NASA CONTRACTOR REPORT

NASA CR-1069

NASA CR-1069

LUNAR ORBITER III

Photographic Mission Summary

Prepared by
THE BOEING COMPANY
Seattle, Wash.
for Langley Research Center

NATIONAL AERONAUTICS AND SPACE ADMINISTRATION • WASHINGTON, D. C. • MAY 1968

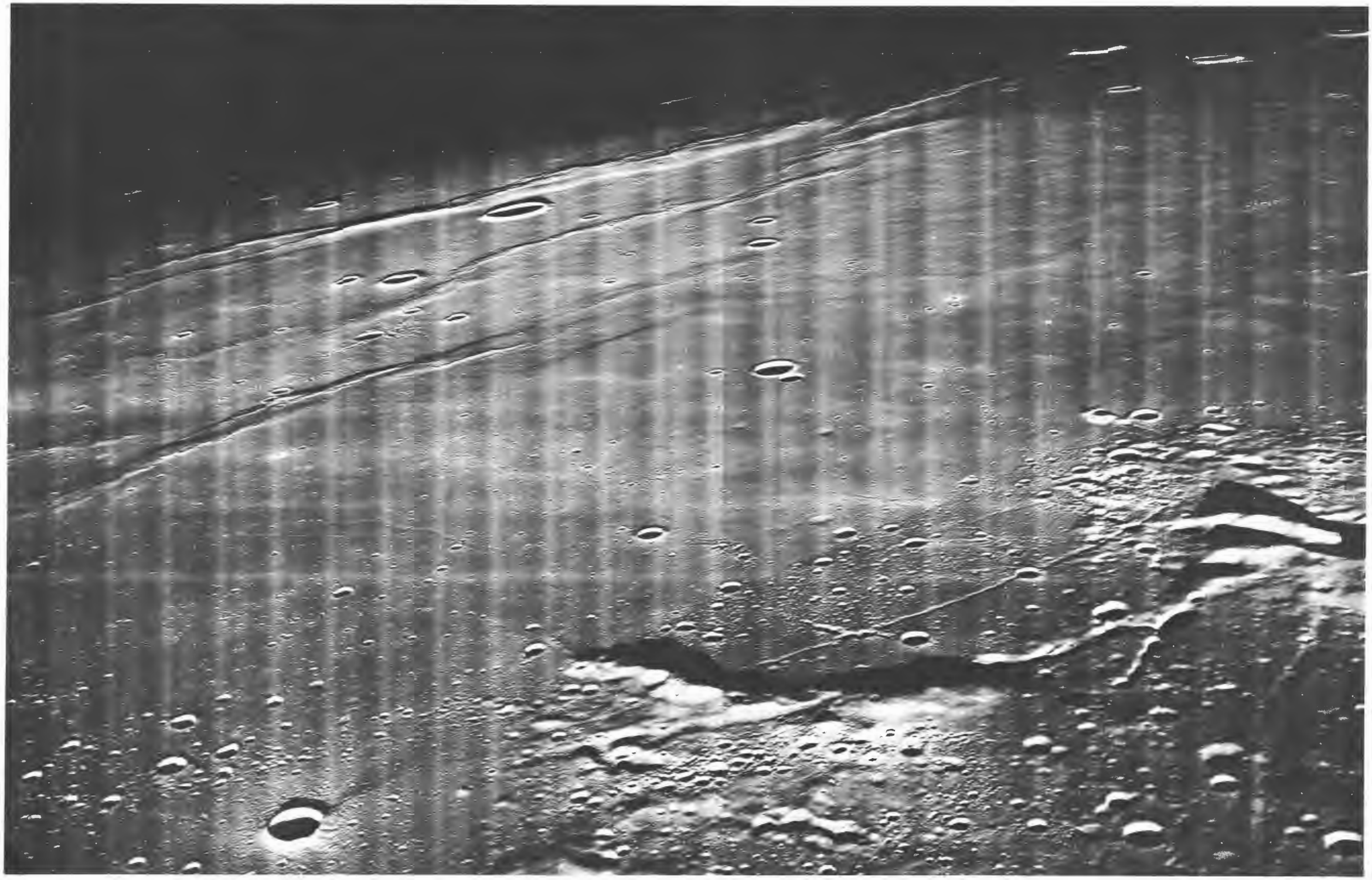

Lunar Landing Approach
—Astronaut's View

Photo taken by NASA-Boeing Lunar Orbiter III, Feb. 21, 1967, 01:33:37 GMT from an altitude of 52 km.

NASA CR-1069

LUNAR ORBITER III

Photographic Mission Summary

Prepared under Contract No. NAS 1-3800 by
THE BOEING COMPANY
Seattle, Wash.

for Langley Research Center

NATIONAL AERONAUTICS AND SPACE ADMINISTRATION

For sale by the Clearinghouse for Federal Scientific and Technical Information
Springfield, Virginia 22151 – CFSTI price $3.00

CONTENTS

CONTENTS (Continued)

FIGURES

TABLES

ILLUSTRATIONS

Wide-Angle Frame 162—Site III S-26
(Oblique to north toward crater Kepler)

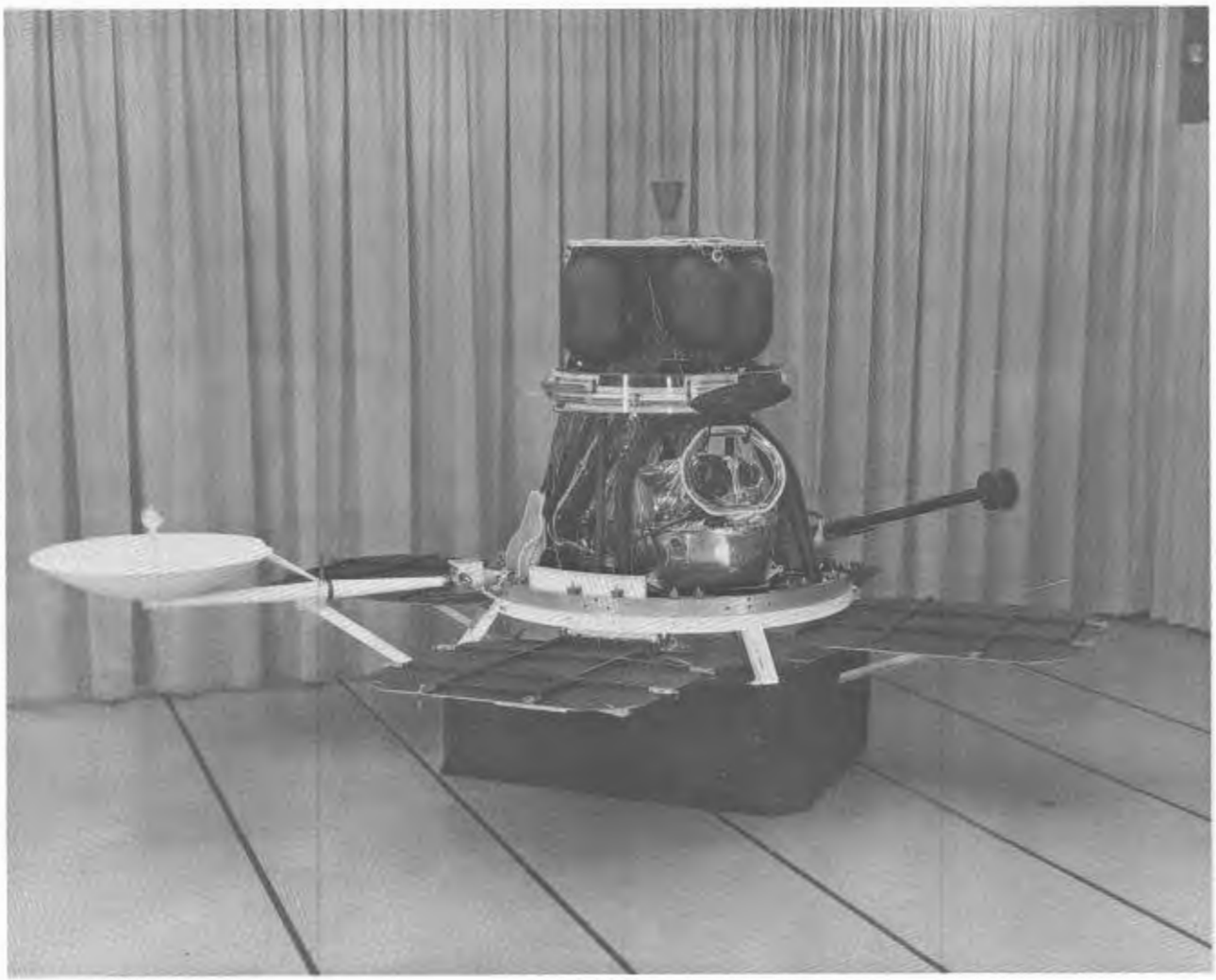

LUNAR ORBITER III FINAL REPORT

PHOTOGRAPHIC MISSION SUMMARY

The third of five Lunar Orbiter spacecraft was successfully launched from Launch Complex 13 at the Air Force Eastern Test Range by an Atlas-Agena launch vehicle at 01:17 GMT on February 5, 1967. Tracking data from the Cape Kennedy and Grand Bahama tracking stations were used to control and guide the launch vehicle during Atlas powered flight. The Agena-spacecraft combination was boosted to the proper coast ellipse by the Atlas booster prior to separation. Final maneuvering and acceleration to the velocity required to maintain the 100-nautical-mile-altitude Earth orbit was controlled by the preset on-board Agena computer. In addition, the Agena computer determined the maneuver and engine-burn period required to inject the spacecraft on the cislunar trajectory 20 minutes after launch. Tracking data from the downrange stations and the Johannesburg, South Africa station were used to monitor the entire boost trajectory.

Antenna and solar panel deployment sequences and Sun acquisition were initiated by stored commands shortly after spacecraft separation and before acquisition by the Deep Space Network tracking stations.

Events of significance during the cislunar trajectory were the star map and Canopus acquisition sequence initiated about 11 hours after launch, and the single midcourse correction of only 5.09 meters-per-second velocity change nearly 38 hours after launch. Both of these functions were satisfactorily completed. Injection into the initial lunar orbit occurred 92.5 hours after launch. The velocity change maneuver resulted in a 13-degree plane change at injection and an orbit perilune of 210 kilometers. After nearly 4 days of this orbit to acquire tracking data for a 21-degree orbit inclination angle, transfer to the final photographic elliptical orbit (49 kilometers) was completed.

The active photographic period was initiated during Orbit 44 on February 15, 10 days and 9 hours after launch. During the next 7 days the 12 primary and 31 of the 32 planned secondary sites were photographed. A total of 156 photographs were taken of the primary sites during 20 orbits. Secondary-site photography was completed by taking 55 photos during 31 separate orbits. During this photographic period, 78 telephoto and 39 wide-angle photos were read out in whole or in part in the priority readout mode. Intermittent film advance stoppages occurred during priority readout, but were overcome by slight changes in operating procedures. The photographic phase was completed on February 23 when the desired film processing was completed, the Bimat cut command executed, and the final readout period initiated.

Readout and examination of photos continued in a near-routine manner for the next 7 days during 51 readout periods. Shortly after initiation of the "readout on" command during Orbit 149, a transient or momentary voltage dropout upset the photo subsystem control logic. As a result, the film advance was turned on while the film supply brake was applied, which caused the ultimate failure of the film advance motor. At the time of failure on March 2, the final readout had recovered telephoto photography of Frames 79 through 215 and Wide-Angle Frames 78 through 215.

Primary-site photography was accomplished by a complex integration of vertical, near vertical, and cross-track tilt orientations to provide the monoscopic, stereoscopic, and converging telephoto stereoscopic coverage outlined in the mission objectives. Secondary-site photography included vertical, near vertical, and low-and high-oblique angles. Except for minor changes in site location, the addition of a fourth photo pass over Primary Site IIIP-12, and the deletion of Secondary Site IIIS-32, all photography was completed as planned.

There were no micrometeoroid impacts recorded during the photographic mission and the radiation dosage was low.

All mission objectives—except for reconstruction of approximately 73 dual frames during the final readout—were satisfactorily accomplished. This mission represents the first comprehensive site-examination photographic mission of the lunar surface and satisfies the Apollo minimum requirement.

Eight Apollo landing-site candidates have been selected by the NASA screening group from data obtained from the first three Lunar Orbiter missions.

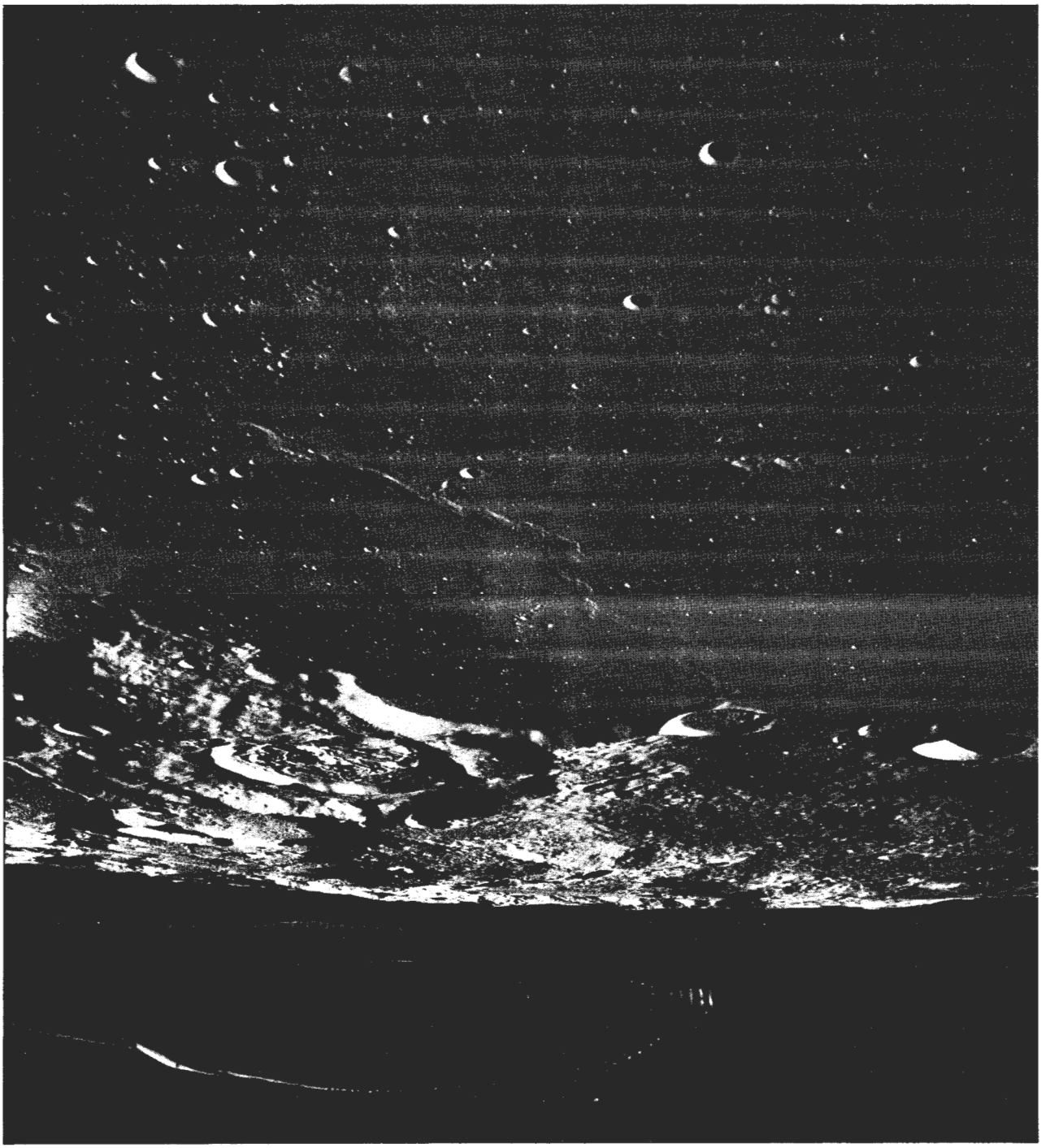

Wide-Angle Frame 213—Site III S-29
(Oblique to south toward crater Damoisseau)

1.0 INTRODUCTION

The Lunar Orbiter program was formalized by Contract NAS1-3800 on May 7, 1964, as one of the lunar and planetary programs directed by the NASA headquarters Office of Space Sciences and Applications. The program is managed by the Langley Research Center, Hampton, Virginia, with The Boeing Company as the prime contractor. Lunar Orbiter is the third in a succession of unmanned missions to photograph the Moon and to provide lunar environmental data to support the Apollo manned lunar landing mission.

The three successful Ranger flights each provided a series of photographs of decreasing area and increasing resolution (to a fraction of a foot) as each spacecraft approached and impacted the Moon. The Surveyor provides detailed information on lunar surface characteristics (with resolution in millimeters) in the immediate area of each successful soft landing. Surveyor contributes small-scale relief and soil mechanics data limited to the line of sight surrounding the landing site.

The Lunar Orbiter prime mission is to photograph large areas at a resolution level adequate to provide information for selection and verification of suitable landing sites for manned Apollo vehicles and unmanned Surveyor vehicles. Monoscopic coverage at approximately 1-meter resolution and stereoscopic photographs at approximately 8-meter resolution at a nominal altitude of 46 km are to be obtained of each primary photo site.

1.1 PROGRAM DESCRIPTION

The Lunar Orbiter system design was based on the requirement to photograph specific target sites within an area of interest bounded by ± 10-degree latitude and ± 60-degree longitude. Types of photo missions within the primary region are classified as:

- Single-site search and examination;
- Large-area search;
- Spot photos;
- Combinations of the above.

Designated areas of scientific interest and landmarks for Apollo navigation outside of the primary area may also be photographed.

Lighting conditions and altitude must be adequate for detection of:

- Features equivalent to a cone having a 2-meter base diameter and 0.5-meter height;
- An area 7 by 7 meters of 7-degree slope (when sloped in a direction to provide maximum contrast with surrounding area).

The original plan required that each of the five missions (during the 1966 to 1967 period) provide topographic information of at least 8,000 square kilometers at nominal 1-meter resolution and approximately 40,000 square kilometers at nominal 8-meter resolution. This coverage can be obtained by single photographs or by 4-, 8-, or 16-exposure sequences in either of two automatic sequencing modes (nominal 2 or 8 seconds between exposures).

In addition to the five flight spacecraft, three ground test spacecraft are included in the comprehensive ground test and flight program. The ground test spacecraft were used for the qualification test program, mission simulation testing in an environmental space chamber, and the performance demonstration and tests of the spacecraft compatibility with the ground support facilities.

Additional program requirements include collection of selenodetic data that can be used to improve the definition of the lunar gravitational field, and knowledge of the size and shape of the Moon. Radiation intensity and micrometeoroid impact measurements are also to be obtained to further define the lunar environment.

At the completion of each photographic mission (approximately 30 to 35 days after launch), the spacecraft may remain in lunar orbit for an extended period to obtain additional tracking data, continue environmental monitoring, and conduct scientific experiments.

The Lunar Orbiter I mission provided extensive moderate-resolution coverage of nine primary Apollo sites, as well as photographs of eight proposed site areas for the Lunar Orbiter II mission. Wide-angle and telephoto coverage of 13 primary sites was provided by the Lunar Orbiter II mission. Primary photo sites for Mission I were located along a southern latitude band with Mission II sites along a northern latitude band within the Apollo zone of interest (± 5° latitude and ± 45° longitude). These two missions provided an immense volume of detailed lunar photographic data and completed the Apollo minimum requirement of two site-search missions.

Mission III differed from previous Lunar Orbiter missions in that it was a site-confirmation rather than a site-search mission. The primary objective was to photograph promising areas identified by screening Lunar Orbiter I and II photos, thereby providing the additional data needed to confirm the adequacy of such areas as Apollo and/or Surveyor landing sites.

1.2 PROGRAM MANAGEMENT

Successful accomplishment of Lunar Orbiter program objectives requires the integrated and cooperative efforts of government agencies, private contractors, numerous subcontractors, and the worldwide data collection system of the NASA Deep Space Network. The functional relationship and responsibilities of these organizations is shown in Figure 1-1.

As the prime contractor, Boeing is responsible to the Lunar Orbiter Project Office of the NASA-Langley Research Center for the overall project management and implementation of the complete operating system. Boeing is also responsible for the establishment—with and through the NASA-Langley Research Center—of effective working relationships with all participating government agencies.

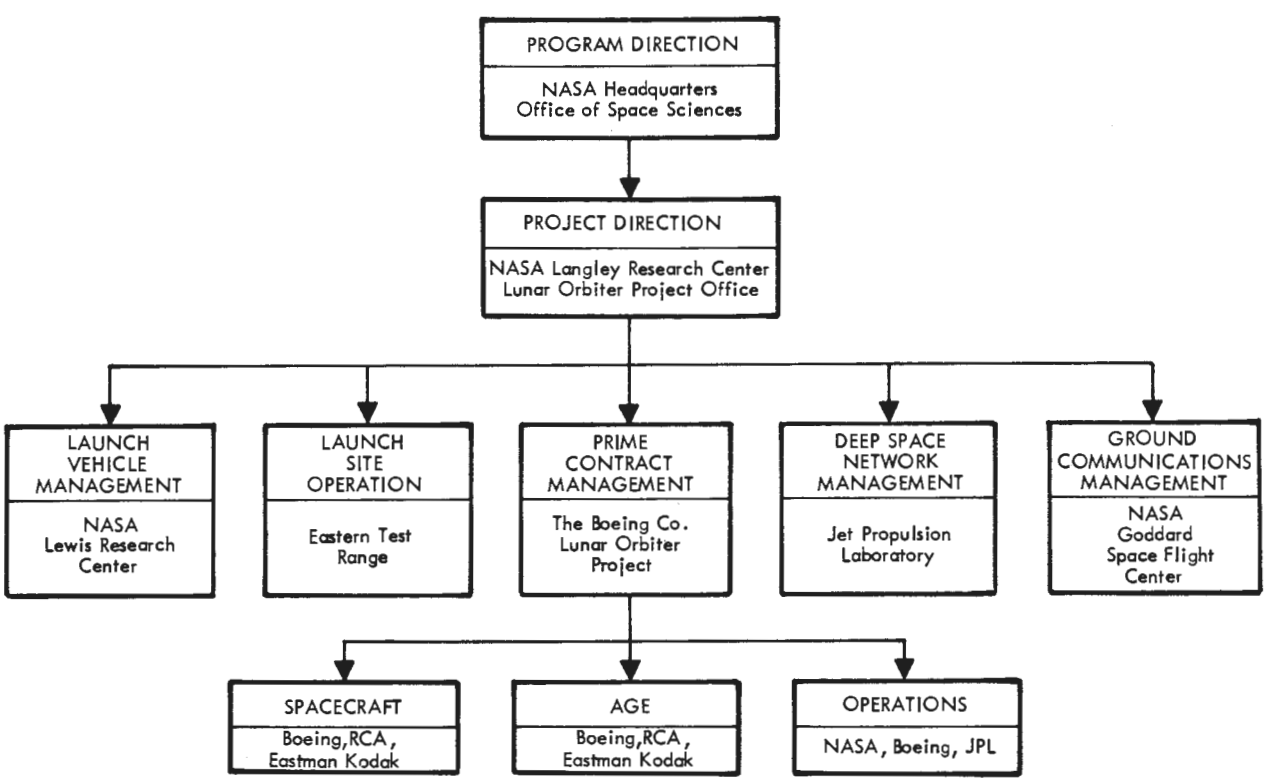

Figure 1-1: Lunar Orbiter Project Organization

The NASA Lewis Research Center supports the Lunar Orbiter program by providing the Atlas-Agena launch vehicle and associated services that are necessary to: (1) ensure compatibility of the spacecraft with the launch vehicle; and (2) launch and boost the spacecraft into the proper cislunar trajectory.

The Air Force Eastern Test Range (AFETR) provides facilities, equipment, and support required to test, check out, assemble, launch, and track the spacecraft and launch vehicle. The AFETR also controls the Atlas launch vehicle trajectory and monitors Agena performance through cislunar injection, separation, and retrofire to ensure orbital separation. Appropriate instrumentation facilities, communications, and data recorders are provided at downrange stations and instrumentation ships to ensure the availability of data for boost trajectory control, acquisition by the Deep Space Station tracking radars, and postmission analysis.

The Deep Space Network (DSN) is managed by the Jet Propulsion Laboratory. This network, consisting of the Space Flight Operations Facility (SFOF) and the Deep Space Stations (DSS), provides two-way communications with the spacecraft, data collection, and data processing. Facilities are provided for operational control which interface with Lunar Orbiter mission-peculiar equipment. Support is also provided in terms of personnel, equipment calibration, and housekeeping services.

Goddard Space Flight Center is the agency responsible for the worldwide network of communication lines necessary to ensure prompt distribution of information between the several tracking stations and the Space Flight Operations Facility during the mission and mission training periods.

1.3 PROGRAM OBJECTIVES

The prime project objective of the Lunar Orbiter mission is to secure topographic data regarding the lunar surface for the purpose of extending our scientific knowledge, and selecting and confirming landing sites for Apollo. To accomplish the objective, high-resolution photographic data covering specified areas on the lunar surface and moderate-resolution photographic data coverage of extensive areas are necessary.

Other objectives are to secure information concerning the size and shape of the Moon, the properties of its gravitational field, and lunar environmental data.

Selection of the photo sites for each Lunar Orbiter mission are based on Apollo constraints and preferences as modified to reflect the knowledge gained by preceding missions. The present Apollo constraints and preferences indicate that a minimum of two Lunar Orbiter site-search missions are required. Lunar Orbiters I and II satisfied this requirement by photographing the selected primary sites located along southern and northern latitude bands within the Apollo zone ($\pm$ 5-degree latitude and $\pm$ 45-degree longitude). Following the site-search missions, additional data on promising areas is required by a site-confirmation mission before selection and certification of Apollo and/or Surveyor landing sites. Landing sites are desired at a number of locations to fulfill the exploration and scientific objectives of the Apollo program and to provide an adequate launch window. The topography of an Apollo landing site must be smooth enough for an Apollo landing module (LM) landing. The approach terrain must be reasonably level to allow satisfactory LM landing radar performance. The surface resolution requirement to enable the selection of suitable sites for Apollo landings is approximately 1 meter.

The selenodetic and environmental mission data objectives require the use of operational equipment and detectors on the spacecraft. Tracking data obtained throughout the mission produce the basic data required to satisfy selenodetic objectives. Micrometeoroid detectors mounted on the periphery of the spacecraft and radiation detectors mounted internally monitor the lunar environmental data on each flight for transmission to the ground stations.

1.3.1 Mission III Objectives

The specific objectives for Mission III were defined by NASA as follows:

"Primary:

- To obtain, from lunar orbit, detailed photographic information of various lunar areas, to assess their suitability as landing sites for Apollo and Surveyor spacecraft, and to improve our knowledge of the Moon.

Secondary:

- To provide precision trajectory information for use in improving the definition of the lunar gravitational field;

- To provide a spacecraft which can be tracked in lunar orbit by the Manned Space Flight Network (MSFN) stations for the purpose of exercising and evaluating the tracking network and Apollo Orbit Determination Program."

The primary objective of Lunar Orbiter III was to continue the Lunar Orbiter I and II task of photographing promising areas to determine their adequacy as Apollo and/or Surveyor landing sites considering location, topography, and soil mechanics. The site photography was expected to provide some engineering geology data to support the extrapolation of Surveyor data. Mission III differs from the previous two missions in that it was a site-confirmation mission rather than a site-search mission. To provide access to both the Mission I and II primary sites with acceptable lighting conditions, the orbit inclination was increased to 21 degrees.

Primary photo site selection was based on screening of the Lunar Orbiter I and II photos by representatives of the Apollo project, the Surveyor project, the U. S. Geological Survey, Bellcomm, and the Lunar Orbiter project. Twelve primary sites (including the landing area of Surveyor I) and 32 secondary sites were selected for Mission III. The 12 primary sites were to be photographed with a total of 156 frames during 19 orbits. These were to be taken in 8- or 16-frame fast-mode sequences for all sites except IIIP-3 and -6, which were to use four-frame slow-mode sequences.

In addition, the 32 secondary-site coverage required 56 separate exposures. All secondary sites employed single-frame exposures—except for Sites IIIS-1, -7, -10, -15, -17, -18, -19, and -23, which were to be four-frame sequences. Some of the secondary photo sites were selected to obtain oblique coverage of specified primary sites. Photography of primary and secondary sites was to include: vertical, oblique, forward and side stereo, and converging telephoto stereo coverage.

Other photographic mission considerations were the requirements to:

- Read out selected frames between sites for mission control.

- No photography in the initial lunar orbit.

- Minimum priority readout shall provide complete wide-angle coverage of primary sites.

Tables 1-1 and -2 tabulate the location and the number of exposures for each of the primary and secondary photo sites selected. In addition, comments are given with respect to the type of photos taken and a cross reference to related primary sites of Missions I and II. In all such cases the Mission III area covers a particular area within the previous mission coverage. Figure 1-2 graphically identifies each of the primary photo sites and indicates the corresponding photo orbit and spacecraft altitude.

Other objectives, in addition to continuing to provide precision tracking information and monitoring lunar environmental conditions, included providing a spacecraft that can be tracked in lunar orbit by the MSFN for the proposed exercising and evaluating of the tracking network and Apollo Orbit Determination Program.

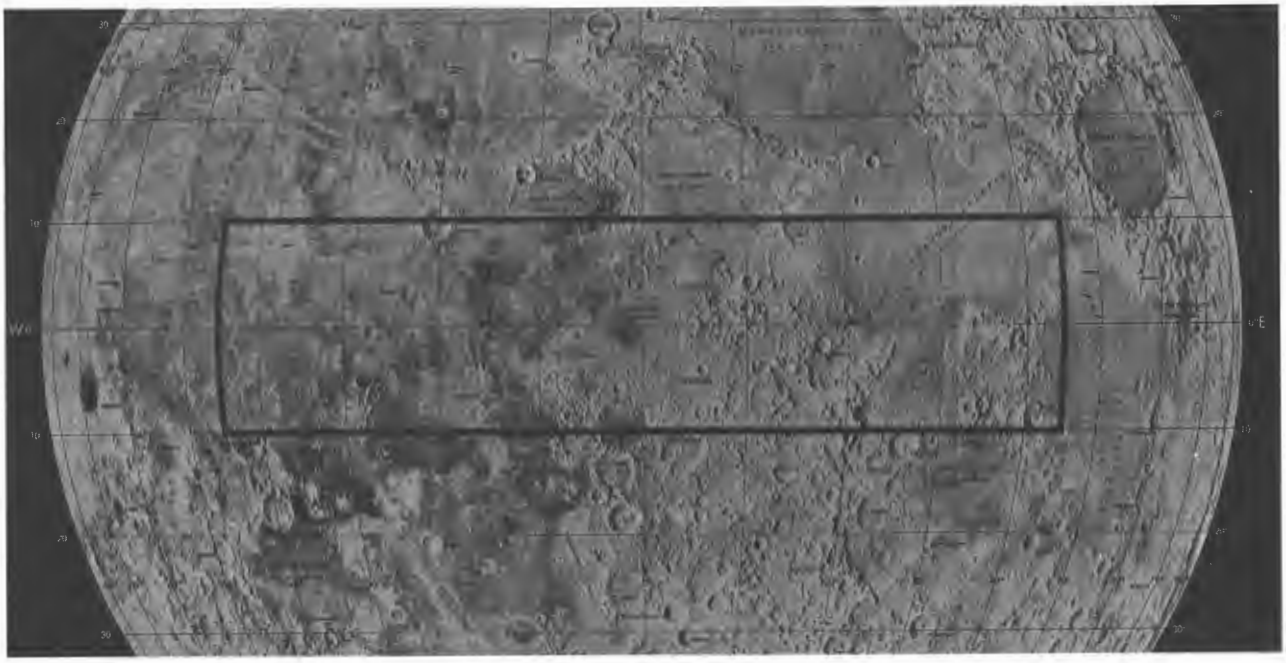

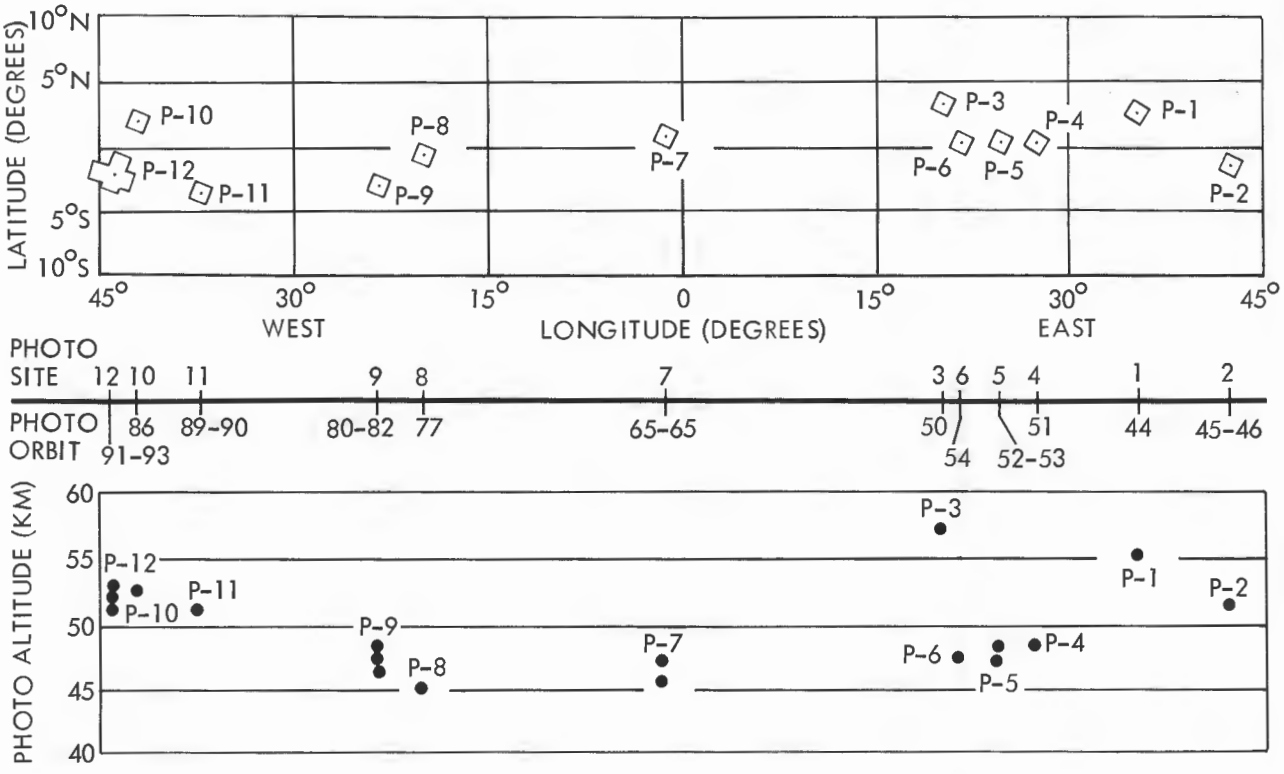

Figure 1-2: Primary-Photo-Site Distribution

Table 1-1: PRIMARY-PHOTO-SITE IDENTIFICATION

Site Number	LOCATION		PHOTO COVERAGE			Comments
	Longitude	Latitude	Orbit	Exposure	Total	
IIIP-1	35° 15′ E	2° 55′ N	1	16	16	Northeast area of Site IIP-2
IIIP-2a	42° 25′ E	0° 50′ S	1	8	8	Within Site I-1
IIIP-2b	42° 41′ E	0° 55′ S	1	4	4	Portion of Site IIP-3b (Note 1)
IIIP-3	20° 15′ E	3° 20′ N	1	4*	4	Southwest portion of Site IIIP-3b, Surveyor candidate
IIIP-4	27° 27′ E	0° 37′ N	1	8	8	Northeast area of Site I-3
IIIP-5a	24° 31′ E	0° 27′ N	1	8	8	Portions of Sites I-3 and IIP-6 (Note 1)
IIIP-5b	24° 31′ E	0° 27′ N	1	8	8	Portions of Sites I-3 and IIP-6, Surveyor candidate
IIIP-6	21° 30′ E	0° 20′ N	1	4*	4	Surveyor candidate
IIIP-7a	1° 17′ W	1° 02′ N	1	8	8	Portions of Sites I-5, IIIP-7 and -8 (Note 1)
IIIP-7b	1° 20′ W	0° 55′ N	1	8	8	Portions of Sites I-5, IIIP-7 and -8, Surveyor candidate
IIIP-8	19° 50′ W	0° 50′ S	1	8	8	Site IIP-11
IIIP-9a	23° 11′ W	3° 09′ S	1	8	8	Site I-7 (Note 1)
IIIP-9b	23° 11′ W	3° 09′ S	1	8	8	Site I-7, Surveyor candidate
IIIP-9c	23° 11′ W	3° 09′ S	1	8	8	Site I-7, Surveyor candidate
IIIP-10	42° 00′ W	1° 45′ N	1	8	8	Site IIP-13 (Note 2)
IIIP-11	36° 56′ W	3° 17′ S	1	8	8	Site I-8.1
IIIP-12a	43° 52′ W	2° 23′ S	1	16	16	Site I-9.2, Surveyor I landing site
IIIP-12b1			1	4	4	Site I-9.2 (Note 3)
IIIP-12b2			1	4	4	Site I-9.2 (Note 3)
IIIP-12c			1	8	8	Site I-9.2 (Note 3)

* Slow Mode

Note 1: Pass produces convergent telephoto stereo coverage of specific target area or photography obtained on the other pass.

Note 2: Convergent telephoto stereo coverage with Mission II Site IIP-13 data.

Note 3: Convergent telephoto stereo coverage of specific sections of Site IIIP-12a photography.

Table 1-2: SECONDARY-PHOTO-SITE IDENTIFICATION

Site Number	Location		Photo Coverage			Comments
	Longitude	Latitude	Orbit	Exposure	Total	
IIIS-1	47° 10′ E	1° 50′ S	1	4	4	Messier and Messier A
IIIS-2	104° E			1		Along Sun's rays
IIIS-3	38° 45′ E	4° 30′ S		1		Oblique covering Colombo quadrangle
IIIS-4	24° 31′ E	0° 27′ N		1		Oblique of Site IIIP-5 looking west
IIIS-5	24° 12′ E	0° 35′ S		1		Oblique looking north to Moltke
IIIS-6	6° 20′ E	7° 45′ N		1		Oblique looking north to Rima Hyginus
IIIS-7	6° 50′ E	3° 40′ N	1	4*	4	Vicinity of Dembowski
IIIS-8	26° 25′ E	11° 20′ S		1		Oblique to south to Theophilus
IIIS-9	17° 35′ E	1° 25′ S		1		Oblique to north to Delambre
IIIS-10	13° 30′ E	1° 30′ S	1	4*	4	Surveyor candidate site
IIIS-11	1° 20′ W	0° 55′ N		1		Oblique of Site IIIP-7 looking west
IIIS-12	DELETED					
IIIS-13	0° 30′ W	5° 00′ N		1		Oblique to north of Murchison and Pallas
IIIS-14	9° 00′ W	5° 00′ N		1		Oblique to north of Surveyor site
IIIS-15	5° 30′ W	0° 40′ N	1	4*	4	Near Schröter
IIIS-16	5° 40′ W	0° 20′ S		1		Mösting
IIIS-17	4° 05′ E	4° 45′ S	1	4*	4	Surveyor candidate site
IIIS-18	8° 02′ W	1° 50′ S	1	4	4	Mösting C
IIIS-19	3° 40′ W	3° 20′ S	1	4*	4	Surveyor candidate site
IIIS-20	27° 45′ W	7° 40′ N		1		Oblique to north - Hortensius domes
IIIS-21	20° 00′ W	0° 30′ S		1		Oblique of Site IIIP-8
IIIS-21.5	126° E					Oblique to south - Farside
IIIS-22	22° 05′ W	1° 10′ N		1		Surveyor candidate site
IIIS-23	17° 14′ W	3° 31′ S	1	4*	4	Oblique to south - Fra Mauro

cont.

* Slow Mode

Table 1-2 (Cont.)

Site Number	Location		Photo Coverage			Comments
	Longitude	Latitude	Orbit	Exposure	Total	
IIIS-24	23° 15′ W	3° 05′ S		1		Oblique of Site IIIP-9
IIIS-25	42° 00′ W	1° 45′ N		1		Oblique of Site IIIP-10
IIIS-26	37° 50′ W	8° 10′ N		1		Oblique to north - Kepler
IIIS-27	37° 10′ W	3° 30′ S		1		Oblique of Site IIIP-11
IIIS-28	43° 55′ W	2° 20′ S		1		Oblique of Site IIIP-12
IIIS-29	60° 33′ W	5° 00′ S		1		Oblique to south - Damoiseau
IIIS-30	64° 35′ W	7° 00′ N		1		Oblique to north - Luna 9 area
IIIS-31	67° 00′ W	1° 50′ N		1		Floor of Hevelius
IIIS-32	68° 00′ W	5° 00′ S		1		Oblique to south - Grimaldi

1.4 MISSION DESIGN

The Lunar Orbiter spacecraft was designed around its photo subsystem to ensure the maximum probability of success of the photographic mission. Similarly, the mission design maximized the probability of quality photography by placing the spacecraft over the mission target(s) in the proper attitude, altitude, and within the established lighting limitations. Launch vehicle, spacecraft, and photographic considerations were integrated into the design effort to optimize the trajectory and sequence of events to satisfy mission photographic objectives. Primary mission events as related to the Earth-Moon-Sun-spacecraft orbit geometry are shown in Figure 1-3.

Selection of the trajectory was based on conditions that must be satisfied, such as:

- Transit time (Earth to Moon) of approximately 90 hours;
- Initial orbit of 1850-km apolune and 200-km perilune;
- Nominal photographic altitude of 45 km;
- Orbit inclination of approximately 21 degrees at lunar equator;
- Descending-node photography for lighting;
- Posigrade orbit for visibility of injection.

Trajectory and orbit data used for mission design were based upon computations using Clarke's model of the Moon with Earth effects. The data used were the output of computer programs covering the following phases:

- Translunar Search Program;
- Translunar Orbit Description Program;
- Lunar Orbit Description Program.

Table 1-3 tabulates launch window characteristics for the February launch periods. The nominal sequence of events presented in the mission event sequence and time line analysis was based on a launch time approximately 30 minutes into the first launch window.

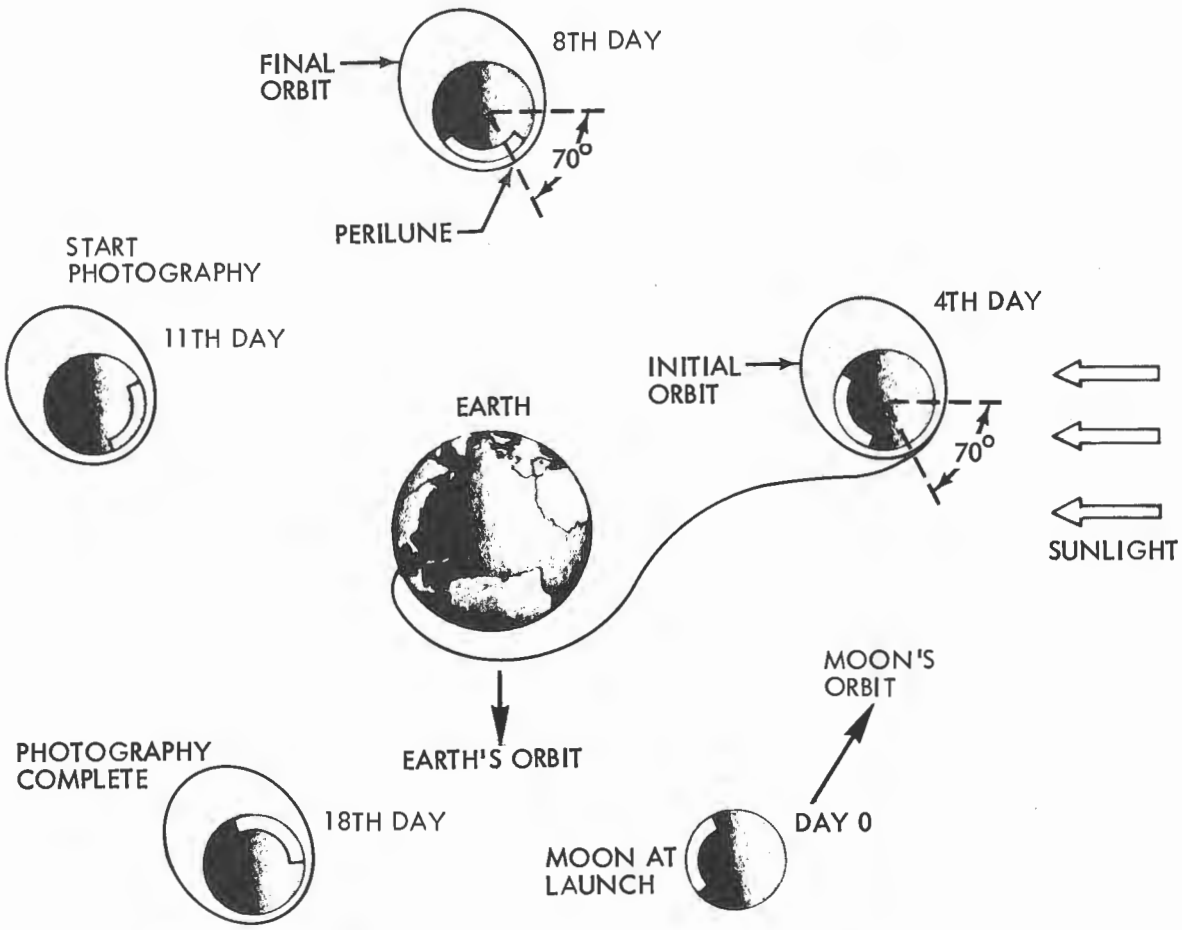

Figure 1-3: Sun-Earth-Moon-Spacecraft Relationships

Table 1-3: FEBRUARY LAUNCH WINDOW SUMMARY

Launch Date	Launch Time (GMT)		Launch Azimuth (deg)	
	Start	Stop	Start	Stop
Feb. 3-4	23:11	02:53	70	92
5	00:51	03:50	79	101
6	01:48	04:25	85	106
7	02:36	04:58	90	113
8	02:34	05:06	91	113

The trajectories required to accomplish the photographic objectives during these launch periods were documented in the form of:

- Targeting specifications for the booster agency;
- Tracking trajectory data;
- Tracking and telemetry coverage plan;
- Deep Space Station view periods;
- Mission error analysis;
- Alternate mission studies.

The set of orbit parameters that provided the required coverage of the photo sites determined the sequence and timing of events to obtain the desired photo coverage. Other factors that affected photo subsystem sequences included such operational and spacecraft performance limitations as:

- Start readout no sooner than 18 minutes after Earthrise to ensure spacecraft acquisition and photo subsystem video adjustments;
- End readout 7 minutes before expected sunsets to prepare spacecraft for Sun occultation operation;
- Interval of 14 minutes between end of processing and start of readouts to allow traveling-wave-tube amplifier (TWTA) warmup and video adjustments;
- Interval of 2 minutes between end of readout and start of processing to turn off readout and activate processor;
- Inhibit processing at least 5 minutes before Sun occultation to prevent processing on battery power only;
- Advance one frame every 8 hours to avoid film set;
- Process two frames every 4 hours to reduce Bimat dryout;
- Read out as many frames as possible between photo passes to support the near-real-time mission operation and control functions.

The requirement to photograph specific primary sites from both Missions I and II necessitated increasing the orbit inclination angle from 12 to 21 degrees to obtain acceptable coverage and lighting conditions. This change resulted in a 19% gap in telephoto coverage on successive orbits for Mission III rather than the contiguous side coverage obtained on previous missions. To ensure the capability of covering the required sites, the photo maneuver was made from the closest orbit and the computation included a roll maneuver to properly orient the spacecraft cameras. The resulting off-vertical photography produced a slight degradation in the resolution capability of the photos.

Based upon excellent results from the evaluation of photos taken in the experimental convergent telephoto stereo mode during Mission II, this technique was specified for six of the 12 Mission III primary sites. To ensure retention of the best resolution integrity, one photo pass was made with the camera axis as near vertical as possible and the other with the camera axis tilted as required to obtain the overlapping coverage.

The nominal planned sequence of significant events from the transfer to final ellipse (end of Orbit 38) to the completion of film processing and "Bimat cut" command (Orbit 104) is shown in Figure 1-4. The ordinate covers the period of one complete orbit (3 hours, 28 minutes, 13.2 seconds) and the abscissa covers successive orbits during the photographic phase of the mission. Time progresses from the bottom to the top and the time at the top of any orbit is identical to the bottom of the next orbit. Three bands are shown in the figure which represent the periods when the Earth, the Sun, and the star Canopus are not visible to the spacecraft. The bar charts at the top represent the approximate viewing periods of the three primary Deep Space Stations. The figure also shows where the photos were taken with respect to time from orbit perilune as well as the times alloted to film processing and priority readout.

Figure 1-5 shows spacecraft exposure numbers of each photo and shows the planned sequence of primary and secondary photo sites. The shaded portions indicate the wide-angle photos read out in the priority mode. Partial-frame readouts for telephoto coverage on either or both sides of the wide-angle photos are not shown.

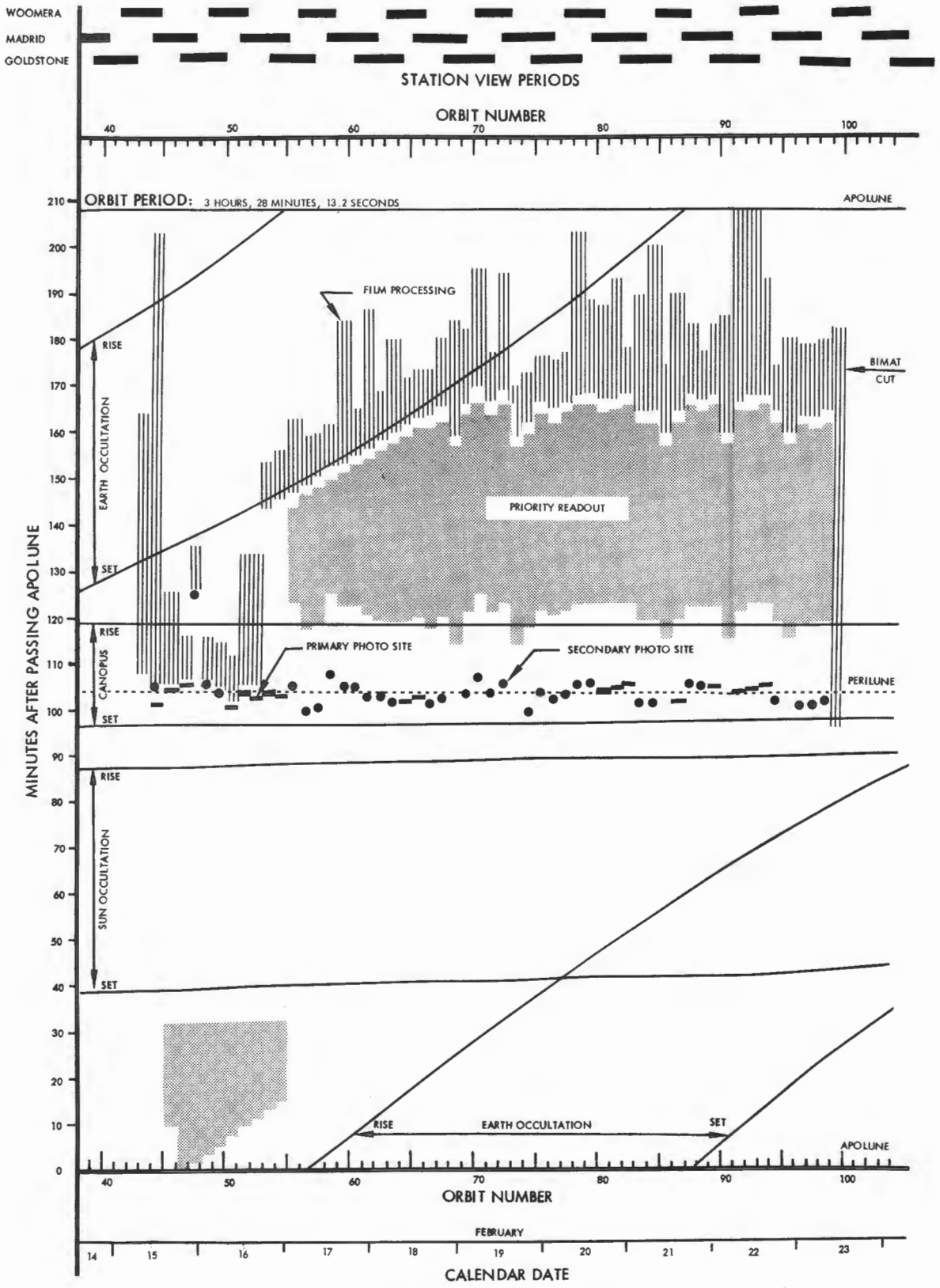

Figure 1-4: Planned Photo Period Sequence of Events

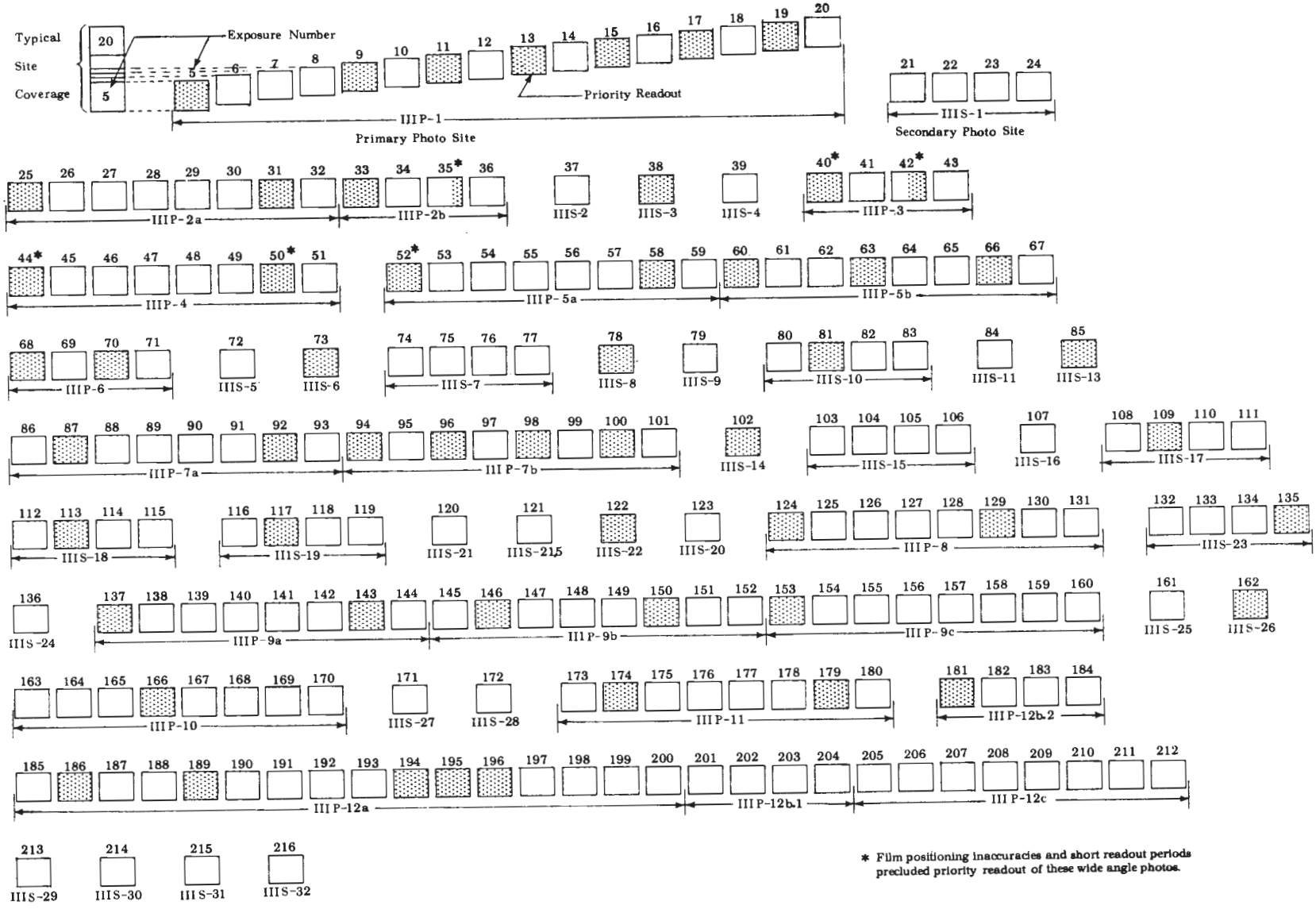

Figure 1-5: Exposure Sequences and Wide-Angle Priority Readout

1.5 FLIGHT VEHICLE DESCRIPTION

The Lunar Orbiter spacecraft is accelerated to injection velocity and placed on the cis-lunar trajectory by the Atlas-Agena launch vehicle.

Spacecraft Description—The 380-kilogram (853-pound) Lunar Obiter spacecraft is 2.08 meters (6.83 feet) high, spans 5.21 meters (17.1 feet) from the tip of the rotatable high-gain dish antenna to the tip of the low-gain antenna, and measures 3.76 meters (12.4 feet) across the solar panels. Figure 1-6 shows the spacecraft in the flight configuration with all elements fully deployed (the mylar thermal barrier is not shown). Major components are attached to the largest of three deck structures which are interconnected by a tubular truss network. Thermal control is maintained by controlling emission of internal energy and absorption of solar energy through the use of a special paint covering the bottom side of the deck structure. The entire spacecraft periphery above the large equipment-mounting deck is covered with a highly reflective aluminum-coated mylar shroud, providing an adiabatic thermal barrier. In addition to its structural functions, the tank deck is designed to withstand radiant energy from the velocity control engine to minimize heat losses. Three-axis stabilization is provided by using the Sun and Canopus as primary angular references, and by a three-axis inertial system when the vehicle is required to operate off celestial references, during maneuvers or when the Sun and/or Canopus are occulted by the Moon.

The spacecraft subsystems (as shown in the block diagram of Figure 1-7) have been tailored around a highly versatile "photo laboratory" containing two cameras, a film supply, film processor, a processing web supply, an optical-mechanical electronic readout system, an image motion compensation (IMC) system (to prevent image smear induced by spacecraft velocity), and the control electronics necessary to program the photographic sequences and other operations within the photo subsystem. Operational flexibility of this photo subsystem includes the capability to adjust key system parameters (e.g., number of frames per sequence, time interval between frames, shutter speed, line-scan tube focus) by remote control from the ground.

The influence of constraints and requirements peculiar to successful operation in lunar orbit are apparent in the specific design selected.

- A three-axis stabilized vehicle and control system were selected to accommodate the precise pointing accuracies required for photographs and for accurate spacecraft velocity-vector corrections during midcourse, lunar orbit injection, and orbit-transfer maneuvers.

- The spacecraft is occulted by the Moon during each orbit, with predictable loss of communication from Earth. Since spacecraft operations must continue behind the Moon, an on-board command system with a 128-word memory was provided to support up to 16 hours of automatic operation. It can be interrupted at virtually any time during radio communication to vary the stored sequences or introduce real-time commands. The selected programmer design is a digital data processing system containing register, precision clock, and comparators, to permit combining 65 spacecraft control functions into programming sequences best suited to spacecraft operations required during any phase of the mission.

- The communications system high-gain antenna was provided with a ± 360-degree rotation capability about the boom axis to accommodate pointing errors introduced by the Moon's rotation about the Earth.

- Two radiation detectors were provided to indicate the radiation dosage levels in the critical unexposed film storage areas. One detector measured the exposure seen by the unexposed film re-

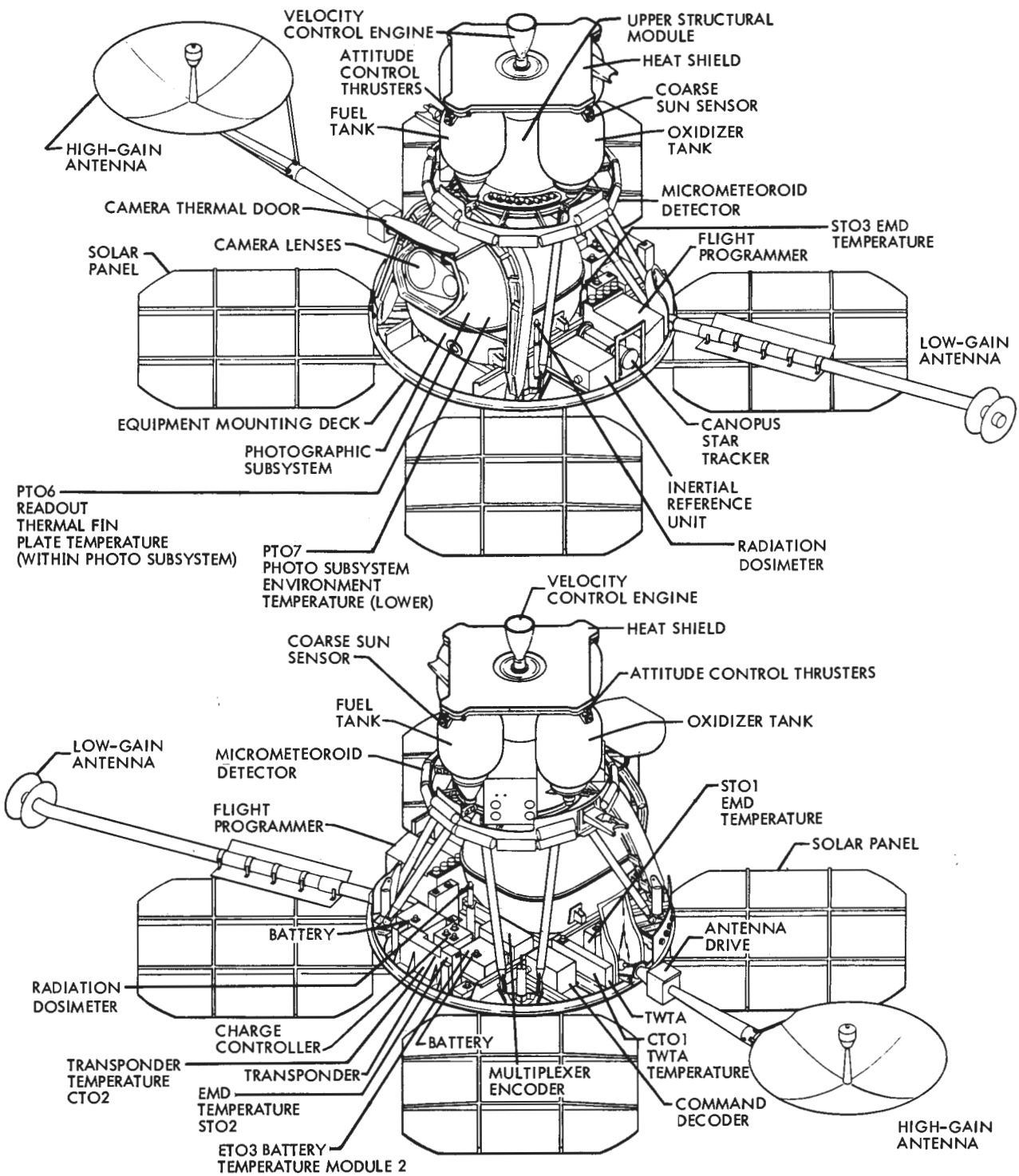

NOTE: SHOWN WITH THERMAL BARRIER REMOVED

Figure 1-6: Lunar Orbiter Spacecraft

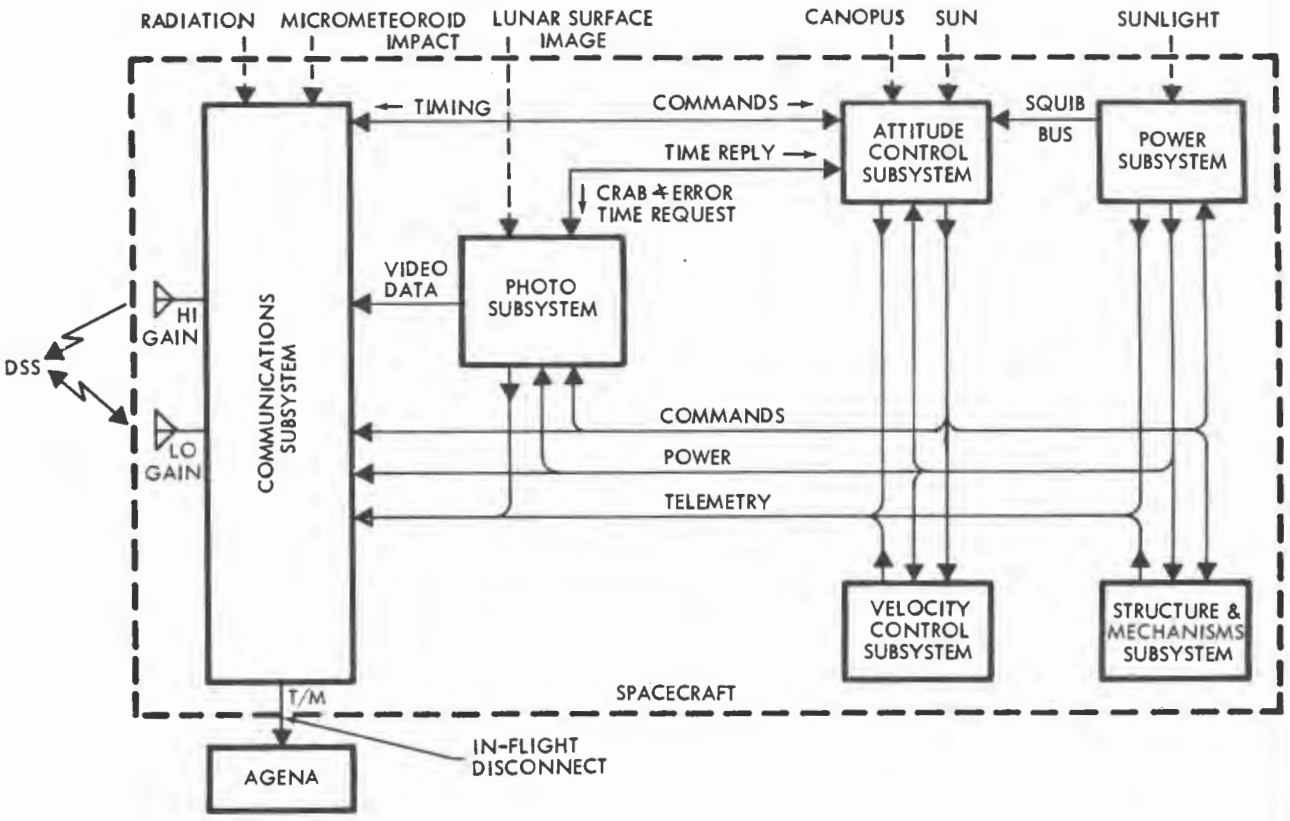

Figure 1-7: Lunar Orbiter Block Diagram

maining in the shielded supply spool, the second, the integrated radiation exposure seen by undeveloped film in the camera storage looper. The data from these detectors allow the selection of alternate mission plans in the event of solar flare activity.

The overall operation of taking the lunar pictures, processing the film, and readout and transmission of the photo video data within the spacecraft is shown in schematic form in Figure 1-8. In addition, the photo reconstruction process at the Deep Space Stations and the reassembly process at Eastman Kodak, Rochester, N. Y., are also shown.

Significant changes from the spacecraft configuration, defined in more detail in NASA Reports CR 782 and CR 883 Lunar Orbiter I and II — Photographic Mission Summary— Final Reports, respectively, based on performance during Missions I and II include:

- Added a 0.21 neutral-density filter in front of the wide-angle lens to equalize the film exposure levels from the two lenses.
- Modified the Reseau mark pattern preexposed on the spacecraft film, to ensure that two lines appear on each framelet and alternate lines are staggered.
- Minor changes in thermal coating coupon types and location.
- Employed the backup inertial reference unit with Kearfott gyros rather than previously used Sperry gyros.
- Revised inertial reference unit temperature control system to eliminate possible electromagnetic interference.
- Revised inertial reference unit conformal coating.

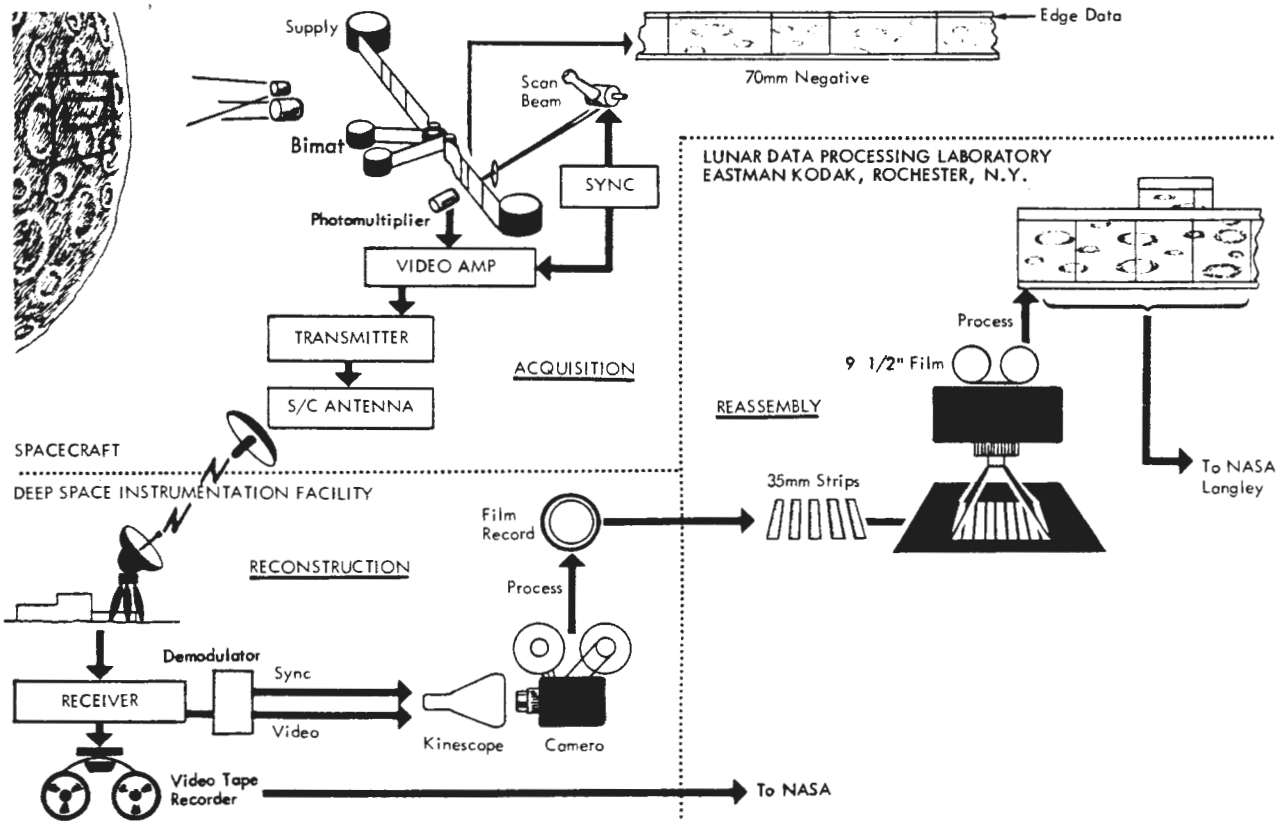

Figure 1-8: Photographic Data Acquisition, Reconstruction, and Assembly

Launch Vehicle Description—The Atlas-Agena combination is a two-and-a-half-stage vehicle as shown in Figure 1-9.

Two interconnected subsystems are used for Atlas guidance and control—the flight control (autopilot) and radio guidance subsystems. Basic units of the flight control subsystem are the flight programmer, gyro package, servocontrol electronics, and hydraulic controller. The main ground elements of the radio guidance subsystem are the monopulse X-band position radar, continuous-wave X-band doppler radar (used to measure velocity), and a Burroughs computer. The airborne unit is a General Electric Mod III-G guidance package which includes a rate beacon, pulse command beacon, and decoder. The radio guidance subsystem interfaces with the flight control (autopilot) subsystem to complete the entire guidance and control loop. All engines of the SLV-3 Atlas are ignited and stabilized prior to launch commitment.

The upper stage is an Agena space booster and includes the spacecraft adapter. It is adapted for use in the Lunar Orbiter mission by inclusion of optional and "program peculiar" equipment. Trajectory and guidance control is maintained by a preset on-board computer. The Agena engine is ignited twice: first to accelerate the Agena-Lunar Orbiter combination to the velocity required to achieve a circular Earth orbit, and second to accelerate the spacecraft to the required injection velocity for the cislunar trajectory.

The Agena Type V telemetry system includes an E-slot VHF antenna, a 10-watt transmitter, and individual voltage-controlled oscillators for IRIG standard channels 5 through 18 and channel F. Channels 12 and 13 are used to transmit spacecraft vibrational data during the launch phase. Channel F contains the complete spacecraft telemetry bit stream during the launch phase.

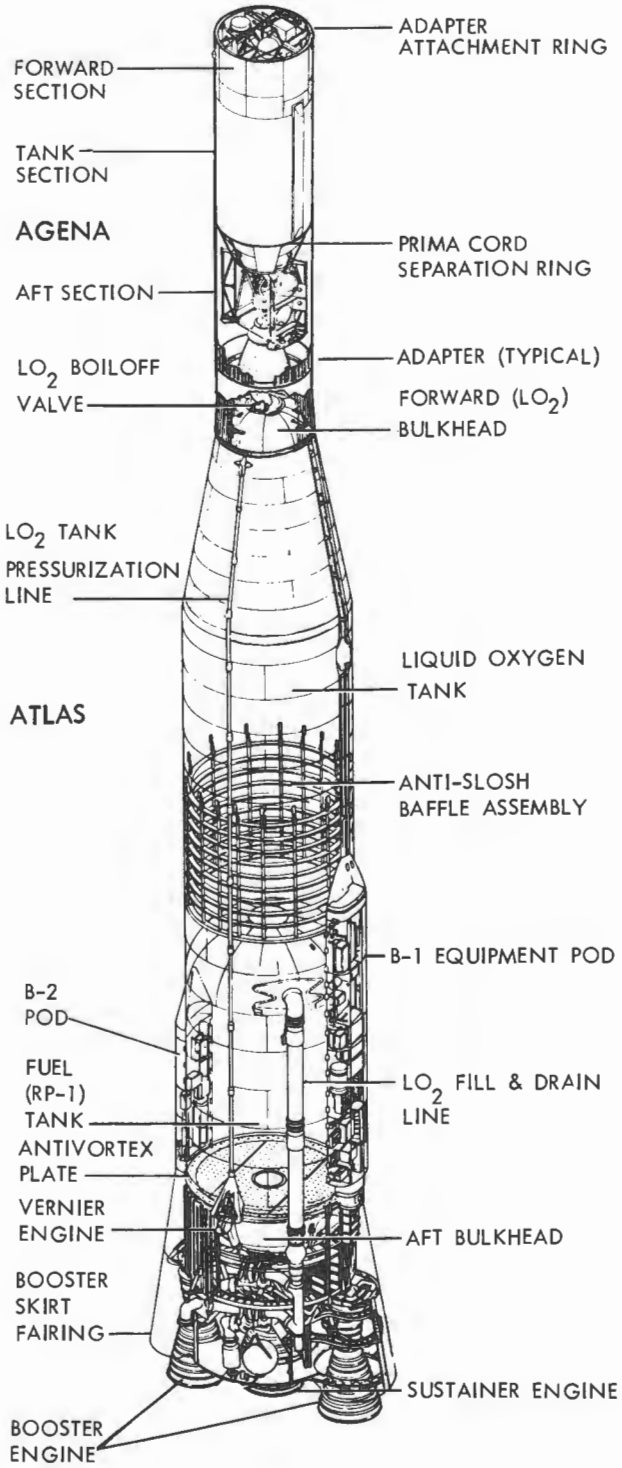

Figure 1-9: Launch Vehicle

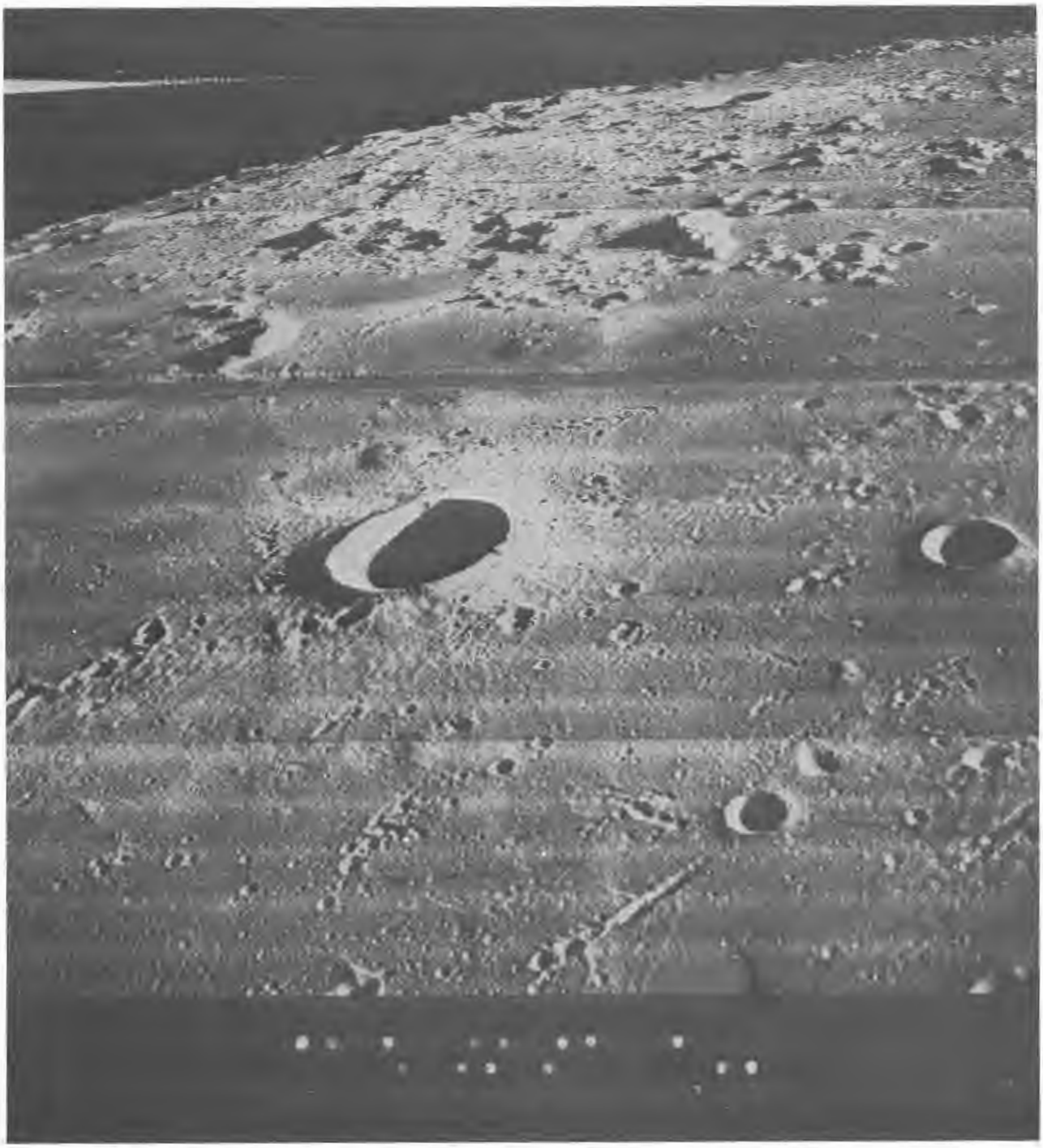

Wide-Angle Frame 123—Site III S-20
(Oblique to north toward Hortensius domes)

2.0 LAUNCH PREPARATION AND OPERATIONS

Lunar Orbiter III mission preparation started with arrival of the spacecraft at AFETR, where it was assembled, tested, and readied for launch. The Atlas-Agena boost vehicle and the Lunar Orbiter spacecraft each received quality acceptance tests at the individual contractor's plants prior to delivery to the AFETR. Early planning included dissemination of information to the launch agency for proper programming of the Atlas-Agena system for the projected launch days. Activities at AFETR of the Atlas, Agena, and Lunar Orbiter spacecraft were integrated so that all systems were properly checked out to support the scheduled launch date. Lunar illumination requirements, Earth-Moon geometry, and Sun-Moon relationships required that these plans be geared to use the available launch windows.

The mission was controlled by the mission director of Langley Research Center, who delegated control of the launch to Lewis Research Center. The launch director was supported by data and tracking instrumentation facilities at the downrange stations and appropriate instrumentation ships located in the Atlantic and Indian Oceans. Upon acquisition of the spacecraft by the Deep Space Network tracking stations, control of the Lunar Orbiter mission was passed from the AFETR to the Space Flight Operations Facility at Pasadena, California.

The following sections summarize the activities and performance prior to acquisition by the Deep Space Network.

2.1 LAUNCH VEHICLE PREPARATION

The Lunar Orbiter III launch vehicle consisted of the Atlas SLV-3, Serial Number 5803, and the Agena-D, Serial Number 6632, boosters. Significant prelaunch events in launch vehicle preparation are shown in Table 2-1.

Upon arrival at AFETR, each vehicle was prepared for launch as summarized in Figure 2-1. This figure shows the test and checkout functions performed in the buildup of the integrated flight vehicle.

Table 2-1: LAUNCH VEHICLE PREPARATION SUMMARY

Date	Event
11-22-66	Agena arrived at AFETR
12-5-66	Atlas booster arrived at AFETR
12-8-66	Atlas erected on Pad 13
12-21-66	B-FACT conducted
1-13-67	Fuel and LOX tanking test
1-16-67	Second fuel and LOX tanking test
1-21-67	Atlas - Agena mated
1-25-67	Second B-FACT conducted

During normal test and checkout procedures, the following problems were encountered and corrected as indicated.

2.1.1 Atlas SLV-3

- A faulty weld on the propellant loading control unit probe tank boss was detected during fuel-tanking operations. Because the leaking weld was inside the fuel tank, the probe boss was encapsulated with a teflon bag to contain the leak.
- The sustainer liquid-oxygen reference regulator was changed three times prior to launch. The original regulator was changed prior to system testing per a Rocketdyne request. Erratic output pressures upon reapplication of supply pressure necessitated two additional replacements and a change in the regulator control setting procedures.
- Both vernier engines were rejected prior to installation, when fibrous (lint) contamination was found in the inlet lines. After sampling and cleaning the lines and associated hardware, the system was

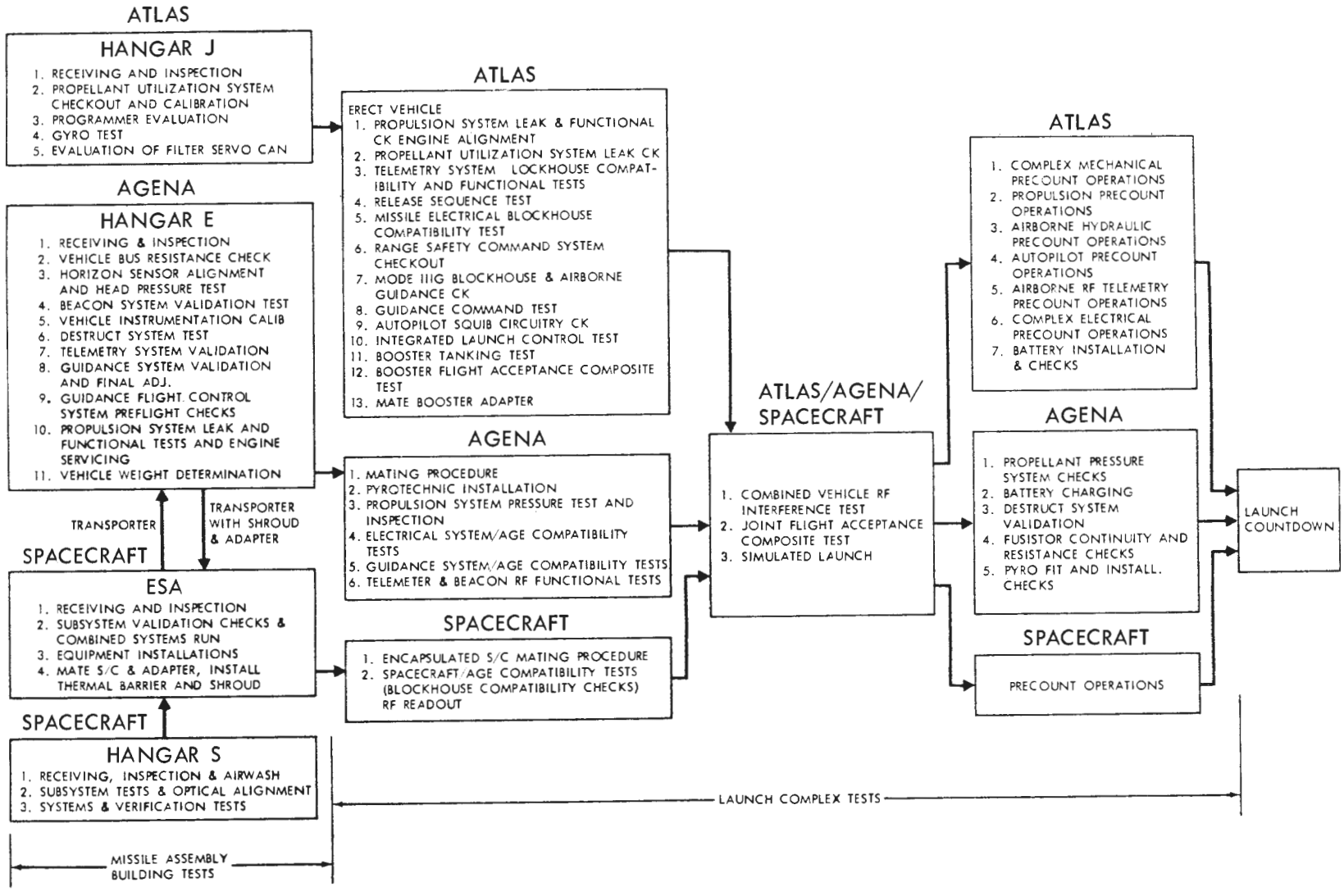

Figure 2-1: Launch Operations Flow Chart

determined to be flight acceptable and reinstalled.

- The sustainer liquid-oxygen pump seal showed an excessive leakage rate at standby pressures. Investigation tests showed that the leakage reduced to well within acceptable limits as the pressure was increased to operational values. This indicated that the lip seal at low pressures was the basic problem, and the installation was determined to be acceptable for flight with no further corrective action required.
- A displacement gyro package and the two-rate package were replaced because of faulty circuits. Failure analysis confirmed the improper operation. Replacement packages performed satisfactorily.
- During the booster flight acceptance composite test, (FACT), loss of the telemetered pitch torque monitor measurement resulted in rejection and replacement of the telemetry package. Failure analysis confirmed the failure in the demodulator unit.

2.1.2 Agena

- The primary timer was replaced during missile assembly building testing when it failed to start and imposed a heavy load on the three-phase inverter. Investigation revealed a bearing retainer mounting screw had grounded phase A of the timer motor.
- Excessive secondary seal leakage resulted in removal of the engine fuel pump and its return to the manufacturer. After necessary repairs, the unit was returned and reinstalled.
- Voltage Control Oscillator (VCO) 18 was found to be faulty and was replaced during pad checkout operations.

Minor test anomalies were detected during the J-FACT, B-FACT, and simulated-launch tests. All were identified and corrected prior to the scheduled launch countdown.

2.2 SPACECRAFT PREPARATION

Lunar Orbiter Spacecraft 6 arrived at Cape Kennedy on August 26, 1966, and was checked out and processed as a backup for Mission II. After the November launch of Mission II, the spacecraft was placed in storage until needed to support Mission III. Spacecraft 7 arrived at Cape Kennedy on November 21 to be prepared and used as a backup unit for Mission III. The significant spacecraft preparation events are shown in Table 2-2.

Table 2-2: SPACECRAFT PREPARATION SUMMARY

Date	Event
January 2, 1967	Spacecraft removed from storage
January 3, 1967	Start processing photo subsystem
January 16-18, 1967	Spacecraft fueling
January 21, 1967	Install photo subsystem in spacecraft
January 23, 1967	DSIF checks without shroud; spacecraft mated to adapter
January 25, 1967	Shroud installation; DSIF checks with shroud installed
January 26, 1967	Mate spacecraft to Agena
January 31, 1967	Simulated launch test
February 3, 1967	Ground power supply troubleshooting

Spacecraft 6 was removed from storage for modification and retest on January 2, 1967. Retest was necessary in accordance with the requirement of Section 5.0 of Boeing Document D2-100111-3, Spacecraft Test Specification—Eastern Test Range—Lunar Orbiter. Limited modifications were also required as a result of experience gained from Missions I and II.

All tests were completed successfully at Hangar S. On January 15, the spacecraft was transferred to the Explosive Safe Area for final testing, installation of ordnance, loading of the photo subsystem, fueling, and final weight and balance checks. Prior to the final move to Launch Pad 13 on January 26, the thermal barrier and nose fairing (shroud) were installed around the spacecraft.

The following major problems were encountered and corrected during prelaunch testing and checkout at ETR.

- The accelerometer in the inertial reference unit failed during tests, necessitating replacement of the unit.
- The traveling-wave-tube amplifier, Serial Number 23, was replaced due to suspect test history.
- A damaged micrometeoroid detector was not replaced.
- The Canopus star tracker was removed for a special engineering test and subsequently reinstalled.
- A bent solar panel actuator arm was found. The actuator was replaced.
- The film advance motor in the photo subsystem was replaced due to erratic film advance behavior.

All retests and special tests were satisfactorily concluded.

2.3 LAUNCH COUNTDOWN

Following matchmate of the encapsulated spacecraft to the Agena on January 26, tests were run to verify impedance and interface compatibility between the Agena and the spacecraft.

When an attempt was made to apply power to the spacecraft, no indication of spacecraft power was evident. Investigation disclosed that a shorting bar on the chart recorder, used to record bus voltage and current, was shorting out the ground power supply. As a precautionary measure, the ground power supply was replaced by the spare ground power supply. Ground power was then applied to the spacecraft, and the pad checkout completed satisfactorily. Upon completion of these tests, the spacecraft was ready for simulated launch.

Simulated launch on January 31 began with the spacecraft count being picked up at T-520 minutes at 10:50 GMT. During the test, there was a noticeable variation of as much as 15 db below normal in the "up" link power to the spacecraft. During the plus count, the link returned to nominal values experienced during previous Lunar Orbiter operations.

At T-55, the spacecraft ground power supply failed and was replaced. During the changeover and subsequent ground power turn-on, power transients were observed and a single photo subsystem film advance was noted. After determination was made that no damage had been done to the photo subsystem, the count was resumed and the test continued through the plus count without further incident. This incident caused 73 minutes of unplanned hold time during the simulated countdown.

The following minor problems were encountered during the simulated launch:

- Readouts by the Agena beacon indicated a signal strength 2 db below downrange requirements. The beacon was later removed and a bench power reading confirmed satisfactory signal strength.
- An interlock circuit "program open loop" light was observed in the Burroughs guidance computer. Investigation revealed that the door covering the manual constant setting switches was open. Closing the door corrected the situation.
- A switch malfunctioned in the automatic checkout sequence circuit of the track checkout equipment panel. Installation of a spare panel corrected the problem.
- Intermittent flashing of the track trans-

mitter confidence circuit light was traced to the automatic frequency control circuit. This was corrected by an adjustment of the confidence circuitry tolerance.

Tests conducted with the spacecraft van after the simulated launch test to investigate the rf level variations showed the anomaly to be caused by signal multipath between the complex and the DSIF-71. Boresighting the 10-foot parabolic antenna on the complex with DSIF-71 resulted in signal gain of 10 db.

On February 2, a test was conducted on the spacecraft to exercise the external ground power supply and repeat that portion of the spacecraft countdown where the film advance had been experienced on the simulated launch test. Power supply problems were again encountered. The launch attempt scheduled for February 3, 1967, was cancelled and processing of the backup spacecraft, Lunar Orbiter Serial Number 7, was initiated.

Trouble shooting continued on February 3. After initial duplication of the power supply problem with the spacecraft simulator, all further attempts to reproduce the anomaly were without results in approximately 20 tests. A test was run on the spacecraft simulator and then the spacecraft was put through that portion of the test where all the problems had been encountered. As these tests were completely successful, the launch was rescheduled for the following day. Prior to turning power on the spacecraft, it was discovered that the Agena umbilical cable release mechanism was not in the flight configuration. The cable was disconnected from the vehicle, the release mechanism was mechanically preloaded, and then reconnected to the Agena.

The spacecraft count was picked up at T-520 minutes on February 4, 1967. After power was supplied to the spacecraft at T-420 minutes, there was some fluctuation in signal between the spacecraft and DSIF-71. Prior to T-315 minutes, when the traveling-wave-tube amplifier (TWTA) was checked, a requirement for the TWTA to be at 45°F was imposed. Spacecraft air conditioning was stopped and the nitrogen purge was started to facilitate this requirement. A few seconds after this was implemented, variations in signal were noticed. The air conditioning was cycled up and down with corresponding variations in signal. The TWTA was finally checked successfully at about T-250 minutes, causing the silent period at T-255 minutes to be delayed for approximately 5 minutes. From this point, a normal spacecraft countdown was conducted to liftoff. Primary spacecraft air conditioning was lost at about T-30 minutes and a switchover to the backup system was accomplished without incident. Liftoff occurred at 01:17:00.120 GMT with favorable weather conditions.

A simplified countdown sequence for the spacecraft and supporting function is shown in Figure 2-2.

2.4 LAUNCH PHASE

The launch phase covers performance of the Lunar Orbiter C flight vehicle from liftoff through spacecraft separation from the Agena and subsequent acquisition of the spacecraft by the Deep Space Network.

2.4.1 Launch Vehicle Performance

Analysis of vehicle performance, trajectory, and guidance data indicated that all launch vehicle objectives were satisfactorily accomplished. Atlas objectives were to:

- Place the upper stage in the proper coast ellipse as defined by the trajectory and guidance equations;
- Initiate upper-stage separation;
- Start the Agena primary timer;
- Relay the jettison spacecraft shroud command;
- Start the secondary timer commands of the launch vehicle.

Agena objectives were to:

- Inject the spacecraft into a lunar-coincident transfer trajectory within prescribed orbit dispersions;

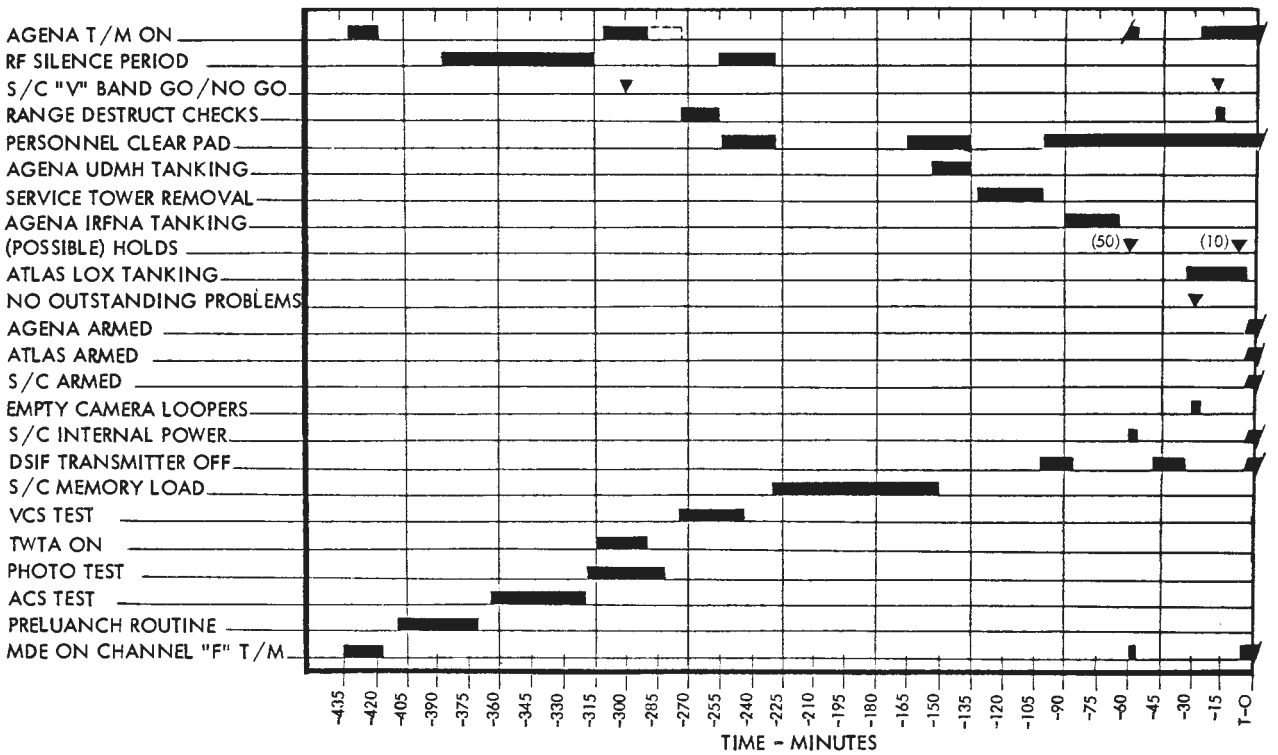

Figure 2-2: Master Countdown Time Sequence

- Perform Agena attitude and retro maneuvers after separation to ensure non-interference with spacecraft performance.

All of these objectives were accomplished.

Table 2-3 provides a summary of planned and actual significant events during the ascent trajectory. All times are referenced to the liftoff time of 01:17:01.120 GMT on February 5, 1967.

2.4.1.1 Atlas Performance

Atlas SLV-3 (Serial Number 5803) operational performance was satisfactory throughout the flight. All engine, propulsion, and prepellant utilization functions were within tolerances. Peak accelerations of 6.0 and 3.2 g were indicated at booster and sustainer engine cutoffs, respectively. Calculations based on performance parameters indicated that approximately 1,376 pounds of liquid oxygen and 764 pounds of fuel remained at SECO. This was equivalent to 7.5 seconds of additional engine burn time.

Vehicle stablitiy was maintained throughout all phases of powered flight by the Atlas flight control system. Staging and separation operations were satisfactory. Satisfactory response was observed to the programmed maneuvers and programmed switch functions. Vehicle angular displacements and rates at vernier engine cutoff were negligible. The flight control system responded correctly to all guidance discretes, and relayed all appropriate information to the upper-stage vehicle.

Evaluation of ground-recorded and telemetry data indicated that both the Mod III-A ground station and the Mod III-G airborne-guidance equipment performed satisfactorily. The system properly acquired the vehicle as planned and maintained solid lock in both the track and rate subsystems until launch plus 375.7 seconds (well beyond Atlas-Agena separation).

The following coast ellipse and insertion parameters at VECO + 2 seconds were obtained from guidance system data.

- Semimajor axis — 14,512,049 feet
- Semiminor axis — 12,708,077 feet
- Velocity magnitude — 18,534 feet per second
- Velocity to be gained — +0.49 foot per second
- Filtered yaw velocity — +2.77 feet per second
- Filtered altitude rate minus desired altitude rate — −1.73 feet per second

Table 2-3: ASCENT TRAJECTORY EVENT TIMES

Event	Programmed Time (+Sec)	Measured Time (TIM) (+Sec)
Liftoff 2-in. Motion	0	01:17:01.120 GMT
Booster Engine Cutoff	129.5	129.7
Sustainer Engine Cutoff	289.2	288.0
Start Primary Sequence Timer	292.4	297.4
VECO - Uncage Gyros, Jettison H/S Fairings	309.4	309.2
Nose Shroud Ejection	311.5	311.4
SLV-3/Agena Separation	313.5	314.4
Separation Backup (Sequence Timer)	338.4	343.5
Initiate - 120 deg/min Pitch Rate	345.4	350.3
Transfer to −3.21 deg/min Pitch Rate; Pitch H/S to IRP	350.4	355.5
Arm Engine Control	365.4	370.4
First Burn Ignition (90% Pc)	366.6	371.7
First Burn Cutoff (V/M Cutoff Switch)	521.2	527.5
Transfer to −4.20 deg/min Pitch Rate	542.4	547.6
Horizon Sensors to 0.12-degree Bias Position	545.4	550.8
Second Burn Ignition (90% Pc)		1105.68
Second Burn Cutoff		1194.38
Agena - Spacecraft Separation		1358.55

2.4.1.2 Agena Performance

Operational performance of the Agena D (Serial Number 6632) was satisfactory during the flight.

The primary sequence timer was started, by a discrete command from the Atlas guidance system to ensure proper Agena-spacecraft separation, 5.2 seconds later than the preflight predictions; therefore, the Agena functions initiated by the timer were all shifted in time by this amount. Performance data showed the average combustion chamber pressure during the first burn period was

503.3 psig, which produced a calculated thrust of 15,960 pounds. Based on a computed total flow rate of 53.73 pounds per second, the specific impulse was calculated to be 291.9 pound-seconds per pound. The first burn period of 155.8 seconds was 1.1 seconds longer than predicted. The second burn period of 88.8 seconds was 0.2 second longer than predicted. Performance data during the second burn period indicated an average combustion chamber pressure of 501.3 psi with a calculated thrust of 15,897 pounds. The specific impulse was computed as 295.8 pound-second per pound based on a computed total propellant flow rate of 53.73 pounds.

Velocity meter performance was satisfactory, although the accelerometer pulse rate under zero gravity in the later phases of flight indicated a larger-than-allowable null torque value. As expected, small disturbances were observed when thrust terminations changed and at vehicle separations. Flight control action quickly reduced all disturbances subsequent to Atlas-Agena separation.

Agena computer performance was satisfactory in controlling the vehicle attitude during the Earth orbit period and controlling the cislunar trajectory injection maneuver.

2.4.1.3 Spacecraft Performance

Spacecraft performance during the period from liftoff to acquisition by the Deep Space Network was satisfactory. Performance telemetry data showed that the spacecraft antennas were successfully deployed 1 minute, 50 seconds after spacecraft separation. The solar panels were deployed and functioning properly 26 seconds later.

2.5 DATA ACQUISITION

Earth track of the Lunar Orbiter III mission is shown in Figure 2-3. Significant events and planned coverage of the AFETR facilities are shown on this trajectory plot.

The AFETR preliminary test report showed the data coverage presented in the following tables. A list of electronic tracking coverage from all stations is contained in Table 2-4, together with the type of tracking operation employed for each period. Telemetry data recording is summarized in Table 2-5 by recording station and telemetry frequency.

Lunar Orbiter telemetry data were recorded via Channel F of the Agena link and also via the spacecraft telemetry system. Prior to spacecraft separation, the spacecraft transmissions (2298.3 MHz) were made with the antenna in the stowed position.

Weather conditions during the launch operation were favorable. The upper wind shears were within acceptable limits. At liftoff the following surface conditions were recorded.

- Temperature 54.3°F
- Relative humidity 94%
- Visibility 10 miles
- Dew Point 53°F
- Surface winds calm
- Clouds clear
- Pressure 29.970 inches of mercury

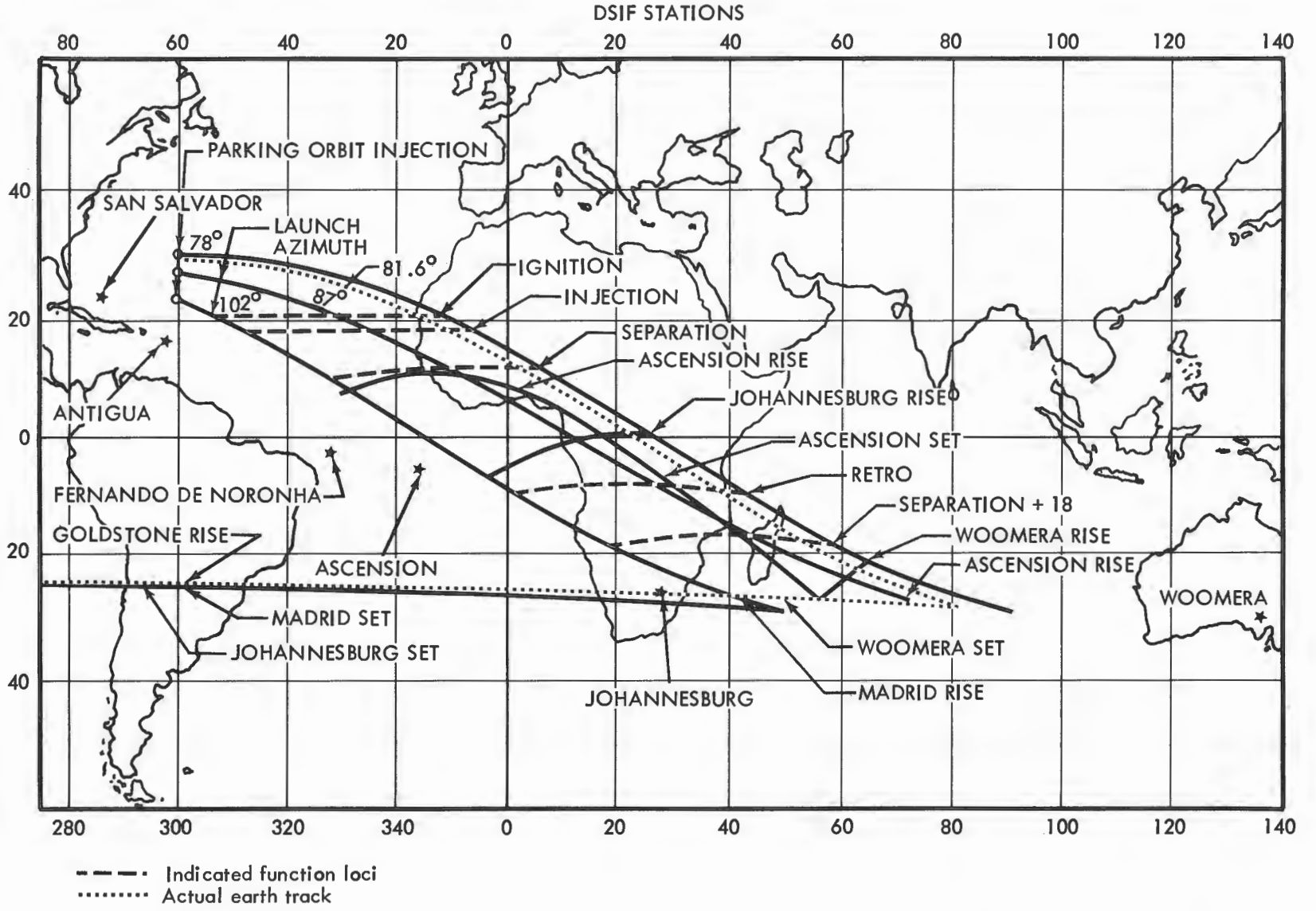

Figure 2-3: Earth Track for February 5, 1967

Table 2-4: AFETR Electronic Tracking Coverage

Location	Radar No.	Period of Coverage (sec)		Mode of* Operation
		From	To	
Radar:				
Station 0	0.18	12	472	AB
Patrick				
Station 1	1.1	0	2	TV
Cape Kennedy		2	28	IR
		28	119	AS
	1.2	0	3	TV
		3	121	IR
		121	126	AS
	1.16	8	62	AS
		76	265	AS
Station 19	19.18	14	82	AS
Kennedy Space Center		82	262	AB
		262	365	AS
		365	477	AB
Station 3	3.16	68	250	AB
Grand Bahama	3.18	92	451	AB
Station 7	7.18	208	574	AB
Grand Turk				
Station 91	91.18	476	706	AB
Antigua				
Station 12	12.16	-	-	(No track
Ascension	12.18	-	-	below horizon)
RIS Uniform	T-11-C	1310	2073	AB
Special Instrumentation:				
Station 1	Tel ELSSE	12	110	F
		4	457	
		13	110	
		4	443	

* Modes of Operation:
AB = Automatic Beacon Track
AS = Automatic Skin Track
F = Flight Line
IR = Infrared Track
TV = Television

Table 2-5 : AFETR Telemetry Coverage

	Location	Link (mc)	Period of Coverage (sec)	
			From	To
	Station 1 Tel II	Agena 244.3	-420	479
	Cape Kennedy	Atlas 249.9	-420	479
		Lunar 2298.3 Orbiter	-420	149
	Station 1 Tel IV	244.3	-420	479
	Cape Kennedy	249.9	-420	479
		2298.3	-420	163
	Station 3	244.3	40	501
	Grand Bahama	249.9	40	501
		2298.3	100	501
	Station 4	249.9	80	560
	Eleuthera			
	Station 91	244.3	380	633
	Antigua	2298.3	377	710
	Station 12	244.3	(No Signal	
	Ascension	2298.3	below horizon)	
	Station 13	244.3	1604	5519
	Pretoria, Africa	2298.3	1594	1779
Mobile Range - Instrumentation Facilities	RIS Lima	244.3	610	920
	RIS Whiskey	244.3	920	1133
		2298.33	922	1140
	Audit 1 No. 490	244.3	890	1490
	Audit 2 No. 627	244.3	839	1053
	RIS Yankee	244.3	1613	4179
		2298.33	1609	5585
	RIS Uniform	244.3	1234	2540
		2298.33	1234	1461
		2298.33	1634	1688
		2298.33	1719	1740

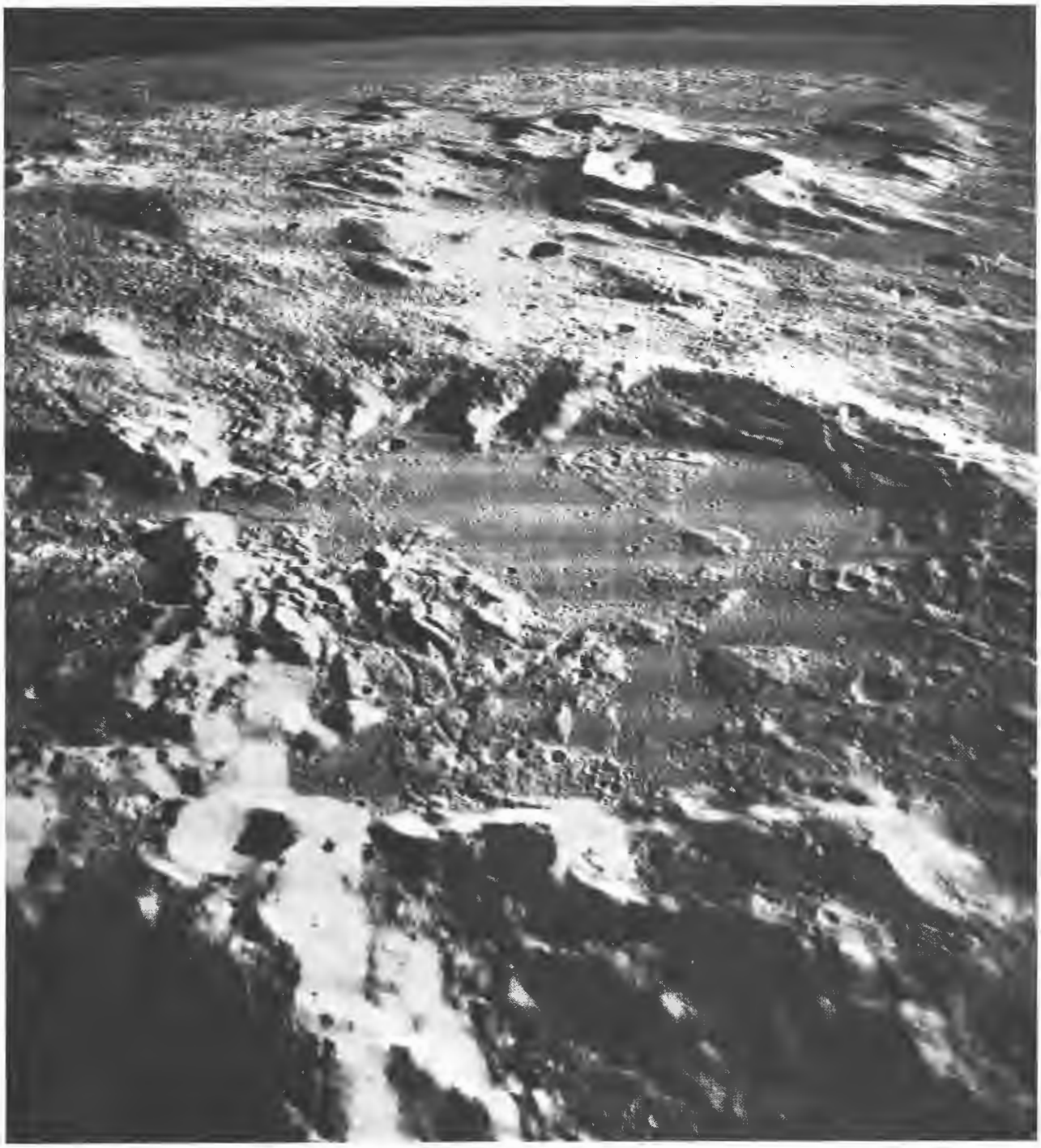

Wide-Angle Frame 85—Site III S-13
(Oblique to north toward craters Murchison and Pallas)

3.0 MISSION OPERATIONS

Operation and control of Lunar Orbiter III required the integrated services of a large number of specialists stationed at the Space Flight Operations Facility (SFOF) in Pasadena, California, as well as at the worldwide Deep Space Stations. The Langley Research Center exercised management control of the mission through the mission director. Two primary deputies were employed: the launch operations director located at Cape Kennedy and the space flight operations director located at the SFOF in Pasadena.

Launch vehicle and spacecraft performance data and tracking information were recorded by AFETR during the launch and boost phases. At the launch mission control center at Cape Kennedy, the primary concern was the monitoring of launch vehicle performance and the ascent trajectory obtained. Spacecraft performance telemetry data was also retransmitted, in real time through the Cape Kennedy Deep Space Station, to the SFOF where it was closely monitored and evaluated by the flight operations specialists. This dissemination of data to both the launch and space flight operations centers enabled the efficient and orderly transfer of control from Cape Kennedy to the SFOF.

Flight control of the mission was centralized at the SFOF for the remainder of the mission. All commands to the spacecraft were coordinated by the spacecraft performance analysis and command (SPAC) and flight path analysis and command (FPAC) team of subsystem specialists and submitted to the space flight operations director for approval prior to being transmitted to the DSIF site for retransmission to the spacecraft.

Operational performance of the spacecraft and the worldwide command, control, and data recovery systems are presented in the following sections.

3.1 MISSION PROFILE

The Lunar Orbiter space vehicle (consisting of Atlas SLV, Serial Number 5803; Agena D, Serial Number 6632; and Lunar Orbiter C) was successfully launched at 01:17:01.120 GMT on February 5, 1967 from Launch Complex 13 at AFETR. Liftoff occurred at the opening of the window for February 5. The flight azimuth of 81.6 degrees required by Launch Plan 5C was satisfied.

Figure 3-1 provides a pictorial summary of the 25-day photographic mission of Lunar Orbiter III. The timing of events during the countdown and through the "start Canopus acquisition" function are referenced to the liftoff time. The remainder of the mission is referenced to Greenwich Mean Time. Photography of each of the primary sites is indicated by site and orbit number and GMT. The corresponding information for the 32 secondary sites is not shown on the chart. With the exception of minor changes in site location for primary and secondary sites and the cancellation of the last secondary site, the photographic mission was conducted as planned.

Two types of photo readout periods are shown in the shaded areas. The "priority readout" was limited to one spacecraft frame or less by photo subsystem internal limitations and the available view periods when the Sun was visible to the spacecraft. This period was terminated upon completion of photography when the "Bimat cut" command was transmitted and executed. During the "final readout" period the readout time per orbit was limited only by the available view periods when the spacecraft was in the sunlight and by operating temperatures within the photo subsystem.

Also shown in Figure 3-1 are the major events during the powered portion of flight necessary to inject the spacecraft on the cislunar trajectory. The major spacecraft functions required to make it fully operational and attain the desired lunar orbits are also shown.

The Lunar Orbiter III spacecraft was acquired by the Deep Space Network 50 minutes after launch by the Woomera, Australia, station. Initial performance data verified that the spacecraft antenna and solar panel

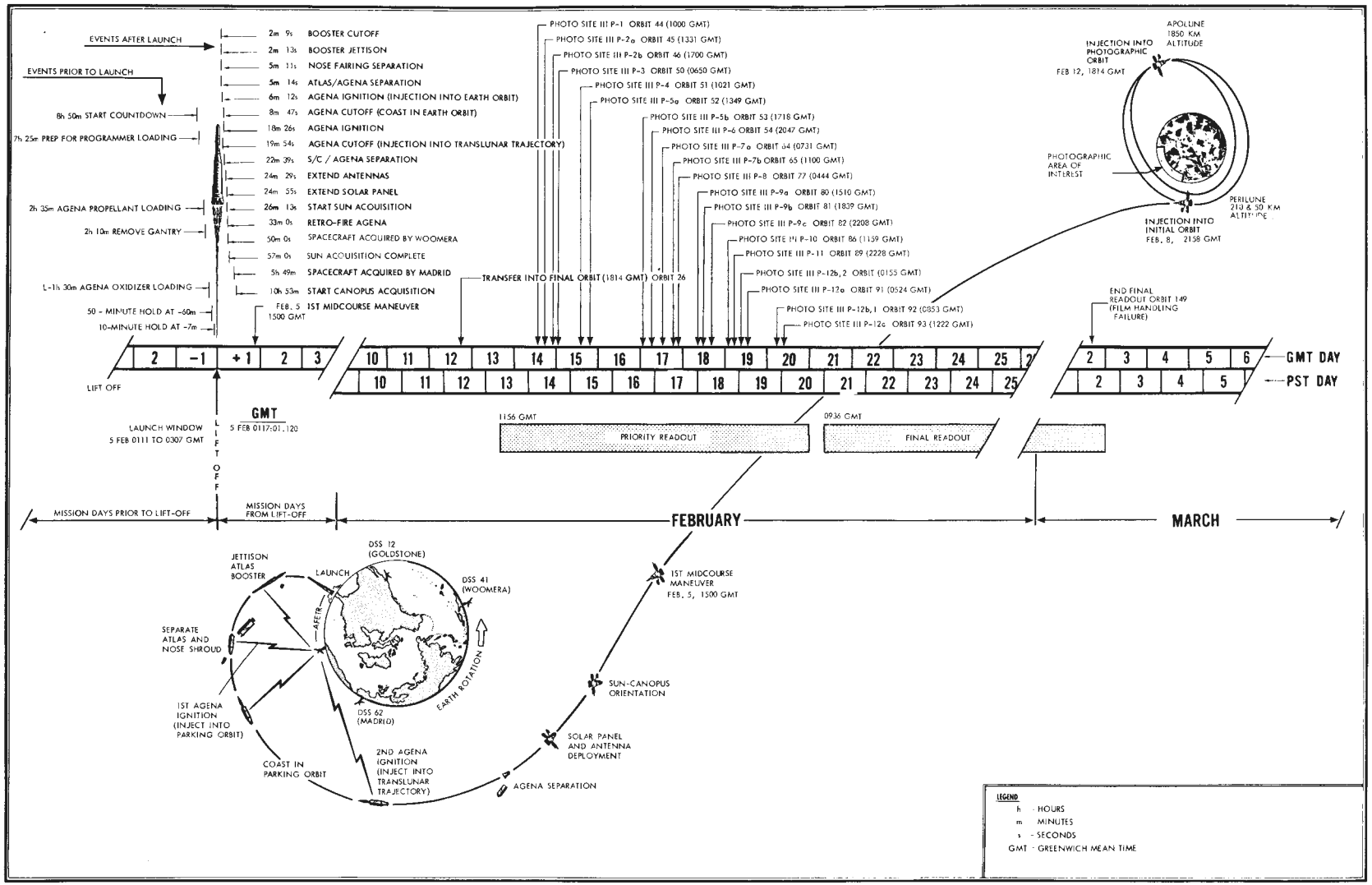

Figure 3-1: Lunar Orbiter III Flight Profile

deployment sequences and Sun acquisition had been accomplished. A star map roll maneuver was initiated 10 hours and 53 minutes after launch as part of the Canopus acquisition sequence. At 37 hours and 43 minutes after launch, a velocity change of 5.09 meters per second and midcourse guidance correction maneuver were initiated.

Injection into the initial lunar orbit, initiated at 92 hours and 37 minutes, produced a 13-degree plane change and a velocity reduction of 704.3 meters per second during the 542.5 seconds of engine operation. The initial orbit parameters were: apolune, 1802 km; perilune, 200 km; and orbit inclination, 20.94 degrees. Spacecraft tracking data was obtained during the next 4 days to determine the orbit parameters for a 21-degree inclination and define the transfer maneuver required to conduct the photographic mission.

Transfer to the final orbit was performed during Orbit 26 by reducing the spacecraft velocity by 50.7 meters per second by a 33.7-second engine-burn period. During Orbits 39 and 42, the Goldstone test film in the spacecraft was read out and recorded at two stations to verify photo subsystem operation. A 16-frame exposure sequence was taken of Primary Site IIIP-1 on Orbit 44. After a 4-minute delay, a series of four additional exposures was made of Secondary Site IIIS-1 without any additional spacecraft maneuver. The first of a series of 54 priority readout sequences was initiated during the next orbit and recorded at the Madrid, Spain, DSS. (Early evaluation of these photos verified proper operation of the photo subsystem and that the wide-angle-lens filter equalized the exposure by the two lenses).

During 54 successive orbits, a total of 211 dual-frame (wide-angle and telephoto) exposures were taken of the 12 primary and 31 secondary sites. Mission photography was conducted as planned except for minor shifts in some photo site locations, the addition of a fourth photo pass over the Surveyor I landing site, and the real-time cancellation of the last (IIIS-32) secondary site. As the mission progressed, the primary sites were photographed with near-vertical and off-vertical camera axes, and converging telephoto stereo to obtain the desired site coverage. Secondary-site photography subjects included selected primary sites and areas of scientific interest, which were photographed as near-vertical, tilted, and high-oblique views. The actual landing site and the shadow of Surveyor I were identified in Telephoto Frame 194. Spacecraft Frame 214 was an oblique photo of the general area of the Luna 9 landing site. The "Bimat cut" command was executed during Orbit 98, thus ending the photo taking portion of the mission.

The final readout phase was initiated by Readout Sequence 57 during Orbit 99. This readout progressed normally through Orbit 148 with an average readout of 2.7 frames (about 32 inches) per orbit. During this period, all spacecraft frames from 215 to 83 were read out, transmitted, and recorded. During initiation of the readout sequence during Orbit 149 on March 2, a transient or momentary power outage reset the photo subsystem control logic to an abnormal state which was not immediately recognized and eventually resulted in electrical failure of the film-advance motor. Repeated attempts to move the film from the readout looper to the supply reel were not successful. Approximately four additional frames, however, were read out (the capacity of the readout looper) during the next few orbits before the photo mission was terminated. The final readout completed Primary Sites IIIP-7 through IIIP-12 and Secondary Sites IIIS-10 through IIIS-31, as well as portions of Secondary Sites IIIS-8 and -9. Priority readout provided additional photos of segments of each of the additional primary photo sites.

There were no recorded micrometeoroid impacts recorded during this 26-day photo mission. The total radiation dosage detected was 2.5 rads near the film cassette and 3.0 rads in the vicinity of the camera looper. These levels had no fogging effect on the spacecraft film. The spacecraft was commanded to pitch off the sunline for approximately one half of the mission to maintain spacecraft temperatures within design operating limits.

3.2 SPACECRAFT PERFORMANCE

The performance of Lunar Orbiter III is best evaluated with respect to program and specific mission objectives. Accordingly, the performance of each of the subsystems as it relates to these objectives is discussed in the following paragraphs, which also include a brief functional description.

To place the photo subsystem in the proper location and attitude at the right time to obtain the desired photographs, the Lunar Orbiter must:

- Be injected into a selected orbit about the Moon whose size, shape, and center of gravity and mass are not precisely known.
- Perform a critical attitude maneuver and a precise velocity reduction to transfer into a specified lower photographic orbit.
- Continue to operate in an unknown radiation environment and in an unknown density of micrometeoroids over an extended time.
- Accomplish a precise attitude maneuver prior to photographing each specified site and actuate the cameras at precisely the commanded time.
- Provide the tracking and doppler signals required to determine the orbit parameters and compute the photographic mission maneuvers.

Failure to satisfy any of these conditions could jeopardize successful accomplishment of the Lunar Orbiter mission. How well Lunar Orbiter III accomplished these critical tasks is shown in Table 3-1, which is indicative of the control accuracy accomplished by the attitude and velocity control subsystems.

During the 92-hour cislunar trajectory and the 149 lunar orbits, the spacecraft satisfactorily accomplished the many sequences of events and multiaxis maneuvers required to establish the desired lunar orbits, photograph the specified areas, and transmit the photo video, tracking, and performance data to the Deep Space Stations. Each of the 12 primary and 31 secondary sites was photographed essentially as planned. Although there was some film-advance sticking, which caused repeated readout of single framelets in priority readout, only a few framelets of two wide-angle photos were lost because most of the photos involved were read out during final readout. (Operational control proce-

Table 3-1: TRAJECTORY CHANGE SUMMARY

FUNCTION	DESIRED TRAJECTORY	VELOCITY CHANGE (Meters Per Second)		ACTUAL TRAJECTORY
		Desired	Actual	
Cislunar Midcourse	Aim Point 6123 km	5.11	5.09	Aim Point 6143 km
Lunar Orbit Injection	Perilune 213 km Apolune 1850km Inclination 21.05	704.3	704.3	Perilune 210 km Apolune 1802 km Inclination 20.94
Orbit Transfer	Perilune 54.8 Apolune 1846 Inclination 20.87	50.7	50.7	Perilune 54.8 Apolune 1847 Inclination 20.91

dures were developed during the mission to reinitiate film advance when the film stoppage was detected.) The photo mission was terminated prematurely when the film-advance motor failed as a result of an improper camera control logic sequence attributed to a power transient or momentary power failure within the photo subsystem. At the time of mission termination, 74 telephoto and 73 wide-angle photographs remained to be read out in final readout. Priority readout provided reconstructed photos of both telephoto and wide-angle photos of many of the frames missed in final readout.

3.2.1 Photo Subsystem Performance

Photo subsystem performance was generally satisfactory during the active photo taking portion of the mission. Intermittent film-advance problems were encountered during priority and final readout periods. A failure of the film-advance motor, attributed to an improper film advance logic during Orbit 149 prevented further movement of the film.

The Lunar Orbiter photo subsystem simultaneously exposes two pictures at a time, processes film, and converts the information contained on the film to an electrical signal for transmission to Earth.The complete system, shown schematically in Figure 3-2, is contained in a pressurized temperature-controlled container.

The camera system features a dual-lens (telephoto and wide-angle) optical system that simultaneously produces two images on the 70-mm SO-243 film. Both lenses operate at a fixed aperture of f/5.6 with controllable shutter speeds of 0.04, 0.02, and 0.01 second.

A double-curtained focal-plane shutter is used with the telephoto lens and a between-the-lens shutter is used with the wide-angle lens. Volume limitations within the photo system container necessitated the use of a mirror in the optical path of the 610-mm lens. This mirror causes reversal of all telephoto images on the spacecraft film (from left to right across the flight path) with respect to the wide-angle system.

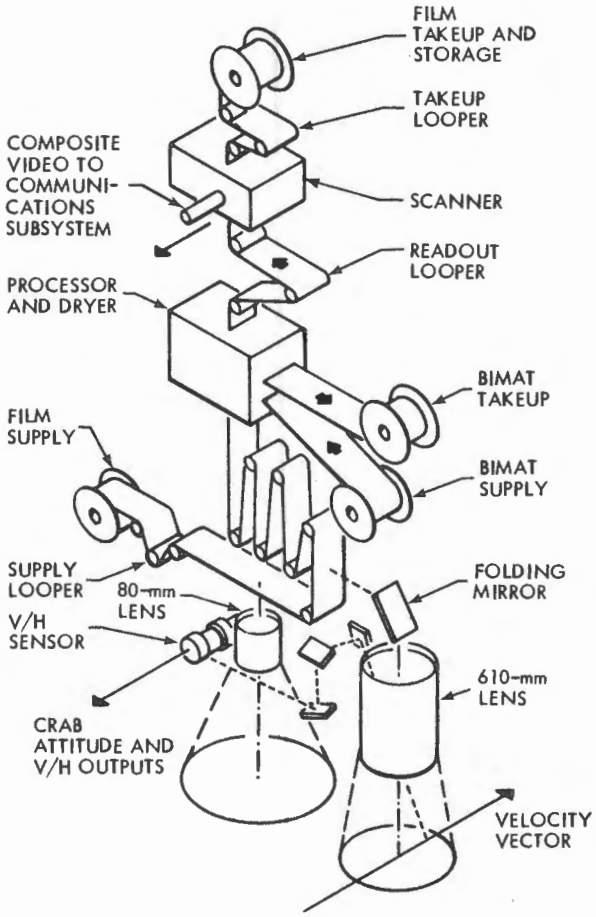

Figure 3-2: Photo Subsystem

An auxiliary optical system, which operates through the telephoto lens, samples the lunar-terrain image and determines a velocity-to-height (V/H) ratio. This output controls the linear movement of each camera platen to compensate for image motion at the film plane (IMC). The V/H ratio also controls the spacing of shutter operations to provide the commanded overlap. Camera exposure time for each frame is exposed on the film in binary code by 20 timing lights.

The latent-image (exposed) film is developed, fixed, and dried by the processor-dryer. processing is accomplished by temporarily laminating the emulsion side of the Bimat film against the SO-243 film emulsion as it travels around the processor drum.

Photographic data are converted by the readout system into an electrical form that can be transmitted to the ground receiving station. Scanning the film with a 6.5-micron-diameter high-intensity beam of light produces variations in transmitted light intensity proportional to the changes in film density. A photomultiplier tube converts these variations to an analog electrical voltage, and the readout system electronics adds timing and synchronization pulses, forming the composite video signal shown in Figure 3-3. Thus, it is possible to transmit continuous variations in film tone or density rather than the discrete steps associated with a digital system. The electrical signals are fed to a video amplifier and passed to the modulation selector; transmission is via a traveling-wave-tube amplifier (TWTA) and high-gain antenna.

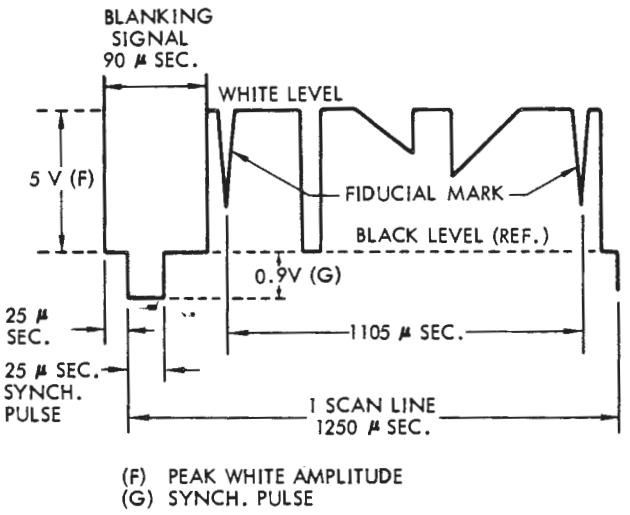

Figure 3-3: Video Signal Waveform

As a result of the previous mission photographic results, the need to more nearly equalize the light transmission characteristics of the two lens systems was identified. To accomplish this change, a 0.21 neutral-density filter was installed in front of the wide-angle (80-mm) lens. Evaluation of the telephoto and wide-angle photos indicated that the filter produced the desired equalization of exposure in the two lenses. The observed density differences were less than 0.1.

Operation of the photo subsystem during the photo exposure and processing periods was satisfactory, although blemishes noted on previous missions were present. Primary-site photo sequences were taken in slow mode (50% forward overlap of wide-angle pictures), fast mode (87% forward overlap of wide-angle photos), from a vertical attitude, and up to 10-degree cross-axis tilt. Secondary-site photos were taken in single frame as well as fast-and slow-mode sequences from a vertical attitude and large off-vertical angles. The photos confirmed proper operation of the photo subsystem during these operations. There were 55 processing periods during the mission. A stop line and Bimat pull-off line on the spacecraft film, and local degradation in film processing, were associated with each period.

Intermittent film stoppages in the readout looper were experienced during the last half of the priority readout phase, resulting in repeated readout of a single framelet. Commanding the optical-mechanical scanner to the focus-stop position for 10 minutes and then reinitiating "readout drive on" generally removed the hangup and the readout continued. A small fraction of two wide-angle photos was lost by the stoppage because those areas on the spacecraft film were not reached prior to the failure in final readout. During final readout, similar stoppages occurred after readout storage looper contents reached approximately 19 inches. An alternate procedure, employed to compensate for the abnormality, was to temporarily stop readout while the looper was emptied and then reinitiate readout. An average of 2.6 frames (nearly 32 inches) was read out during each orbit.

Postmission analysis of data indicates that the repeated readout of a single framelet was indicative of a loss of proper film tension within the readout looper. Evaluation of possible causes led to the conclusion--based partially upon observations and results from assembly and tests--that the problem could have been caused by an over-long readout looper mounting screw. An over-long screw could, depending on assembly tolerance

buildup, depress the teflon separators of the readout looper against the looper rollers, thereby interferring with the free movement of film and causing loss of tension in the readout looper. The loss of tension results in the failure to advance film through the optical-mechanical scanner into the readout looper.

Telemetry data indicates that the turn-on sequence for Readout Sequence 110 on Orbit 149 was interrupted between the first and second telemetry frame (23-second interval between frames) after initiation of the "readout electronics on" command. Data contained in the second telemetry frame indicated several abnormal operations within the photo subsystem. When the time to complete the "readout electronics on" sequence had elapsed, there was no video data transmitted. The "readout electronics on" sequence was then reinitiated and all photo subsystem telemetered data associated with the readout operation appeared normal. After optimizing the video signal by line-scan-tube gain and focus adjustments, the readout proceeded normally for about 68 minutes. When an attempt was made to empty the readout looper, at the end of the readout period, there was no indication of film movement. Repeated attempts failed to move any film from the readout looper to the supply reel. This failure occurred when reading out Telephoto Frame 79.

Subsequent evaluation of the performance telemetry data, supported by additional test sequences, indicated that the film-advance motor had failed during the 68-minute readout period. The time of failure was indicated by a 1.2-ampere drop in the power subsystem load current data about 29 minutes after reinitiation of Readout Sequence 110. The significance of the abnormal operational data during the interruption of the first "readout electronics on" command was not fully evaluated in real time. This evaluation was influenced by the fact that, upon reinitiation of the command for the turn-on sequences, telemetry performance data and video data received appeared normal. Real-time evaluation of performance data indicated that the additional current could be attributed to camera heaters operating. There was no data to indicate that the additional load current observed was in any way associated with abnormal operation of the photo subsystem until automatic emptying of the readout looper, at the end of the readout period, failed to occur.

Postmission data analysis and tests indicated that the failure was the result of an improper film handling logic in which the film-advance motor was commanded to wind forward while the film supply motor brake was also applied. The film-advance motor attempted to advance film during Readout Sequence 110 as evidenced by the increased load current. This overload condition caused the motor to overheat and eventually fail.

The performance data, sampled at 23-second intervals, did not show the exact cause of the improper sequence of events. Analysis of the photo subsystem data verified that a change in the control logic occurred shortly after initiation of the readout sequence. The most logical assumption, relative to the cause, was a momentary power dropout or a transient in the photo subsystem from an unknown source or cause, even though the telemetered power data does not provide any confirmation.

3.2.2 Power Subsystem Performance

Power subsystem performance throughout Mission III was satisfactory in all respects. The only operational constraint imposed during the mission was that the solar array illumination be sufficient to meet the electrical loads imposed on the power subsystem.

All electrical power required and used by the spacecraft is generated by the solar cells mounted on the four solar panels. Solar energy is converted into electrical energy to supply spacecraft loads, power subsystem losses, and charge the hermetically sealed nickel-cadmium battery. The subsystem is shown schematically in Figure 3-4. Excess electrical energy is dissipated through heat dissipation elements. The shunt regulator

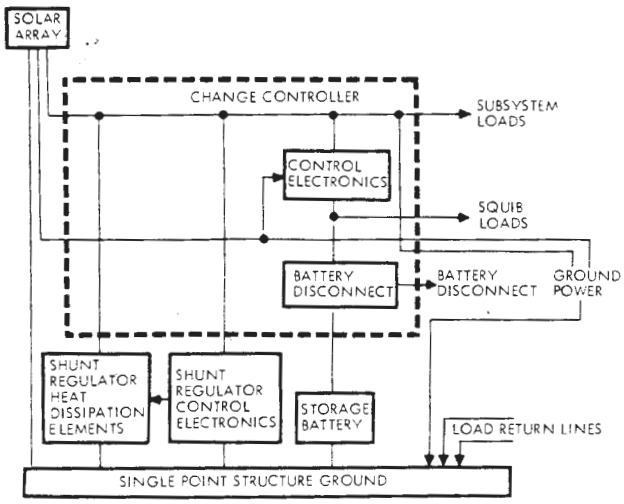

Figure 3-4: Power Subsystem Block Diagram

also limits the output of the solar array to a maximum of 31 volts. Auxiliary regulators provide closely regulated 20-volt d.c. outputs for the temperature sensors and the telemetry converter. Charge controller electronics protect the battery from overvoltage and overtemperature conditions by regulating the charging current. The 12-ampere-hour battery (packaged in two 10-cell modules) provides electrical power at all times when there is insufficient output from the solar array.

Each of the four solar panels has 2,714 individual solar cells mounted in a 12.25-square-foot area. The N-on-P silicon solar cells on each solar panel are connected into five diode-isolated circuits. Individual circuits are connected in series-parallel combinations.

The spacecraft battery provided all electrical demands from 6 minutes prior to launch until Sun acquisition approximately 26.3 minutes after launch. Solar panel deployment and Sun acquisition occurred during a period when performance telemetry was not recorded; it was estimated, however, that the battery was discharged approximately 3.1 ampere-hours for a 23.8% depth of discharge. At 66 minutes after launch, when spacecraft telemetry data was acquired, the solar array was deployed and supplying 13.33 amps at 30.56 volts. The array temperature at this time was approximately 100°F.

Beginning about 16 hours after launch, the spacecraft was pitched 36 degrees off the sunline, for spacecraft temperature control, and the array output was reduced to 10.7 amperes. Both the midcourse correction and lunar orbit injection maneuvers were performed on battery power. The maximum load current during the orbit injection engine-burn period was 7.93 amps. The orbit transfer maneuver required a 19.9-degree pitch off the sunline and the array output of 12.49 amps more than satisfied spacecraft load requirements.

Performance of the power subsystem during the photo orbit period is typified by the parameters shown in Figure 3-5. The dotted portions of the curves were extrapolated to cover the Earth occultation phase based on data obtained in other orbits for the corresponding times after sunrise.

As the mission progressed, the relative position of the Earth occultation on this type of plot slowly moved in time until, by Orbit 104, Earth occultation completely overlapped the Sun occultation period for the remainder of the photo mission. Representative power subsystem loads for various spacecraft operating modes are shown in Table 3-2.

Evaluation of the solar array output data showed a nearly linear rate of degradation during the first 100 lunar orbits. Thereafter, the rate was nearly constant at about 2%. The apparent slow decrease in output after 100 orbits was found to be approximately equal to the rate of change of the solar intensity or solar constant as the mission progressed.

Bus voltage was limited to 30.56 volts whenever the array output exceeded spacecraft load demands. During the mission a maximum of 250 watts was dissipated through the load resistors.

3.2.3 Communications Subsystem Performance

Communications subsystem performance was satisfactory through all phases of the mission. All photo video, performance telem-

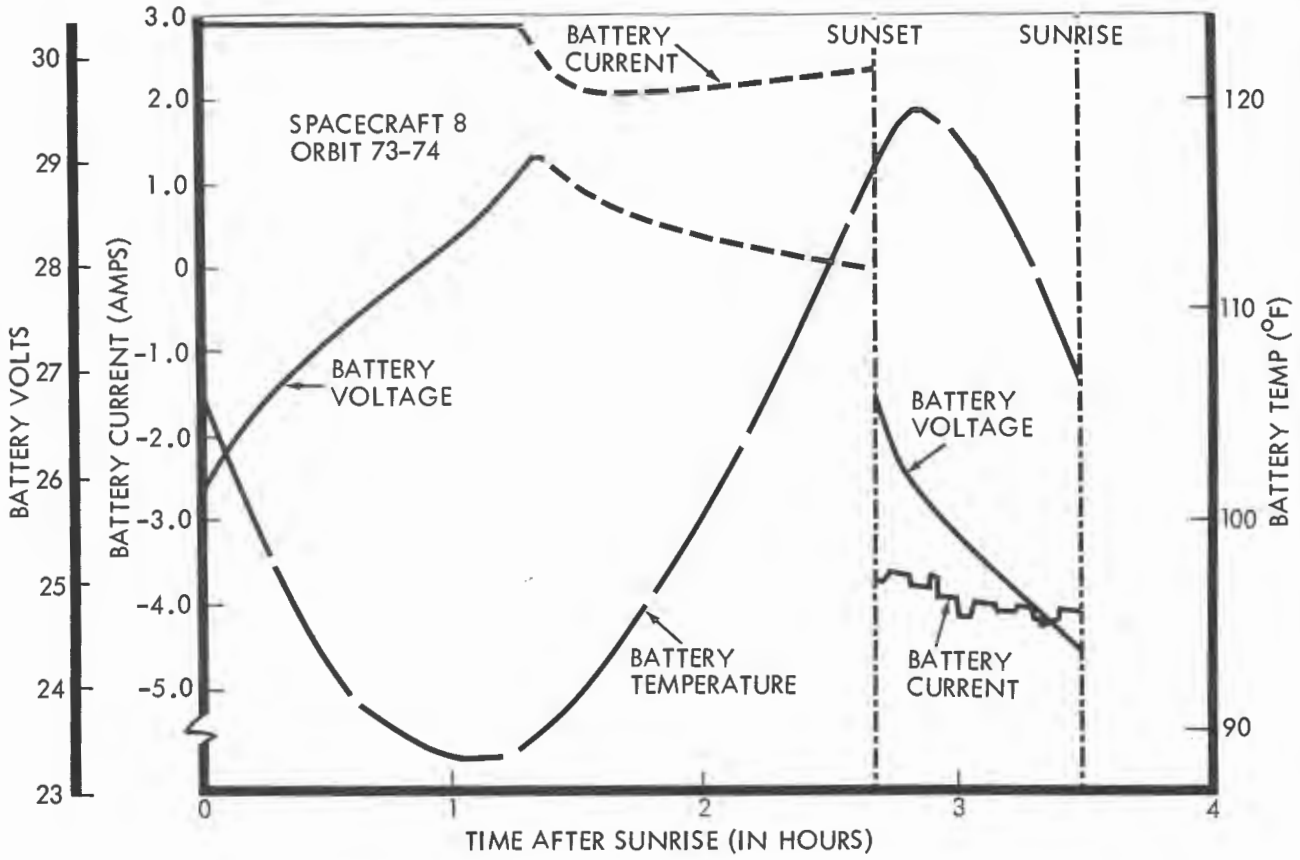

Figure 3-5: Battery Characteristics

Table 3-2: SPACECRAFT LOAD CURRENTS

Operational Mode	Photo Heaters			Spacecraft Load		
	Day	Night	Inhibited	Min.	Nom.	Max.
DAYTIME						
Cruise			X	3.49	3.62	3.75
Photo Standby	X			3.37	3.49	3.81
Camera On			X	3.49	3.49	3.93
TWTA On	X			5.11	5.17	5.78
R/O Electronics On			X	6.20	6.32	6.56
R/O Drive On			X	6.26	6.56	6.68
Processing	X			4.18	5.84	6.26
NIGHTTIME						
Photo Standby		X		4.06	4.12	4.18
Canopus Tracker On		X		4.25	4.31	4.37

etry, and tracking information presented to the communications subsystem was transmitted to the ground-based receiving stations with adequate signal strength.

The Lunar Orbiter communications system is an S-band system capable of transmitting telemetry and video data, doppler and ranging information, and receiving and decoding command messages and interrogations. Major components of the communication subsystem, shown in Figure 3-6, are the transponder, command decoder, multiplexer encoder, modulation selector, telemetry sensors, traveling-wave-tube amplifier, and two antennas.

The transponder consists of an automatic phase tracking receiver with a nominal receiving frequency of 2116.38 MHz, narrow-and wide-band phase detectors, a phase modulator, and a 0.5-watt transmitter with a nominal frequency of 2298.33 MHz. In the two-way phase-lock mode the transmitted frequency is coherently locked to the received frequency in the ratio of 240 to 221.

The command decoder is the command data interface between the transponder receiver and the flight programmer. To verify that the digital commands have been properly decoded, the decoded command is temporarily stored in a shift register, and retransmitted to the DSIF by the telemetry system. After validating the proper decoding of the command, appropriate signals are transmitted to the spacecraft to shift the stored com-

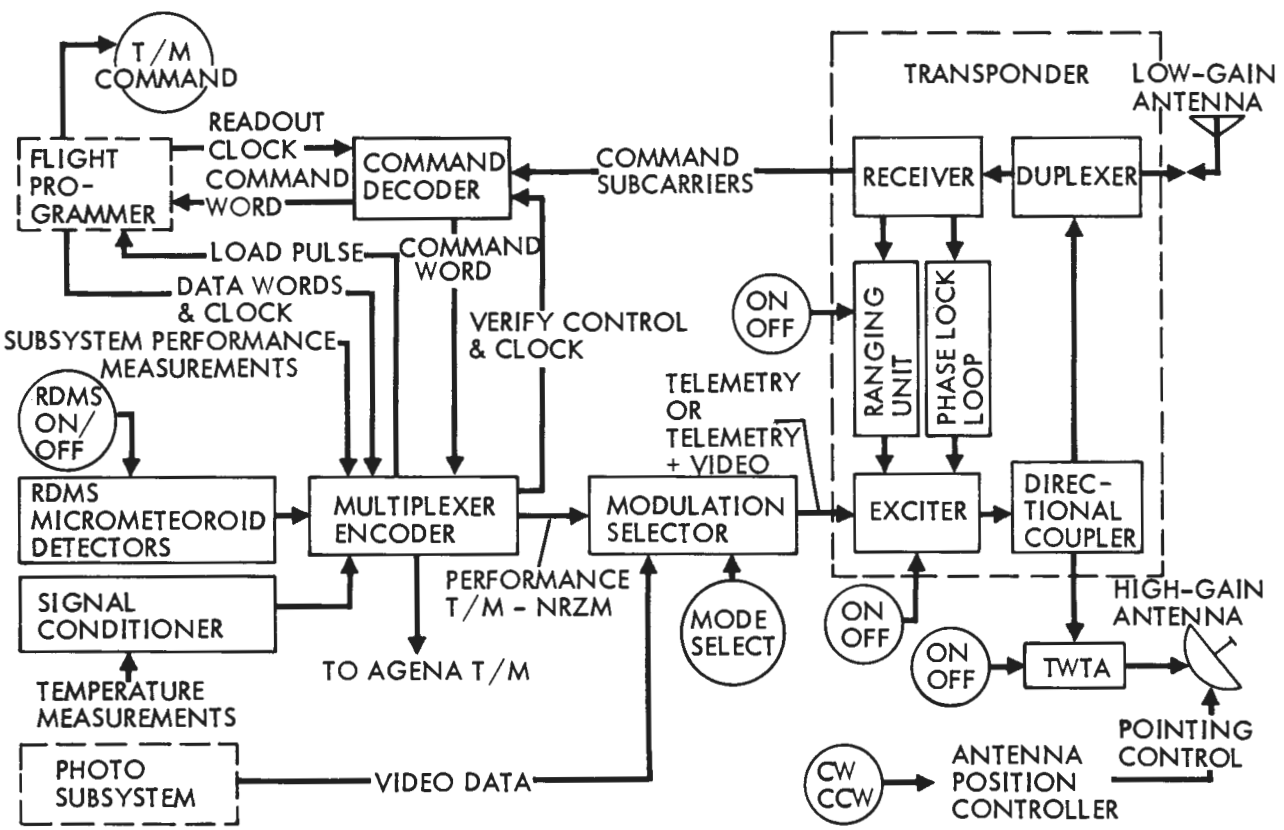

Figure 3-6: Communications Subsystem Block Diagram

mand into the flight programmer for execution at the proper time. The command decoder also contains the unique binary address of the spacecraft.

The PCM multiplexer encoder is the central device that puts performance telemetry data into the desired format for transmission. Seventy-seven inputs are sequentially sampled at one sample per frame, and one channel is sampled at eight times per frame in the analog section. The output of these 85 data samples is converted from analog to digital form. The multiplexer also combines the 20-bit flight programmer words, the 133 one-bit discretes, and the four-bit spacecraft identification code into nine-bit parallel output words.

The modulation selector mixes the photo video information and the 50-bit-per-second performance telemetry information for input to the transponder for transmission. The selector receives control signals from the flight programmer to operate in one of the following modes.

MODE	DATA TYPE	ANTENNA EMPLOYED
1	Ranging and performance telemetry	Low gain
2	Photo video and performance telemetry	High gain
3	Performance telemetry	Low gain

(A Mode 4 exists which is implemented by selecting the normal Mode 2 modulation but exercising the Mode 3 transmission method when no video input data are available. The selection of this particular mode increases the available power in the downlink carrier.)

The telemetry system samples the output of sensors within the various spacecraft subsystems. Normal telemetry data channels include such information as temperatures, pressures, voltages, currents, and error signals. Special instrumentation includes 20 micrometeoroid detectors located on the tank deck periphery. Radiation dosage measurement, in the form of two scintillation counter dosimeters and the associated logic, are mounted in the photo subsystem area.

The traveling-wave-tube amplifier (TWTA) consists of a traveling-wave tube, a bandpass filter, and the required power supplies. This equipment, used only to transmit the wideband video data and telemetry (Mode 2) during photo readout, has a minimum power output of 10 watts. All of the necessary controls and sequencing for warmup of the traveling-wave tube are self-contained.

The spacecraft employs two antennas, a high-gain antenna which provides a strongly directional pattern and a low-gain antenna which is as nearly omnidirectional as practical. The low-gain antenna is a biconical-discone slot-fed antenna mounted at the end of an 82-inch boom. The high-gain antenna is a 36-inch parabolic reflector that provides at least 20.5 db of gain within ±5 degrees of the antenna axis. The radiated output is right-hand circularly polarized. The antenna dish is mounted on a boom and is rotatable in 1-degree increments about the boom axis to permit adjustments for the varying relative positions of the Sun, Moon, and Earth.

Spacecraft performance telemetry data was received at the SFOF via the Agena transmitter, AFETR instrumentation, and the Deep Space Station (DSS-71) at Cape Kennedy for 22 minutes after launch, with only 5 minutes of unusable data. This included about 2.1 minutes of data after cislunar injection.

The Deep Space Station at Johannesburg (DSS-51) first acquired the spacecraft transmissions 29.1 minutes after launch at a signal strength of -132.0 dbm, using the acquisition aid antenna. (This was 6.5 minutes after spacecraft separation.) Two-way lock was established 1.6 minutes later and was maintained solid for about 6.5 hours. The Woomera

Deep Space Station (DSS-41) acquired the spacecraft in three-way lock 50.5 minutes after launch. (These acquisitions were completed prior to execution of the stored-program Mode 4 switchover command.) The expected received signal strength drop was evident when the Mode 4 switchover command was executed. Performance telemetry data, transmitted directly from the spacecraft, was received beginning 66.5 minutes after launch. These data indicated that all deployment sequences were completed and the Sun acquired.

Overall performance of the communications subsystem in the high-power, low-power, command, and ranging and/or tracking modes was satisfactory. In the low-power mode, the received signal strength at the Deep Space Stations varied from 1.5 db below to 8 db above the nominal link design values. During photo readout periods, the high-power-mode received signal strength varied from 1 db below to 6 db above the corresponding nominal link design values. All components of the communications subsystem performed satisfactorily. There were some indications of minor irregularities in performance telemetry data of transponder output power and TWTA turn-on data. This did not, however, cause any degradation in or loss of spacecraft performance or video data.

During the mission the transponder output power measurement indicated the characteristic inverse relationship to the transponder temperature. In general, there was no detectable indication of these changes in the ground received signal strength.

In the early lunar orbit period, the received signal strength at the Deep Space Stations showed a steady decrease in value during the entire Sun occultation period. There was no indication of any corresponding change in the rf power monitored through the telemetry system. In fact, the transponder output power showed the normal increase in value as the transponder temperature decreased. Data obtained from special tests during this period verified the downlink power changes as the spacecraft cooled off, and further indicated that there were no detectable variations in the uplink received signal strength (monitored by the receiver AGC).

Transponder output power variations of 8 mw were repeatedly observed in the telemetry data just before and shortly after sunrise. A correlation was found with the transponder temperature data in that 8-mw variations occurred whenever the temperature passed through a value of about 70°F. It is believed that the 8-mw jump reflected a change in TWTA coupling, reducing the rf drive to the TWTA and resulting in a lower helix current. Based on this assumption, an operational decision was made during the mission to delay turning on the TWTA until the 8-mw jump in transponder rf output occurred. This resulted in shortening the priority readout, but did eliminate the high helix current during that period.

The traveling-wave-tube amplifier was commanded through 114 on-off cycles with a total operating time of 155 hours during the photographic mission and launch countdowns prior to the photo subsystem motor failure. During priority readout, the operating time averaged 41.3 minutes per orbit. In final readout, the average operating time was 129.3 minutes per orbit.

3.2.4 Attitude Control Subsystem Performance

Operational performance of the attitude control subsystem was adequate to support all mission objectives. All components functioned properly or as expected throughout the mission.

•

Execution of all spacecraft events and maneuvers is controlled by or through the attitude control subsystem, Figure 3-7, to precisely position the spacecraft for picture taking, velocity changes, or orbit transfers.

The basic operating modes are:

Celestial Hold—The basic references in this mode are the Sun and Canopus; the gyro sys-

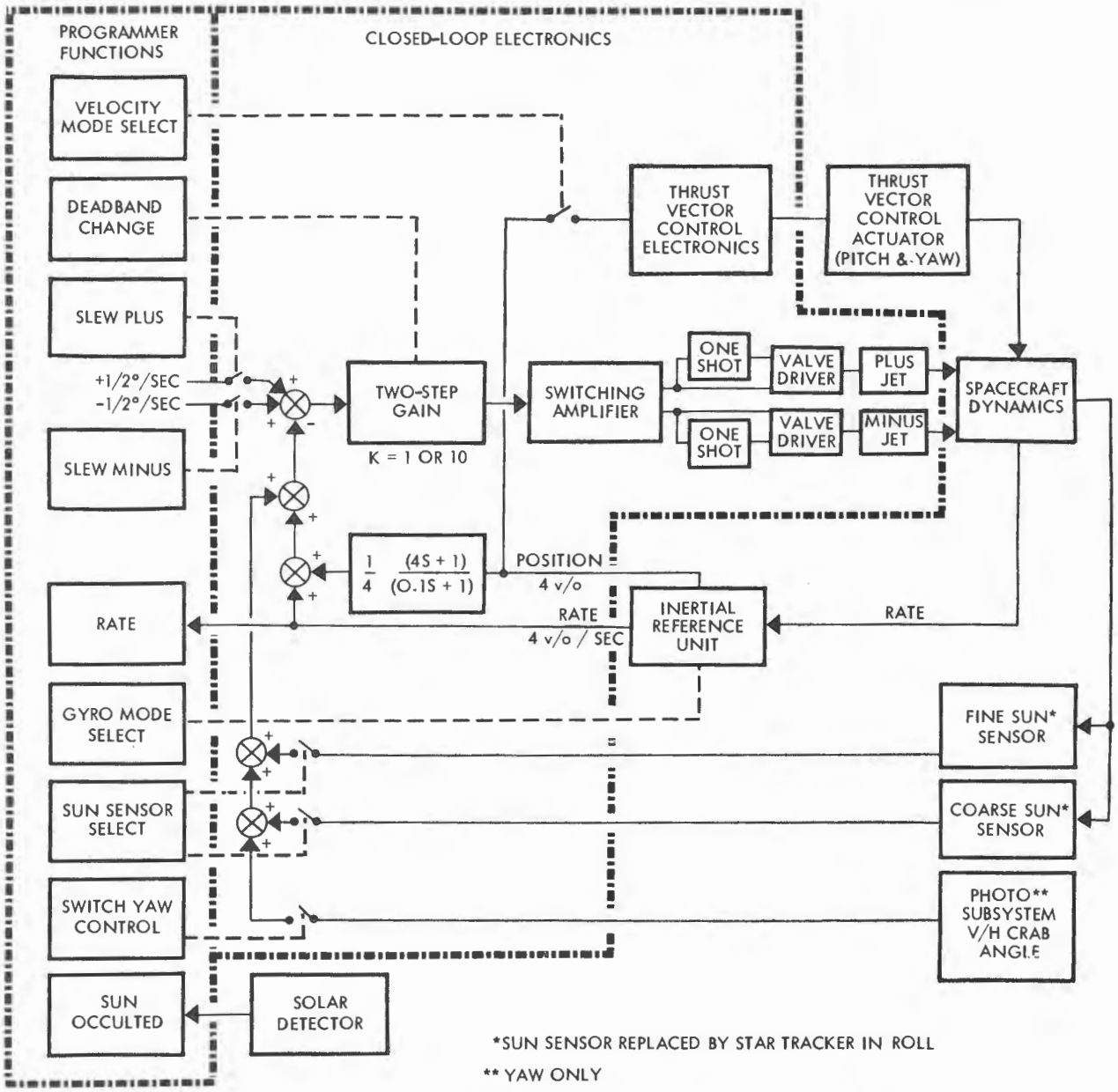

Figure 3-7: Attitude Control Subsystem Functional Block Diagram

tems operate as rate sensors. This mode was planned for use during normal cruise operations and as the initial conditions for all commanded attitude changes. (In practice the spacecraft was locked to the Canopus reference during lunar night.)

Inertial Hold—The basic references in this mode are the three gyros operating as attitude-angle sensors. This mode is used during all attitude and velocity change maneuvers, and whenever the celestial reference system is occulted.

Maneuver Mode—In this mode the spacecraft acquires the commanded angular rate about a single axis. The remaining two gyros may be held in the "inertial hold" mode.

Engine On, Inertial Hold—This mode is similar to the previously defined "inertial hold" mode except that the attitude of the space-

craft during the velocity change is accomplished by feedback control to the engine actuators.

Limit Cycling—The spacecraft is commanded to maintain a position within ±0.2 degree for all photographic and velocity control maneuvers or whenever commanded. (The normal deadband is ±2 degrees.)

The onboard digital programmer directs the spacecraft activities by either stored-program command or real-time command. The unit provides spacecraft time, performs computations and comparisons, and controls 120 spacecraft functions through real-time, stored, and automatic program modes. The information stored in the 128-word memory is completely accessible at all times through approoriate programming instructions. A capability of providing up to 16 hours of stored information and instructions for the spacecraft is inherent in the flight programmer design. This feature provides a high degree of reliability of executing commands without redundant equipment.

The inertial reference unit maintains the spacecraft attitude. Three gyros provide appropriate rate or angular deviation information to maintain proper attitude and position control. A linear accelerometer provides velocity change information in increments of 0.011 foot per second to the flight programmer during any firing of the velocity control engine.

Sun sensors are located in five positions about the spacecraft to provide spherical coverage and ensure Sun acquisition and lock-on and the resulting alignment of the solar panels. Error signals are generated whenever angular deviation from the spacecraft-sunline exists. A celestial reference line for the spacecraft roll axis is established by identifying the celestial body that the star tracker acquires, locks on, and tracks. Under normal conditions the star, Canopus, is used for this purpose; however, any known celestial body of suitable brightness and within the tracker's field of view as the spacecraft is rotated about the roll axis can be used to satisfy this function.

The closed-loop electronics provides the switching and electronic controls for the reaction control thrusters and positioning of the velocity control engine actuators. Attitude maneuver and control are maintained by the controlled ejection of nitrogen gas through the cold-gas thrusters mounted on the periphery of the engine deck. During a velocity control maneuver, gimbaling of the velocity control engine is used to maintain stable orientation of the spacecraft.

The attitude control subsystem maintained stable operation through the velocity change manuevers, normal limit cycle operation, and all photographic maneuvers. A total of 383 single-axis maneuvers was required to support all operational functions during the 25-day mission.

Spacecraft temperature control required the spacecraft to be pitched (15 to 45 degrees during cislunar and 15 to 35 degrees during lunar orbits) away from the Sun for approximately 56% of the mission. There were no control problems associated with these maneuvers. Table 3-3 identifies the maneuvers performed for each requirement.

Table 3-3: MANEUVER SUMMARY

FUNCTION	PLANNED TOTAL	ACTUAL			
		Roll	Pitch	Yaw	Total
Velocity	12	6	6	0	12
Photography	286	104	94	82	280
Star Map	3	3	0	0	3
Thermal Pitch-off	10	0	67	0	67
Attitude Update	30	9	1	1	11
Others	17	5	5	0	10
Total	358	127	173	83	383
Narrow-deadband maneuvers		120	163	83	366
Wide-deadband maneuvers		7	10	0	17
Total		127	173	83	383

The Sun and Canopus were acquired a total of 224 times during the mission with the control mode breakdown as shown in Table 3-4.

Table 3-4: SUN-CANOPUS ACQUISITION SUMMARY

	Narrow Deadband	Wide Deadband	Total
Canopus acquisition	108	19	127
Sun acquisition	116	5	121
Total	224	24	248

All velocity change maneuvers (midcourse, lunar orbit injection, and orbit transfer) were performed based on a normal Sun reference in an automatic control mode for pitch and yaw reference. Roll axis control was based upon Canopus acquisition in the "open loop" mode and employing ground calculations by the subsystem analysts to determine the roll commands required. The roll update maneuver was performed from 2 to 5 hours prior to the maneuver execution. The roll errors, with respect to Canopus, were -0.12, -0.29, and -0.08 degree for the above three maneuvers.

In general, the photo maneuvers required three-axis maneuvers to properly orient the cameras. These were all performed in the narrow deadband (±0.2 degree) control zone (See Table 3-4). The pitch and yaw axes were accurately extablished by Sun lock. An accurate roll position was established by operating the Canopus tracker in the "closed loop" mode during Sun occultation periods. (This mode was used because light from the illuminated limb of the Moon for the existing spacecraft-Sun-Moon-target area relationship could affect Canopus tracker operation by direct or reflected paths.)

The flight programmer properly acted upon all commands received from the command decoder. These included 1266 real-time commands and 2349 stored-program commands. The repetitive execution of stored-program commands increased the total executed by approximately 14,000 individual commands. The total programmer clock drift during the mission was -0.16 second. Canopus track was lost during the cislunar trajectory when the velocity control subsystem squib was fired, from high reflected light from the lunar surface, and four times for no detectable cause. After each loss, track was readily reacquired by performing an off-on cycle. The tracker was operated for a total of 79 hours with 158 on-off cycles during the photo mission with no evidence of any decreased performance.

Initial Sun acquisition was accomplished well within the 60-minute limitation. An exact total of Sun acquisition during the mission could not be determined. Reacquisitions after Sun occultation from attitude maneuvers were performed approximately 121 times, of which 116 were accomplished in the narrow deadband and five in the wide deadband control mode.

Performance of the reaction control thrusters was normal during the mission. Approximately 17,000 thruster operations were computed, of which 1654 operations were for attitude maneuvers and the remainder for limit cycle operation. Performance data indicated that 0.069 pound of thrust was developed by the roll thrusters and 0.065 pound by the pitch thrusters. The telemetry sampling interval was such that the corresponding value for the yaw thruster was not obtained.

Operation of the inertial reference unit was satisfactory. The gyro rate-integrating mode drifts were low and stable. During the mission the drift rates were found to be:

- Roll −0.12 ±0.01 degree per hour
- Pitch +0.15 ±0.03 degree per hour
- Yaw 0.02 ±0.03 degree per hour

Results from 360-degree spacecraft maneuvers in both directions are summarized in

Table 3-5 for each axis. These errors are attributed to both the gyro rate mode error and the voltage-to-frequency converter error, which cannot be separated within the telemetry data.

Table 3-5: MANEUVER ERROR

MANEUVER COMMANDED (Degrees)	MANEUVER EXECUTED (Degrees)	ERROR	
		(Degrees)	(Percent)
Roll + 360	360.19	+0.19	0.05
Roll - 360	-359.74	+0.26	0.07
Pitch + 360	360.45	+0.45	0.13
Yaw + 360	360.56	+0.56	0.16
Yaw - 360	-359.89	+0.11	0.03

3.2.5 Velocity Control Subsystem Performance

Operation and performance of the velocity control subsystem was excellent during the three propulsion maneuvers performed.

The velocity control subsystem provides the velocity change capability required for midcourse correction, lunar orbit injection, and orbit adjustment as required. The spacecraft includes a 100-pound-thrust, gimbaled liquid-fuel rocket engine. The propulsion system uses a radiation-cooled bipropellant liquid rocket engine that employs nitrogen tetroxide (N_2O_4) as the oxidizer and Aerozine-50 (a 50-50 mixture by weight of hydrazine and unsymmetrical dimethylhydrazine, UDMH) as the fuel. The propellants are expelled from the tanks by pressurized nitrogen acting against teflon expulsion bladders. The propellants are hypergolic and no ignition system is required.

The engine is mounted on two-axis gimbals with electrical-mechanical actuators providing thrust directional control during engine operations. A central nitrogen storage tank provides (through separate regulators) the gas required to expel: (1) the propellants in the velocity control system and (2) the gas for the attitude control thrusters. Figure 3-8 identifies subsystem components and shows how they are connected. The specified propellant load provides a nominal velocity change capability of 1017 meters per second at an oxidizer-to-fuel ratio of 2.0.

Flight performance data obtained during the three engine-burn periods were evaluated and the velocity control engine performance results are summarized in Table 3-6.

The short duration (4.3 seconds) of the midcourse-correction engine operation made the computation of thrust developed difficult. The three engine-burn periods imparted a total spacecraft velocity change of 760.09 meters per second of the calculated 1010.6 meters-per-second total capability. During the 542.5-second (lunar orbit injection) engine operation, the engine valve temperature remained between 70 and 77°F. Approximately 1 hour later, the valve temperature reached a maximum value of 112.4°F.

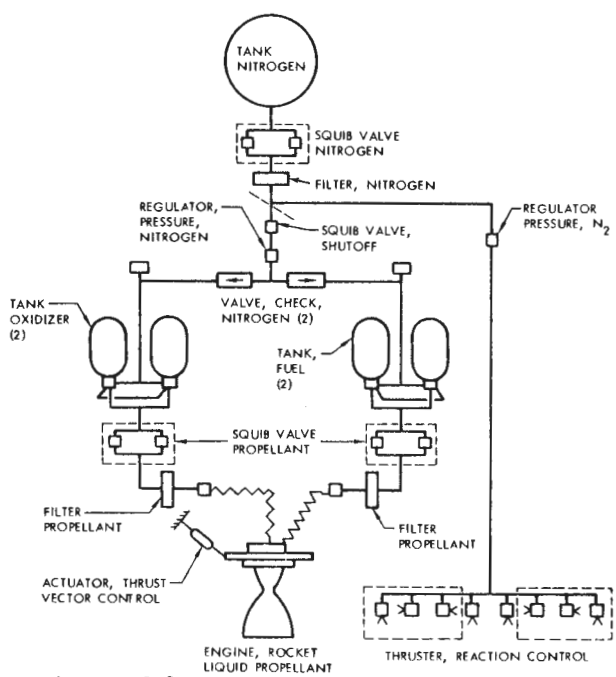

Figure 3-8:
Velocity and Reaction Control Subsystem

Table 3-6: VELOCITY CONTROL ENGINE PERFORMANCE SUMMARY

	VELOCITY CHANGE (meters per sec)	BURN TIME (sec)	THRUST (lb)	SPECIFIC IMPULSE (sec)
MIDCOURSE				
Prediction	5.11	4.5 ± 0.5	99.6	273.2
Actual	5.09	4.3	≈ 102.5	≈ 276
INJECTION				
Prediction	704.3	540.5 ± 10	100	276
Actual	704.3	542.5	99.85	277
TRANSFER				
Prediction	50.7	33.4 ± 1.6	101.3	277
Actual	50.7	33.7	100.3	277

Gimbal actuator position changes during the three engine-burn periods were 0.25 degree or less in pitch and 0.16 degree or less in yaw. These changes reflect the motion of the spacecraft center of gravity. There were one-and two-bit changes in the actuator positions between the end of one burn period and the start of the next period. These changes are believed to reflect the slight changes in the reference voltages. (Ground test data has shown this measurement to be sensitive to these voltage changes when there was no mechanical movement of the actuators.)

Propellant tank heaters were activated 21 times for a total operating time of 1408 minutes to maintain the propellant tank heaters above 40°F. At the end of the photo mission, on Day 61, the spacecraft had a velocity change capability of about 250 meters per second and approximately 6 pounds of nitrogen gas to be used as desired during the extended mission.

3.2.6 Structures, Mechanisms, and Integration Elements Performance

All of the components comprising the structure, thermal control, wiring, and mechanisms operated properly. As in previous missions the spacecraft was periodically oriented off the sunline to maintain spacecraft temperatures within acceptable operating limits.

The Lunar Orbiter spacecraft structure includes three decks and their supporting structure. The equipment mounting deck includes a structural ring around the perimeter of a stiffened plate. Mounted on this deck are the photo subsystem and the majority of the spacecraft electrical components.

The tank deck is a machined ring, v-shaped in cross section, closed out with a flat sheet. Fuel, oxidizer, and nitrogen tanks are mounted on this deck. The 20 micrometeoroid detectors are located on the periphery of the

ring. The engine deck is a beam-stiffened plate that supports the velocity control engine, its control actuators, the reaction control thrusters, and the heat shield that protects the propellant tanks during engine operation.

Prior to deployment, the low- and high-gain antennas are positioned and locked along the edges of these three decks. The four solar panels are mounted directly under the equipment mounting deck and in the stowed position are compactly folded into the space below it. Electrically fired squibs unlock the antennas and the solar panels at the appropriate time to permit them to be deployed into the flight attitude.

Thermal control of the spacecraft is passively maintained. An insolating thermal barrier, highly reflective on both the interior and exterior surfaces, encloses the spacecraft structure, except for the Sun-oriented equipment mounting deck and the insulated heat shield on the engine deck. The objective is to maintain spacecraft temperature within the thermal barrier within a nominal range of 35 to 85°F. The equipment mounting deck exterior surface is painted with a zinc-oxide-pigment, silicone-based paint that was selected to achieve the desired heat balance. This paint has the properties of high emissivity in the infrared region (for dissipation of spacecraft heat) and low absorption at the wavelengths that contain most of the Sun's emitted heat.

A camera thermal door protects the photo subsystem lenses from heat loss and direct sunlight except during photographic periods. Immediately prior to each photographic sequence, the door is opened to permit photography. Fifty-one opening and closing cycles were completed during photography. The antenna and solar panel deployment sequences were satisfactorily completed by stored-program command as planned approximately 25 minutes after launch. Temperatures of the equipment mounting deck increased more rapidly than predicted, but were consistent with Mission II data, when the solar panels were oriented perpendicular to the sunline. The additional coating of S-13G material over the original coating of B-1056 improved the peformance by delaying the start of noticeable degradation.

3.3 OPERATIONAL PERFORMANCE

Operation and control of the Lunar Orbiter III spacecraft required the integrated services of a large number of specialists stationed at the Space Flight Operations Facility (SFOF) in Pasadena, California, as well as at the worldwide Deep Space Stations. Mission advisors and other specialists were assigned from the Lunar Orbiter Project Office, supporting government agencies, Jet Propulsion Laboratory, the Deep Space Stations, and The Boeing Company.

The Langley Research Center exercised management control of the mission through the mission director. Two primary deputies were employed: the first, the launch operations director located at Cape Kennedy; the second, the space flight operations director located at the SFOF. Once the countdown started, the launch operations director directed the progress of the countdown on the launch pad, while the space flight operations director directed the countdown of the Deep Space Network. From the time that these countdowns were synchronized, all decisions (other than Eastern Test Range safety factors) regarding the countdown were made by the mission director, based on recommendations from the launch operations director and/or the space flight operations director.

After liftoff, the performance of the launch vehicle and spacecraft was monitored in the launch mission control center at ETR by the mission director. Telemetry data were used by the launch team and were relayed in real time to the SFOF through the Cape Kennedy DSS. Dissemination of spacecraft performance and tracking data to the launch team and the operations team enabled efficient and orderly transfer of control from Cape Kennedy to the SFOF.

After the spacecraft was acquired by the Deep Space Network (DSN), flight control was assumed by the space flight operations director. Thereafter, the mission director moved from ETR to the SFOF and continued control of the mission. Control of spacecraft operations was delegated to the space flight operations director.

Control of the mission was centralized at the SFOF for the remainder of the mission. All commands to the spacecraft were coordinated by the Spacecraft Performance Analysis and Command (SPAC) and Flight Path Analysis and Command (FPAC) team of subsystem specialists and submitted to the space flight operations director for approval prior to being transmitted to the Deep Space Instrumentation Facility (DSIF) site for retransmission to the Spacecraft. As a backup capability, each prime DSIF was supplied with a contingency capability (including predetermined commands and process tapes) to permit local assumption of the basic mission control function in the event of communications failures.

Mission III was more complex than either of the preceding two missions. In addition to normal vertical photography of the primary sites, Mission III also included converging stereo coverage of specified sites from successive orbits as well as oblique photos of other specified primary sites. Detailed premission planning provided the required control and look-ahead visibility to photograph the 12 primary and 32 secondary sites. Except for the changes in priority readout generated by intermittent film advance, spacecraft performance was so nearly normal that the preplanned sequence was followed with only minor exceptions.

3.3.1 Spacecraft Control

The flight operations team was divided into three groups (designated red, white, and blue) to provide 24-hour coverage of mission operations at the Space Flight Operations Facility. Overlap was scheduled to allow detailed coordination between the on-coming and off-going system analysts. The operations team was essentially unchanged from Mission II.

Spacecraft control was maintained throughout the mission by the generation, transmission, and verification of commands and the transmission of execute tones from the Earth-based facilities. A total of 3615 commands were generated and executed without incident.

Command preparation activity was similar to the method developed for Mission II, namely:

- Off-line planning;
- On-line command preparation.

During the peak activity periods, there was one off-line and one on-line command programmer specialist on each team. The off-line command programmer specialist accomplished the following based upon the film budget and core map schedule of the mission plan as updated by mission directives.

- Planned the layout of each programmer core map;
- Defined the contents of each command sequence;
- Prepared a planning command matrix map;
- Prepared an event flow chart for the on-line programmer;
- Prepared a spacecraft event sequence in GMT for review and approval.

The on-line command programmer specialist accomplished the following, based upon the above planning as approved by the mission advisors and mission control.

- Prepared commands to be transmitted to the spacecraft;
- Incorporated data (magnitude, time, camera mode, etc.) contained in the command preparation directive.

Preparation of each core map was started approximately 14 to 16 hours before the scheduled transmission and ended with the preliminary command conference approximately 7 hours before transmission. In some cases, these functions were delayed by changes

in requirements or desires to incorporate the latest orbit determination information. As in previous missions, the flight programmer breadboard equipment in the SFOF was operated continuously—as if in flight—to follow the mission in real time from launch countdown through the end of photo readout.

As in previous missions, the spacecraft was pitched off the sunline from 15 to 45 degrees for approximately 56% of the mission to maintain spacecraft temperatures within operational limits as outlined in the operational plan.

The increase in orbit inclination from 12 to 21 degrees resulted in a 19% gap in the vertical telephoto coverage from successive orbits. Therefore, in most cases, the cameras had to be pointed off the vertical by a three-axis spacecraft maneuver in order to obtain coverage of the primary photo sites. In addition, the site location of 13 primary and 10 secondary sites was changed for various reasons and one additional primary-site photo pass was added during the mission. Incorporation of the many deviations to the originally complex photo plan (20 primary and 33 secondary sites) was made possible by the experience gained during the first two missions. The majority of site location changes were made to ensure coverage of the desired area and to optimize photo quality.

Evaluation of site characteristics of primary and secondary sites IIIP-1 and IIIS-1 taken on the first photo orbit showed that different shutter speeds were required for the two sites. Actual location of the sites produced a 3-minute, 38.8-second interval between the camera-on times for the two sequences. Considering the time required to photograph Site IIIP-1 and for V/H sensor operation prior to photography of Site IIIS-1 left about 2 minutes to command, verify, and execute the shutter speed change. To provide the highest probability of accomplishing the change, the flight programmer was placed in the "compare time" mode after camera-on command for Site IIIP-1, rather than the normal "wait time" mode.

At the time of implementing this sequence, it was not recognized that, by placing the programmer in the "compare time" mode, the spacecraft time of exposure could not be supplied to the photo subsystem for exposure on the film. As a result, the time codes were blank on the film, necessitating use of estimated exposure or mission predict data to evaluate the photos obtained.

The large number of oblique-and primary-site photos with significant cross-track tilt necessitated the development of a systematic procedure to determine the predicted film density. This was accomplished by computing an equivalent phase angle (angle between the camera axis and the sunline) for use in the Photo Quality Prediction computer program (QUAL). During the mission, film density measurements were made on the GRE film and compared with the predictions. Early results showed the predictions to be approximately 0.2 higher than the actuals and appropriate adjustments were made for the remainder of the mission.

During the February launch period, as in Mission II, the star Canopus approached the limb of the Moon when viewed from the spacecraft as it approached the Apollo zone of interest. Under these conditions the reflections from the illuminated limb, by direct or reflected paths, can interfere with or prevent the retention or reacquisition of Canopus. Since this condition was expected to occur on Mission III prior to executing the photo maneuvers, a backup roll control method was included in premission operational planning. This method was implemented for photo maneuvers as follows. The star tracker was used in the closed-loop mode (tracker error signal fed to the flight programmer) to accurately position the spacecraft in roll. The roll axis was put in the inertial-hold mode. The roll position change from initiation of inertial hold until camera-on time was determined based on the inflight roll drift rate. This roll position change was included in the photo maneuver computation so that the spacecraft was properly oriented over the site.

3.3.2 Flight Path Control

The Lunar Orbiter trajectory was controlled during the boost phase and injection into cislunar orbit by a combination of the Atlas guidance and control system at AFETR and the on-board Agena computers. After acquisition by the Deep Space Station at Woomera, Australia, trajectory control was assumed and maintained by the Space Flight Operations Facility in Pasadena, California. During the first 6 hours of the mission following injection, the Deep Space Network performed orbit determination calculations to ensure DSS acquisition. Guidance and trajectory control calculations for controlling mission trajectories were performed by the Lunar Orbiter Operations group.

Lunar Orbiter flight path control is the responsibility of the flight path analysis and command (FPAC) team located at the Space Flight Operations Facility (SFOF) in Pasadena, California. Flight path control by the FPAC team entails execution of the following functions.

- Tracking Data Analysis—Assessment of tracking data (doppler and range) and preparation of DSS tracking predictions.
- Orbit Determination—Editing of raw tracking data and determination of the trajectory that best fits the tracking data.
- Flight Path Control—Determination of corrective or planned maneuvers based on orbit determination results and nominal flight plan requirements.

FPAC activities during the mission were divided into the following phases.

- Injection through midcourse;
- Midcourse through deboost;
- Initial ellipse;
- Photo ellipse.

Each of the phases is discussed in the following sections.

3.3.2.1 Injection Through Midcourse

The purpose of this phase was to:

- Calculate the optimal orbit injection point;
- Select the cislunar trajectory that satisfies the injection constraints;
- Determine the required midcourse maneuver.

DSS-51, Johannesburg, South Africa, acquired the spacecraft approximately 7 minutes after separation from the Agena. Within 2 hours of cislunar injection, the tracking data showed that the trajectory was well within the midcourse correction capability of the spacecraft. In addition, execution of the midcourse maneuver was not critical and an early maneuver was not necessary. By varying the arrival time for a selected midcourse execution time, the FPAC software programs automatically optimized the deboost, transfer, and midcourse ΔV. On the basis of these computations, the midcourse maneuver was set for 15:00 GMT, February 6, with the spacecraft in view of both Madrid and Goldstone tracking stations.

The midcourse maneuver consisted of a 39.94-degree roll, a 123.39-degree pitch, and a velocity change of 5.11 meters per second (engine-burn time of 4.3 seconds). This maneuver was selected from 12 possible two-axis maneuvers based on:

- Maintaining Sun lock as long as possible;
- DSS line-of-sight vector not passing through an antenna null;
- Minimum total maneuver angular rotation.

The first orbit determination after execution of the midcourse maneuver was not initiated for a period of 8 hours because the trajectory curvature change was too small to provide meaningful results. This initial determination predicted the encounter perilune altitude and time of closest approach within 7.6 km and 1.1 seconds of the best estimate of trajectory prediction based on 10.5 hours of two-way doppler data. These orbit parameters, midcourse-designed encounter conditions, and estimates used for final deboost maneuver calculations are shown in Table 3-7.

Table 3-7: SUMMARY OF ENCOUNTER PARAMETERS

Elements	1st OD	Best Estimate	Midcourse Designed	Final Deboost Calculation
Perilune Altitude (km)	2237.1	2229.5	2224.7	2237.3
Time of Closest Approach (seconds after 22:06 GMT, February 8)	05.7	04.6	00.0	22.2
$\bar{B}\cdot\bar{T}$ (km)	5620.3	5607.1	5604.6	5618.9
$\bar{B}\cdot\bar{R}$ (km)	-2477.2	-2478.7	-2465.2	-2482.4
$\bar{B}$ (km)	6142.0	6130.5	6122.8	6142.9

The final deboost calculation orbit determination was selected from other orbit determinations because:

- The results fitted 37 hours of two-way doppler data after midcourse very well.
- The predicted $\bar{B}\cdot\bar{T}$ was consistent with previous determinations.

Two factors were identified which introduced some uncertainty into the selection of this determination, namely:

- The range unit residuals were on the order of 4 km.
- The time of closest approach was about 17.6 seconds late.

Based on results obtained from previous missions, a serious effort was made to use the ranging unit data obtained with the same confidence level as the two-way doppler data in making the orbit determinations. During the early determinations the results were fairly successful and a very good fit between ranging data solutions and doppler data solutions was obtained. As more data was obtained, the ability to fit the ranging and doppler results together deteriorated markedly. A decision was therefore made to rely exclusively on the two-way doppler data. The discrepancies will be evaluated after completion of the mission to improve the use of this data on the next mission.

The deboost maneuver design and execution commands were based on 37 hours of two-way tracking data. This maneuver was required to guide the spacecraft from the approach hyperbola into an ellipse in which the orbital elements, including a plane change, are as close to nominal as possible. Twelve possible two-axis maneuvers were considered to accomplish the deboost. Based on the same operational requirements used for the midcourse correction, the spacecraft maneuver selected consisted of:

- Roll 30.88 degrees;
- Pitch 125.88 degrees;
- ΔV 704.3 meters per second.

Engine ignition occurred at 21:54:19.0 GMT on February 8 and lasted 543.5 seconds. The spacecraft was tracked by both the Goldstone and Woomera Deep Space Stations during the injection into the initial lunar orbit with a 13.04-degree plane change.

In the event that the spacecraft failed to complete the injection maneuver, a series of fly-by maneuvers and alternate photo mis-

sions had been designed but was not implemented.

3.3.2.3 Initial Ellipse

Occultation occurred 21 minutes after thrust termination. During this short period, sufficient tracking data was required to make a quick orbit determination and generate predictions to ensure rapid reacquisition of the spacecraft by the Deep Space Network as it emerged from behind the Moon. Table 3-8 shows a comparison of orbit elements of the nominal design, first determination, and best estimates. The first estimate was based on approximately 20 minutes of two-station tracking data.

During the 4 days between orbit injection and transfer, orbit determination consisted of routine updating of the spacecraft state vector and support of the orbit transfer maneuver design. Orbit determination results used to design the transfer maneuver were based on 14.3 hours of two-way lock doppler tracking from all three tracking stations.

The orbit transfer maneuver was based on the following requirements.

- Minimum perilune altitude of 48.0 km;
- Illumination band of 60 to 80 degrees for primary sites;
- Transfer at least 24 hours prior to first photo;
- Minimum of 30 minutes between the end of Earth occultation and engine ignition.

Optimizing these requirements resulted in the selection of Orbit 26 to initiate the maneuver, thus allowing 18 orbits to complete the necessary orbit determinations and calculations before the first photo. The required spacecraft maneuver was 51.74 degrees roll and 19.86 degrees pitch. Engine ignition occurred at 18:13:26:6 GMT on February 12 with a burn time of 33.7 seconds. Table 3-9 compares the orbital elements and predictions before and after the transfer maneuver. The first orbit determination was completed 100 minutes after the maneuver and the best estimate was made 7.5 hours after the maneuver was completed.

Photo Ellipse—Beginning immediately after completion of the transfer maneuver, tracking data was logged and edited to support orbit determination as required to complete the photographic mission. The photo ellipse was initiated on Orbit 26 and the photographic mission was terminated during Orbit 154. During this period the primary functions included:

- Generation of a high-quality orbit determination prior to each primary photo event;
- Determination of the attitude maneuver and camera-on times for primary-site photography;
- Design secondary-photo-site attitude maneuvers and camera-on times on a noninterference basis with primary photo activity;

Table 3-8: INITIAL-ELLIPSE ORBITAL ELEMENTS

Element	Nominal	Deboost Design	First Orbit Determination	Best Estimate
Perilune Altitude (km)	200.0	213.38	210.76	210.26
Apolune Altitude (km)	1850.0	1849.97	1803.93	1802.10
Inclination* (deg)	21.00	21.05	20.99	20.94
Longitude of Ascending Node *(deg)	311.16	311.70	311.07	310.33
Argument of Perilune* (deg)	176.22	176.22	176.99	177.3

*Selenographic-of-date coordinates

Table 3-9: ORBIT TRANSFER ELEMENTS

Element	Premaneuver Pretransfers	Prediction Posttransfers	Post maneuver 1st orbit Determination	Determination Best Estimate
Apolune Altitude (km)	1795.26	1846.44	1847.15	1847.35
Perilune Altitude (km)	216.08	54.78	54.92	54.84
Orbit Inclination* (deg)	20.94	20.87	20.86	20.91
Ascending-Node Longitude* (deg)	258.74	258.64	258.75	257.86
Argument of Perilune* (deg)	179.58	178.30	178.12	178.88

*Selenographic-of-date coordinates.

- Determination of trajectory predictions, occultation periods and times of sunrise and sunset.

A total of 50 orbit determinations were made prior to Bimat cut (February 23), of which 30 were used to support photo sequence command conferences. Camera-on-time errors were minimized by predicting the state vector to within a few minutes of the estimated on-time using the orbit determination programs. SPAC software programs applied spacecraft and photo subsystem operational factors to the state vector to determine the camera-on time transmitted to the spacecraft. When the photo maneuver, camera-on time, and attitude maneuvers were determined, they were used as input conditions to the EVAL program and the predicted coverage was checked against the desired coverage.

3.3.2.5 Orbit Phase Kepler Elements

Lunar orbit characteristics from Lunar Orbiter III tracking data are presented in Figures 3-9 through -13. These illustrations are histories of perilune radius, apolune radius, orbit inclination, argument of perilune, and longitude of the ascending node. To clearly show the complete mission, these figures cover the 22-day period from lunar injection (Days 39 to 61) and include both ellipses.

3.4 GROUND SYSTEM PERFORMANCE

The Lunar Orbiter ground system provided the facilities and equipment required to receive, record, and transmit data and commands between the Space Flight Operations Facility and the spacecraft. In addition, all facilities necessary to sustain mission operations were provided by a complex consisting of three primary Deep Space Stations (DSS), the Space Flight Operations Facility (SFOF), and the ground communications system which provided voice and data communication between all locations. Separate facilities were provided at Eastman Kodak, Rochester, N. Y., and at Langley Research Center, Hampton, Virginia, to process and evaluate the photo data obtained.

All of these facilities provided the required support during the mission and only minor irregularities were encountered. Each area is separately discussed in the following sections.

3.4.1 Space Flight Operations Facility (SFOF)

The Space Flight Operations Facility provided the mission control center, as well as the facilities to process and display data to support operational mission control. The entire system performed well.

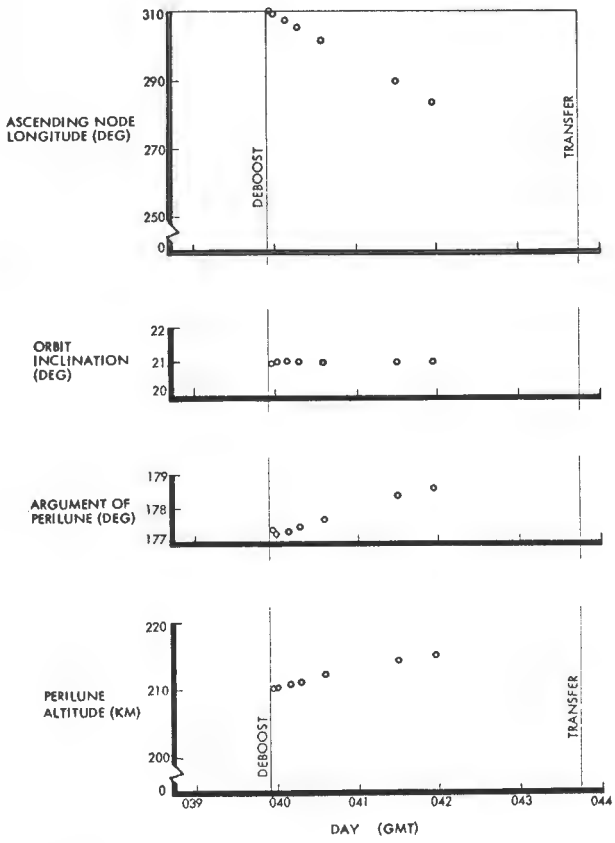

Figure 3-9: Initial-Ellipse Conical Elements

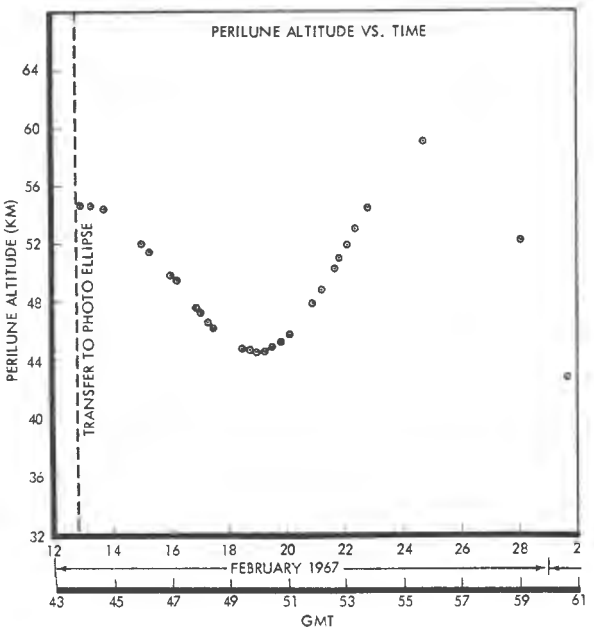

Figure 3-10: Perilune Altitude History

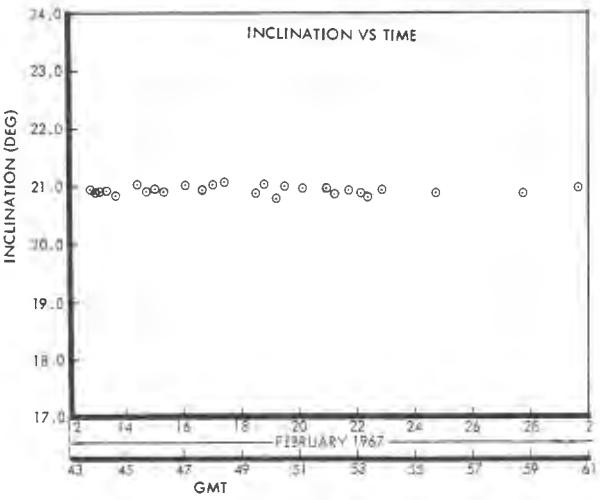

Figure 3-11: Orbit Inclination History

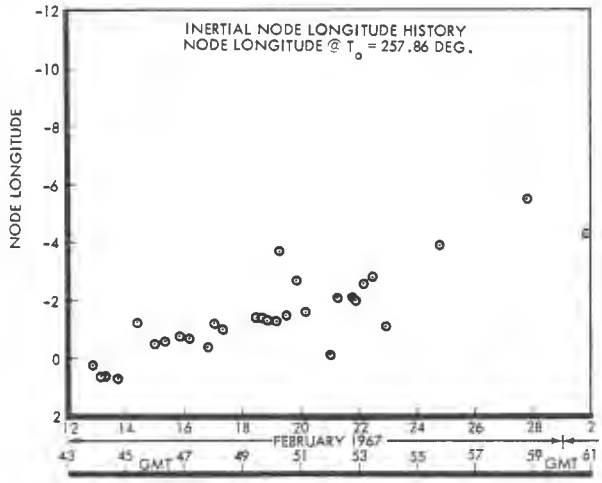

Figure 3-12: Node Longitude History

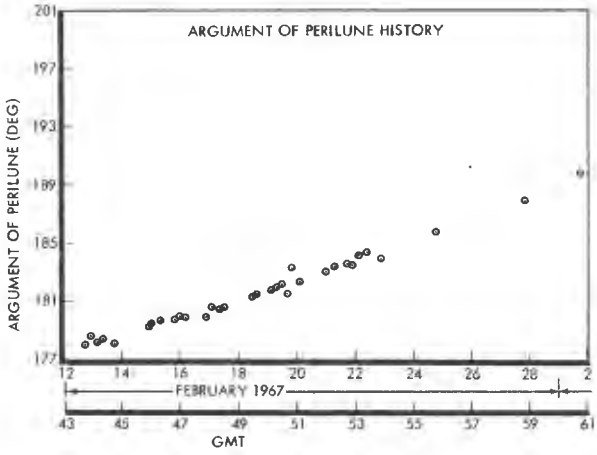

Figure 3-13: Argument of Perilune History

The telemetry processing station and the internal communications system provided telemetry and tracking data from the high-speed data line and teletype lines for use by the SFOF computers and in the operations area.

The central computing complex consists of three computer strings, each of which contain an IBM 7094 computer coupled to an IBM 7044 input-output processor through an IBM 1301 disk file memory and a direct data connection.

All three computer strings were used to support Mission III for the periods indicated. A dual Mode 2 configuration was used to support all critical phases of the mission.

Computer String	Mode 2 (hours)
X string	344
Y string	383.5
W string	37.5
Total	765

These totals also include 253 hours in dual Mode 2 and 1 hour in triple Mode 2.

During the first 6 hours, the DSN was responsible for both orbit determination and data quality determination, as well as the history of data quality and analysis throughout the remainder of the mission. Jet Propulsion Laboratory personnel performed the first orbit determination after cislunar injection. The orbits were determined within the allowable time and showed a nominal injection that was subsequently verified by later orbit-determination computations.

Excellent tracking data was obtained after orbit injection and during the initial orbit. The data-quality determination was consistent among all three stations.

All changes for the Mission III software were demonstrated successfully and frozen prior to the Mission III training exercise. Performance of the mission-independent and mission-dependent software was satisfactory. The minor problems experienced with computer outputs did not affect the operational control of the mission.

The 14 SPAC programs were executed a total of 2,951 times and 2,831 were completed successfully. Of the 120 failures to execute, 102 were attributed to input errors and 18 contained system errors.

The GRE at the SFOF was manned during priority readout only to provide photo data for early analysis, exposure control, and public releases. The video data was received from Goldstone DSS via a microwave link. Video data was recorded by the GRE and also fed to the scan converter for real-time TV presentation within the SFOF.

3.4.2 Deep Space Stations (DSS)

The Deep Space Stations (Goldstone, California; Woomera, Australia; and Madrid, Spain) supported the Lunar Orbiter Mission by:

- Obtaining and processing telemetry and video data from the spacecraft;
- Transmitting commands to the spacecraft;
- Communicating and transmitting both processed and raw data to higher user facilities.

Real-time tracking and telemetry data were transmitted through the ground communications system. The video data were recorded on video magnetic tapes and, by mission-dependent equipment, on 35-mm film. All physical material, such as processed films, video tapes, logs and other reports, were sent to the appropriate destinations via air transportation. All commitments were met and the incident of error was low.

Between Missions II and III, DSS-62 was commissioned and replaced DSS-61 as the primary tracking station at Madrid, Spain.

For a period of 83 minutes on February 14, data was lost at Goldstone DSS when the antenna was stowed to prevent damage due to

high winds at the site. The Madrid DSS was also tracking during this period and the overlapping coverage prevented loss of data.

3.4.3 Ground Communications System (GCS)

Ground communications between the DSS and the SFOF consist of one high-speed-data line (HSDL), three full duplex teletype (TTY) lines, and one voice link. Communication lines to overseas sites are routed through the Goddard Space Flight Center at Greenbelt, Maryland. Performance telemetry data was normally transmitted via the HSDL while the tracking data was transmitted via a TTY line. Telemetry performance data can be transmitted via teletype lines with a reduction in the amount of data transmitted in real time.

Overall performance of the ground communications system was very good. Very little data was lost by transmission losses due to the backup modes provided. Table 3-10 summarizes the "downtimes %" by transmission mode and station.

Table 3-10:
DATA TRANSMISSION OUTAGES

	Downtime (%)		
	HSDL	TTY	Voice
DSS-12	0.1	0.06	0.06
DSS-42	1.8	0.9	0.5
DSS-62	2.2	1.1	0.5

There were isolated times when the HSDL and TTY lines to Woomera and Madrid were down. These periods occurred during non-critical phases of the mission. HSDL down periods at DSS ranged from 1 to 42 minutes while at DSS-62 the period was from 1 to 50 minutes. At DSS-12 the maximum HSDL outage time was 9 minutes.

3.4.4 Photo Processing

Photo processing at Eastman Kodak included printing negative transparencies and positive transparencies by successive-generation contact printing from the original GRE 35-mm positive transparencies. The GRE film was also optically reassembled into 9.5- by 14.5-inch subframes containing 14 framelets. This reassembled negative was used to produce positive and negative transparencies by successive-generation contact printing.

GRE 35-mm film was printed on Type 5234 Eastman Fine-Grain Duplicating Film. Processing goals were to have a density (D) of 0.50 to reproduce on the copy at a value of 2.00 and density of 2.00 to reproduce at a value of 0.50 (where a density of 0.50 corresponds to white and 2.00 corresponds to black). The inverse of densities is the normal result of the film transparency copy process in which white areas on the original produce black areas on the copy. These densities were within ± 0.10 density of the received D-maximum and within ± 0.05 density of the received D-minimum.

Density measurements were made on the GRE film processed from the sites and actually used in the reassembly printing to expose the reassembled subframe negatives. Measurements were made of the test bar pattern in the edge data format pre-exposed on the spacecraft film prior to flight. Results of these measurements are shown in Table 3-11, where D max and D min are the maximum and minimum densities, respectively.

Table 3-11:
MEASURED GRE FILM DENSITY

Station	GRE	D max	2 σ	D min	2 σ
Goldstone	03	2.01	0.10	0.49	0.07
	04	1.98	0.09	0.48	0.05
Woomera	05	1.99	0.07	0.44	0.04
	06	2.00	0.08	0.44	0.03
Madrid	07	1.99	0.04	0.47	0.06
	08	1.96	0.12	0.45	0.06
Average		1.99	0.08	0.46	0.05

Copying results for the 9.5-inch film in terms of density reproduction were as follows.

GRE Film Density	REASSEMBLY PRINTER AVERAGE DENSITY		
	Desired Value	Reassembled Negative Density	
		Average	Range
2.00	0.35	0.35	0.31 - 0.39
0.50	1.80	1.81	1.79 - 1.89

The 0.15 and 0.20 changes in desired value were made to provide an improvement in tone reproduction.

A processing and priority schedule was developed for the 35-mm film to satisfy the urgent requirement for film copies within the daily output capacity (30,000 feet per day) of the assigned facilities.

3.4.5 Langley Photo Data Assessment Facility

The primary functions accomplished at the Photo Data Assessment Facility at Langley Research Center were to make:

- A duplicate copy of the original video tape;
- An analog tape copy containing only the video tape;
- One GRE film for each analog tape;
- Two additional GRE films as priority permitted.

A total of 263 video tapes was received during the mission. These tapes were used to produce:

- 1,555 rolls of 35-mm GRE film;
- 307 analog tape duplicates (many in multiple copies).

A limited number of the GRE film produced were made to improve the photo quality. This was accomplished by playing the video tape through cascaded amplifiers and then into the GRE set. This gain change shifted gray levels to improve the detail contained in lighter areas of selected wide-angle photos.

Electronic equipment was developed for use with the tape playback equipment which automatically compensates for the spacecraft readout density variations. The resultant pictures do not have the characteristic "tiger stripes" observed on previous photos. Figure 3-14 and -15 show representative "before and after" examples of the use of this technique.

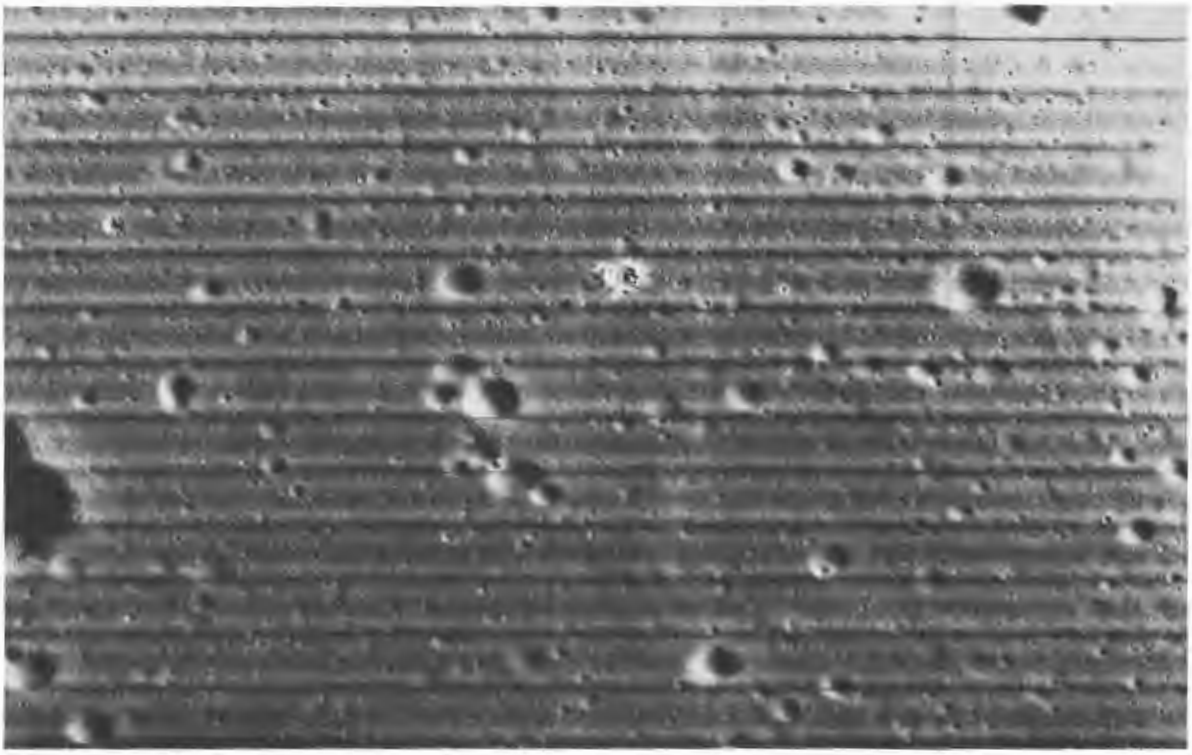

Figure 3-14: Photo without Electronic Augmentation
(Section of Telephoto Frame 212, Site III P-12c)

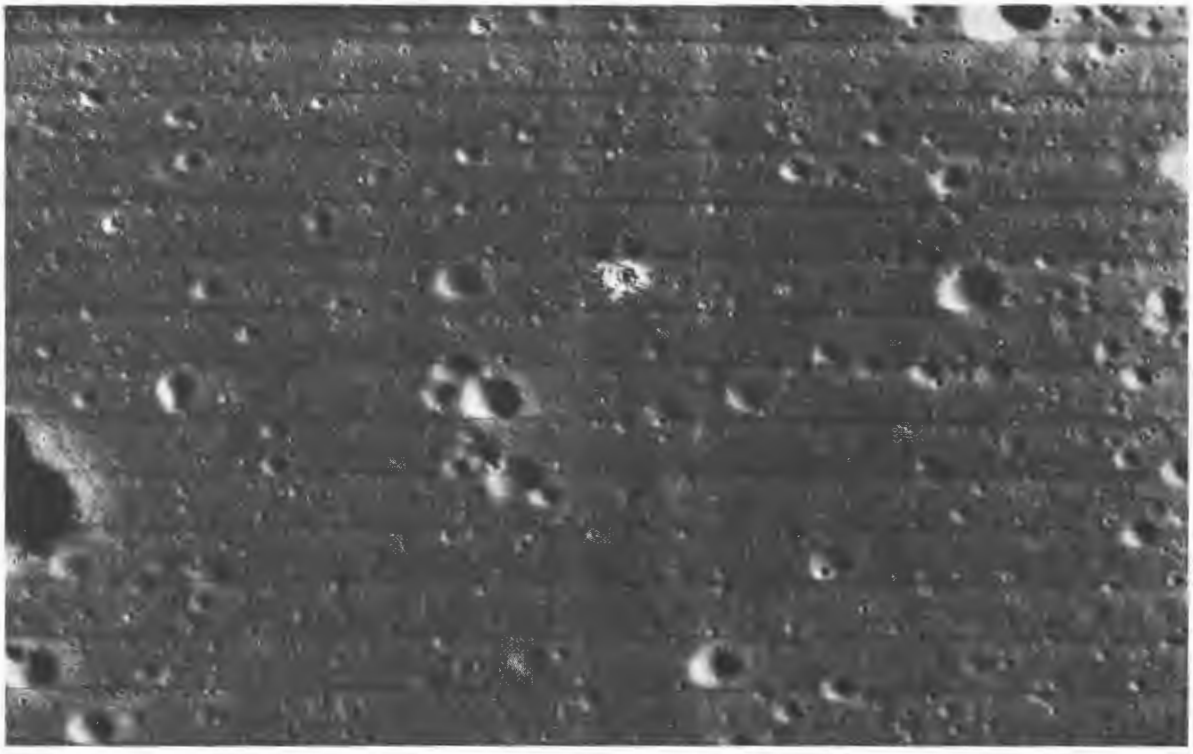

Figure 3-15: Photo with Electronic Augmentation
(Same photo as Figure 4-14)

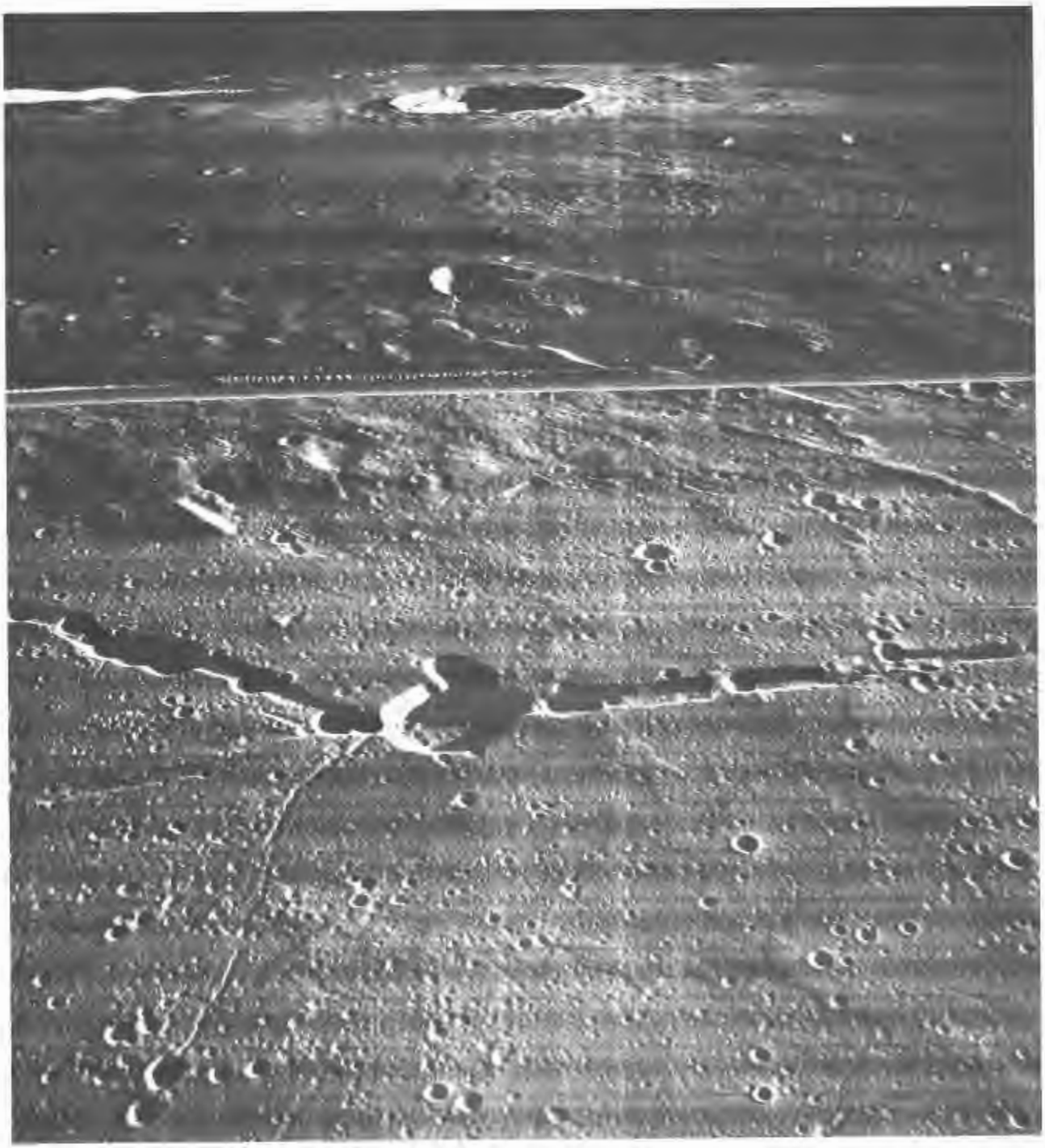

Wide-Angle Frame 73—Site III S-6
(Oblique to north toward Rima Hyginus)

4.0 MISSION DATA

Each Lunar Orbiter mission has an objective to provide four types of data—photographic, lunar environmental, tracking, and performance. All of these objectives were accomplished as verified by the data obtained, except for the premature termination of final readout.

Telephoto coverage of the Surveyor I landing site was examined and the spacecraft with its distinguished shadow was positively identified.

The secondary objective of providing a spacecraft to be tracked by the Manned Space Flight Network (MSFN) to evaluate the Apollo Orbit Determination program will be accomplished during the extended mission.

Each type of data is discussed, in turn, in the following sections.

4.1 PHOTOGRAPHIC DATA

A total of 422 telephoto and wide-angle photographs (211 dual exposure) were taken of the 12 primary and 31 secondary sites essentially as planned. When the failure of the film-advance motor occurred, Telephoto Frames 79 through 215 and Wide-Angle Frames 78 through 215 had been read out in final readout. Of the remaining frames (Telephoto Frames 5 through 78 and Wide-Angle Frames 5 through 77), a total of 51 were read out in whole or in part during priority readout.

Evaluation of the photos by the Lunar Orbiter Photo Data Screening Group resulted in the selection of eight sites suitable for Apollo landing. There were Sites IIP-2, -6, -8, -11, and -13 photographed by Lunar Orbiter II, and partially rephotographed by Lunar Orbiter III; and Sites IIIP-9, -11, and -12 photographed by Lunar Orbiter III and partially by Lunar Orbiter I. From these eight candidate sites, three sites will be chosen by Apollo for the first landing on the Moon. Figure 4-1 shows the location of these sites within the ± 5° latitude, ± 45° longitude Apollo zone.

Primary-site photography was accomplished from altitudes ranging from 45 to 59 kilometers with camera axis orientations between near-vertical and 38 degrees cross-track tilt. The areal coverage of each pri-

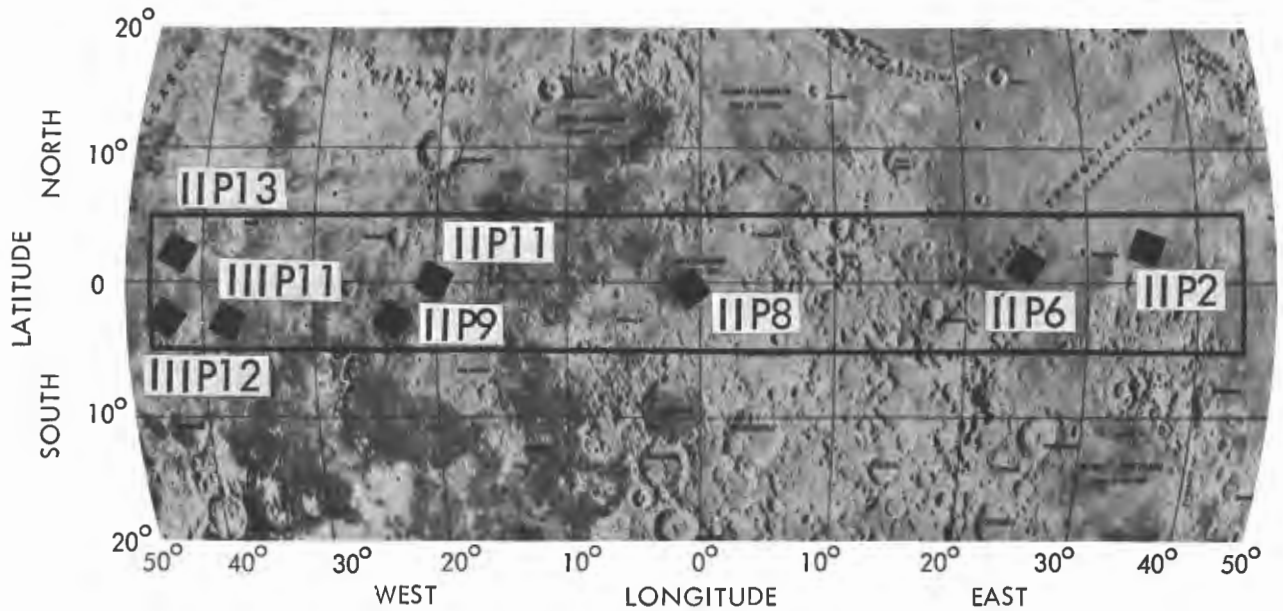

Figure 4-1: Candidate Apollo Landing Site Locations

mary-site photo pass is given in Table 4-1. It must be remembered that priority readout data only was obtained for Primary Sites IIIP-1 through -6. This limited data shows that these sites were photographed as planned.

Secondary-site photography was taken at altitudes between 44 and 63 kilometers on the nearside and from 1460 kilometers on the farside. Camera axis orientations varied from vertical to 69 degrees cross-track tilt. Final readout provided complete photography of Sites IIIS-9 through -31 prior to the mission termination. Secondary Sites IIIS-1 through -5 and -7 were not read out during the priority readout period. The wide-angle photos of Sites IIIS-6 and -8 were read out in primary readout but not the telephoto exposures. Areal coverage of secondary-site photography is summarized in Table 4-2. Over 90% of the secondary-site photography nearside coverage of nearly 520,000 square kilometers was taken from oblique angles, indicating increased realization of the value of this type of photography.

Mission photography was conducted as planned except for minor changes in site coordinates, a change from a single eight-frame sequence over Site IIIP-12b to two four-frame sequences on two passes, and cancellation of Secondary Site IIIS-32. These changes were made to ensure coverage of the desired area and to improve photo quality. The cancellation was made to initiate final readout early and prevent further film hangups from occurring in priority readout.

The 24 priority readout periods (Sequences 005 through 026) which were not duplicated during final readout are shown in Figure 4-2. During this phase it was desired to read out all of the wide-angle photos shown in Figure 1-5 and sections of the telephoto exposure on either side. The processing period was to be adjusted as early as possible so that the processing stop marks occurred in the wide-angle photos. (Readout had progressed to Sequence 018 before a processor stop line was read out.) The processor stop line was also used to establish the actual processor operating speed. Analysis of the TWTA failure data from Mission II resulted in restrictions on when the TWTA could be turned on. These restrictions resulted in a shortening of the priority readout periods. The combined results of these factors resulted in inaccurate positioning of the film at the readout gate and, in some cases, termination of readout before the desired wide-angle photo had been read out. The overall result was a significant reduction of the wide-angle photography of Primary Sites IIIP-2b, -3, -4, and -5a recovered.

4.1.1 Mission Photography

Analysis and assessment of mission photography was based upon visual examination of second-generation GRE positive transparencies, third-generation 9.5-inch reassembled negative transparencies, and paper prints made from manually reassembled GRE film using a 10 to 30X zoom macroscope. Primary-photo-site photography was examined by selecting frames from the start, middle, and end of a photo sequence for critical assessment.

Lunar orbital photography was made particularly difficult by uncertainties in knowledge of the Moon's surface characteristics and its photometric function, both of which are critical to photography. The Moon has unique reflectance characteristics unlike any encountered in terrestial photography. The wide range of reflectance can and did produce photographic images in adjacent areas having a density range that exceeded the capability of the spacecraft readout system (thus obliterating detail in areas of density extremes) while exhibiting excellent detail in the surrounding areas. Experience gained during previous missions was used to refine the selection of photographic parameters needed to determine the required exposure settings.

To aid in evaluating Mission III photos, reseau marks illustrated in Figure 4-3 were pre-exposed on the spacecraft film at the same time as the edge data. The fixed orien-

Table 4-1: PRIMARY-SITE COVERAGE

PHOTO SITE	NUMBER OF FRAMES	APPROXIMATE AREA PHOTOGRAPHED				
		Wide Angle		Telephoto		
		Size (km)	Area (km^2)	Size (km)	Area (km^2)	
Primary Sites						
III P-1	16	108 x 44	4750	75 x 20	1500	
P-2a	8	65 x 42	2730	35 x 18	630	
P-2b	4	52 x 50	2600	19 x 20	380	Converging Telephoto Stereo
P-3	4*	101 x 55	5550	21 x 22	460	
P-4	8	63 x 40	2520	34 x 18	610	
P-5a	8	64 x 42	2690	34 x 18	610	Converging Telephoto Stereo
P-5b	8	63 x 41	2580	34 x 18	610	
P-6	4*	82 x 39	3200	17 x 17	290	
P-7a	8	67 x 47	3150	34 x 18	610	Converging Telephoto Stereo
P-7b	8	59 x 38	2240	32 x 16	510	
P-8	8	58 x 36	2090	31 x 16	500	
P-9a	8	81 x 72	5830	40 x 21	840	
P-9b	8	61 x 40	2440	33 x 17	560	
P-9c	8	63 x 40	2520	34 x 17	580	Converging Telephoto Stereo
P-10	8	68 x 46	3130	37 x 20	740	
P-11	8	67 x 43	2880	36 x 19	680	
P-12b.2	4	51 x 48	2450	19 x 19	360	
P-12a	16	105 x 44	4620	70 x 19	1330	
P-12b.1	4	51 x 44	2240	18 x 19	340	
P-12c	8	83 x 65	5400	42 x 22	920	Converging Telephoto Stereo
			65,610		13,060	

*Slow Mode

Table 4-2: SECONDARY-SITE COVERAGE

PHOTO SITE	NUMBER OF FRAMES	APPROXIMATE AREA PHOTOGRAPHED				
		Wide Angle		Telephoto		
		Size (km)	Area (km^2)	Size (km)	Area (km^2)	
Secondary						
S-6	1	------	44,000	------	------	Oblique
8	1	------	47,000	------	------	Oblique with Horizon
9	1	39 x 32	1,250	17 x 4	70	Near Vertical
10	4*	78 x 37	2,890	16 x 16	260	Near Vertical
11	1	------	37,000	------	2,200	Oblique with Horizon
13	1	142 x 117	16,600	74 x 9	670	Oblique
14	1	96 x 63	6,050	34 x 7	240	Oblique
15	4*	85 x 40	3,400	18 x 18	320	Oblique
16	1	36 x 30	1,080	16 x 4	60	Near Vertical
17	4*	90 x 43	3,870	19 x 19	360	Near Vertical
18	4	51 x 44	2,240	19 x 19	360	Oblique
19	4*	81 x 38	3,080	17 x 17	290	Near Vertical
20	1	------	48,000	------	2,700	Oblique with Horizon
21	1	------	32,000	------	1,800	Oblique with Horizon
21.5	1	1280x1680	215,000	------	12,000	Farside Oblique
22	1	44 x 35	1,540	19 x 4	80	Oblique
23	4*	97 x 46	4,460	20 x 20	400	Oblique
24	1	158 x 140	22,100	------	1,200	Oblique
25	1	160 x 160	25,600	52 x 34	1,400	Oblique
26	1	------	53,000	------	3,000	Oblique with Horizon
27	1	------	51,000	------	2,800	Oblique with Horizon
28	1	------	23,000	------	1,300	Oblique with Horizon
29	1	------	42,000	------	2,300	Oblique with Horizon
30	1	------	46,000	------	2,600	Oblique with Horizon
31	1	50 x 43	2,150	22 x 6	130	Near Vertical

*Slow Mode

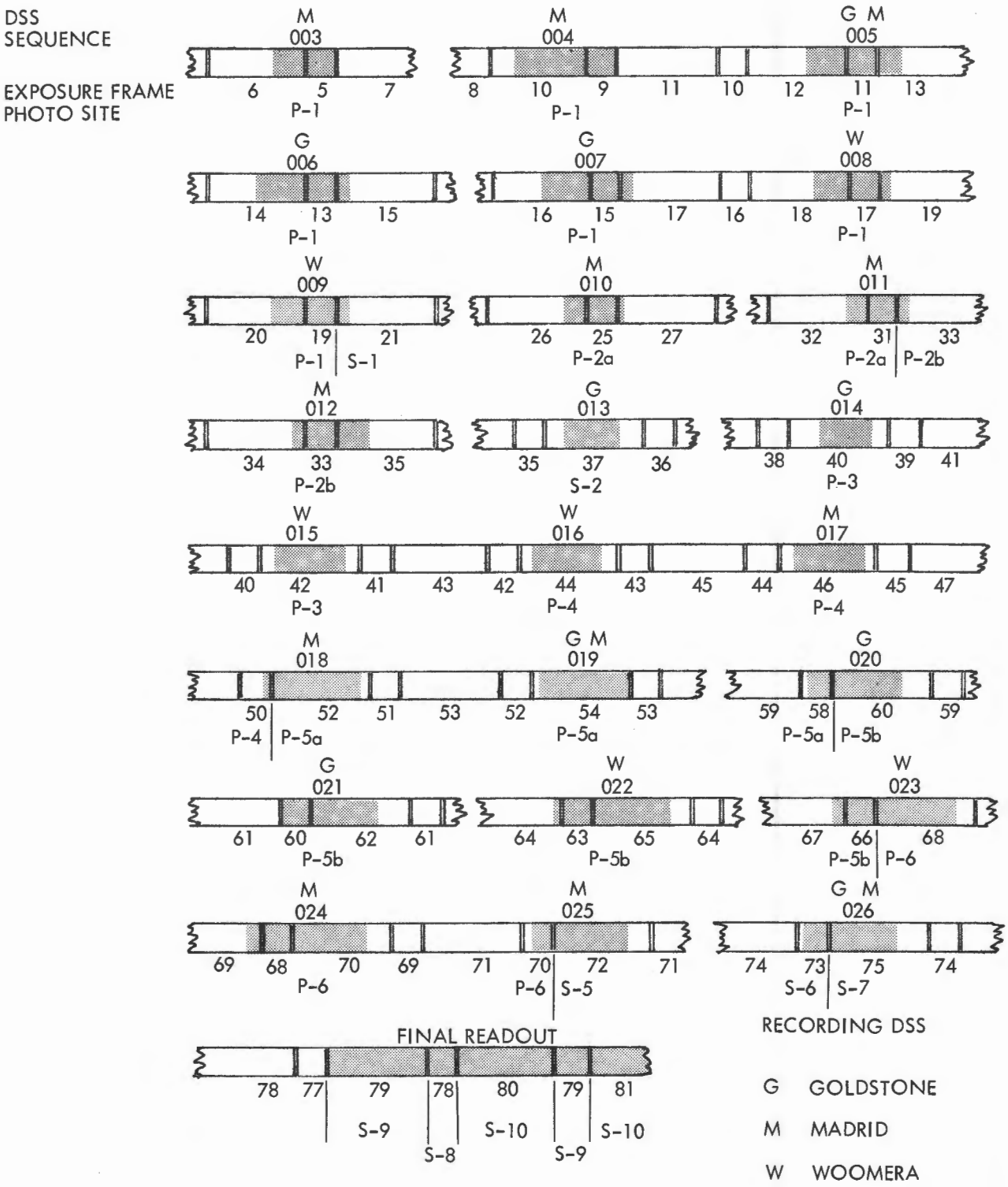

Figure 4-2: Mission III Priority Readout

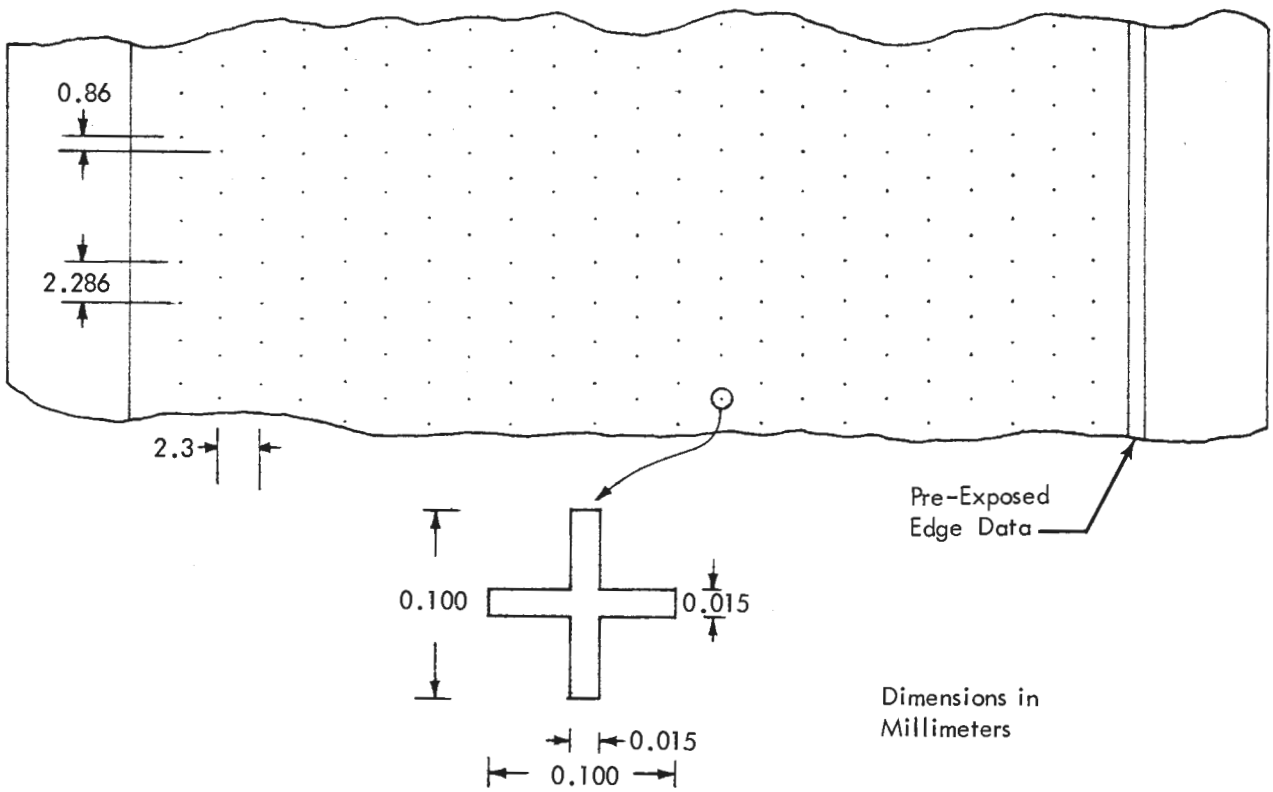

Figure 4-3: Pre-Exposed Reseau Mark Characteristics

tation, which differs from the pattern employed on Mission II, can assist the photo analyst in the detection and compensation for distortions introduced after imaging by the camera lens.

The overall quality of the Mission III wide-angle (80-mm lens) photos was very good and verified the capability to employ a greater diversity of photographic techniques than that used for previous missions. Addition of the 0.21 neutral-density filter to the 80-mm lens successfully balanced the exposure levels obtained with both lenses. A comparison of the predicted and actual densities showed about a 0.2 density consistent differential. Photographs of the first six primary sites ranged from slightly to quite underexposed. Corrections were applied to the exposure computations and the exposure was improved for the remaining sites.

Examination of representative photos of each site showed that the resolution requirements (8 meters plus a correction increment for the altitude difference from 46 kilometers) were met—and in some cases exceeded—at all sites. Craters and rocks spanning as few as three readout scan lines were detected at many sites where image contrast was enhanced by illumination geometry. The ground resolution requirements at 46 kilometers is equivalent to approximately four readout scan lines.

Proper forward overlap was obtained in both the fast mode (87% overlap) and slow mode (50% overlap) employed for the primary and many secondary sites. Side overlap varied depending on the controls employed. In all cases the desired area of coverage was obtained. Many of the secondary-site oblique photos were taken to augment primary-site photography by providing profile visibility of the surrounding area.

Processing marks which result from the intermittent processing schedule employed

during the mission were evident in many of the wide-angle photos. The resulting local degradation was expected because operational control procedures required placing these effects in the wide-angle rather than telephoto exposures.

Telephoto (610-mm lens) photo quality was generally very good. These photos usually displayed a wider range of image densities than the corresponding wide-angle frames. Examination of the photos showed that the resolution requirement (1 meter plus a correction increment for the deviation from 46 kilometers) was met at all sites. The nominal 5% forward overlap desired during each fast-mode sequence was verified at all sites read out. Six of the 12 primary-site photographs included the use of the convergent telephoto stereo methods that were proved feasible on Mission II. Evaluation of Mission II results by the Aeronautical Charting and Information Center showed that 2- to 3- meter form lines are possible as compared to about 25-meter form lines possible from conventional forward-overlap stereo photography. The employment of camera axis tilt to obtain this coverage reduces resolution somewhat. This penalty is offset by retaining maximum resolution of the area by near-vertical photography. The convergent telephoto stereo photos produced the desired results for Mission III primary sites. In addition, the desired convergent telephoto stereo coverage of Mission II Primary Site IIP-13 was attained consistent with the 9-degree difference in orbit inclination of the two missions.

Detailed examination of the telephoto and wide-angle photography of the Surveyor I landing site identified the precise landing site. Spacecraft Frame 194 contained the area in the vicinity of the landing site. Close examination of the telephoto frame covering the estimated location as determined by the use of triangulation methods with Surveyor photos showed the spacecraft, which was identified by the characteristics of its shadow. Confirmation was made by comparison and identification of small craters shown by both Surveyor and Lunar Orbiter photographs.

These areas are shown in Figures 4-14 through 4-17. Figure 4-17 shows an enlargement of the Surveyor I. Knowing the exact location of the Surveyor I, the Mission I telephoto photos of the same area were examined and the smeared image of the reflection from Surveyor I was evident in Frame 208, Framelet 097.

During preparation of this report, the successful flight of Surveyor III was accomplished. A comparison was made of the topographic features contained in the photos from the two missions by Surveyor project personnel. The results of the comparison show that Surveyor III spacecraft had landed in the 200-meter-diameter crater. Figures 4-11a and b show the wide-angle and a section of the telephoto photos (frame 154) nearly centered on the actual Surveyor III landing site. Figure 4-11c, approximately a 100 diameter enlargement of the spacecraft film, indicates the detailed features identified in both Lunar Orbiter III and Surveyor III photos. Analysis of these photos has enabled determination of the actual location of Surveyor III to within 1 meter.

A comparison of the coordinates of the primary-site locations shown in Tables 1-1 and -2 with the results shown in Tables 4-1 and -2 show that the photographic objectives were accomplished. Photographic coverage was not always centered on the specified location because of operational limitations. These included such items as: the photo orbit did not always pass directly over the site; camera-on time was determined for the first frame of the sequence only (subsequent exposures were controlled by the spacecraft velocity-to-height determination); in addition, variations of spacecraft attitude during the photo sequence, variations in lunar surface elevations, uncertainties in the mathematical model of the Moon, and errors in the lunar charts all contribute to the apparent displacements. A similar comparison can be made for the near-vertical secondary sites.

All oblique photos contained the lunar surface features specified for each secondary site.

Matching individual photos with the most recent lunar charts indicates varying degrees of agreement. Some contributing factors to this problem are indicated above. In addition, a secondary objective of the Lunar Orbiter program is to obtain tracking data from which to refine the mathematical model of the Moon. To compute the photo supporting data and predicted photo locations, the best available estimates for these parameters must be used in the orbit determination routines. Therefore, some discrepancies can be expected in coordination of the computed photo location with the maps made from Earth-based observations.

Other errors in locating the photos stem from spacecraft attitude variations within the ±0.2-degree control deadband and the lunar surface elevation changes. It must also be remembered that considerable effort is required to transfer the data from the unrectified, nonorthographic projection photographs to the Mercator projection maps. In general, the lunar feature matching between the photos and lunar charts indicate that the predicted photo locations are generally consistent with the chart "reliability diagram." Continued analysis and comparison of photos obtained from each photo mission will result in more accurately defining the lunar surface, and reducing the positioning error in subsequent lunar charts.

4.1.2 Photo Coverage

Table 4-3 summarizes major photographic parameters of Mission III primary sites and provides significant supporting data for each site. Geometric parameters of photography are illustrated in Figure 4-4. The angle of incidence is defined as the angle between the Sun's rays and the normal to the lunar surface. The phase angle is the angle between the camera axis and the Sun's rays. The angle and altitude ranges are for the first and last frame of the sequence, respectively. The angle "alpha" is defined as the angle between the projection of the surface normal and the camera axis, measured in the phase angle (camera-Sun-principal point) plane. Supporting data presented for Primary Sites IIIP-1 through -6 are based on mission predictions because the exposure times were not read out during priority readout.

Corresponding data for the secondary sites on the nearside are given in Table 4-4. The slant distance is defined as the distance between the camera and the principal ground point (the intersection of the projected camera axis and the lunar surface). Tilt angle is defined as the true angle between the camera axis and the local vertical through the spacecraft. Tilt azimuth is the clockwise angle from lunar north to principal ground point measured from the vertical projection of the spacecraft on the lunar surface. Secondary sites identified as oblique photos have a scale factor that changes throughout the photo. The framelet width numbers given apply at the center of the photo format only. The single farside photo is also shown in the table. During priority readout emphasis was placed on early recovery of primary-site photos with very limited secondary-site photo readouts. As a result, the photos of Sites IIIS-1 through -5 and -7 were not recovered and, therefore, are not included in the table.

The following photographs, Figures 4-5 through 4-21, are representative of portions of the primary and secondary photo sites identified for this mission. Also included are representative farside photography, frontside areas of interest, and examples of moderate resolution and accompanying high resolution. Oblique photos of some secondary sites were of candidate Apollo landing sites. Vertical coverage of these sites is outlined on the oblique photos. Selected photos also provide areas of additional interest within these areas. Each photo contains a descriptive caption.

Table 4-3: PRIMARY-SITE SUPPORTING DATA

PHOTO SITE	SPACECRAFT EXPOSURE NO./ORBIT	SHUTTER SPEED (sec)	LOCATION OF PHOTO CENTER		SPACECRAFT		APPROXIMATE FRAMELET WIDTH		PHASE ANGLE (deg)	ALPHA (deg)	ANGLE OF INCIDENCE (deg)	CAMERA AXIS TILT	
			Long. (deg)	Lat. (deg)	Altitude (km)	Slant Distance (km)	Wide Angle (km)	Telephoto (km)				Angle (deg)	Azimuth (deg)
P-1	5-20/44	0.04	35.2°E	2.7°N	56-54	56-54	1.8-1.7	0.23-0.22	74.8		76.8-74.6		
P-2a	25-32/45	0.02	42.4°E	1.1°N	51	51	1.6	0.21	65.8	1.25	67.1-66.2	3.3	204
P-2b	33-36/46	0.02	42.7°E	1.1°N	52	55	1.8	0.23	73.3	9.9	64.4-64.8	19.9	23
P-3	40-43/50	0.04	20.2°E	3.2°N	59-56	62-59	2.0-1.9	0.26-0.25	73.7		81.1-79.2	17.1	208
P-4	44-51/51	0.02	27.4°E	0.6°N	49	49	1.6	0.20	72.3		71.5-70.6	4.0	11
P-5a	52-59/52	0.02	24.5°E	0.4°N	49	50	1.6	0.21	67.8	4.1	72.7-71.8	14	204
P-5b	60-67/53	0.02	24.6°E	0.5°N	48	49	1.6	0.20	74.5	−4.5	70.8-69.9	11	21
P-6	68-71/54	0.02	21.5°E	0.3°N	48	48	1.6	0.20	69.3	2.9	72.4-70.9	7	200
P-7a	86-93/64	0.04	1.3°W	0°	47-46	51-50	1.6	0.21	69.4	6.1	77.3-76.3	23	203
P-7b	94-101/65	0.04	1.2°W	0.48°N	45	46	1.5	0.19	71.6	3.5	75.5-74.7	10	205
P-8	124-131/77	0.04	19.7°W	1.3°N	45	45	1.5	0.19	72.3	0.2	72.8-72.0	0	---
P-9a	137-144/80	0.04	23.0°W	3.2°S	46-47	59	1.9	0.25	62.3	2.1	70.8-69.7	38	200
P-9b	145-152/81	0.04	22.8°W	2.8°S	47-48	48	1.6	0.20	66.3	1.8	68.8-67.9	8	200
P-9c	153-160/82	0.04	23.1°W	3.1°S	49	49	1.6	0.20	68.5	−1.5	67.4-66.5	2	27
P-10	163-170/86	0.04	41.9°W	1.7°N	52-51	55-54	1.8-1.7	0.23-0.22	84.5	−6.1	79.4-78.4	17	16
P-11	173-180/89	0.04	36.9°W	3.4°S	52	52	1.7	0.21	67.9	0.5	68.9-67.9	3	190
P-12b.2	181-184/90	0.04	43.3°W	2.2°S	51	54	1.7	0.22	67.6	4.5	73.3-72.9	19	200
P-12a	185-200/91	0.04	43.6°W	2.0°S	51-52	53	1.7	0.22	68.2	3.0	72.7-70.6	12	198
P-12b.1	201-204/92	0.04	43.3°W	3.0°S	53	53	1.7	0.22	68.7	0.8	69.8-69.3	4	190
P-12c	205-212/93	0.04	44.2°W	2.6°S	54	62	2.0	0.26	82.3	16.2	69.3-68.2	30	21

Table 4-4: SECONDARY-SITE SUPPORTING DATA

PHOTO SITE	SPACECRAFT EXPOSURE NO./ORBIT	SHUTTER SPEED (sec)	LOCATION OF PHOTO CENTER		SPACECRAFT		APPROXIMATE FRAMELET WIDTH		PHASE ANGLE (deg)	ALPHA (deg)	ANGLE OF INCIDENCE (deg)	CAMERA AXIS TILT	
			Long. (deg)	Lat. (deg)	Altitude (km)	Slant Distance (km)	Wide Angle (km)	Telephoto (km)				Angle (deg)	Azimuth (deg)
Surveyor Screening													
S-10	80-83/61	0.02	13.6°W	1.6°S	45	45	1.5	0.19	69.4	−2.2	68.0–66.5	5	20
S-14	102/66	0.04	9.1°W	4.9°N	52	70	2.2*	0.29*	82.0	−3.8	81.4	41	360
S-17	108-111/70	0.02	4.0°E	4.6°S	52	52	1.7	0.21	62.5	−1.5	61.7–60.1	1	50
S-19	116-119/72	0.02	3.7°E	3.6°S	47	47	1.5	0.19	63.8	1.1	65.9–64.4	6	190
S-22	122/75	0.04	22.0°W	1.0°N	58	50	1.6*	0.21*	72.3	5.4	78.3	18	203
Apollo Landing Sites													
S-11	84/62	0.01	1.1°W	0.9°N	47	134	4.3*	0.56*	15.6	57.9	80.3	67	258
S-21	120/74	0.01	19.5°W	0.7°S	45	120	3.8*	0.50*	15.0	52.1	77.5	66	258
S-24	136/79	0.01	23.1°W	3.1°S	46	112	3.6*	0.47*	17.2	29.2	72.1	64	253
S-25	161/83	0.02	41.9°W	1.6°N	52	131	4.2*	0.54*	15.6	68.4	84.0	65	270
S-27	171/87	0.01	36.8°W	3.8°S	51	115	3.7*	0.48*	15.0	38.7	71.8	62	255
S-28	172/88	0.01	43.8°W	2.3°S	50	134	4.3*	0.56*	16.6	45.9	77.1	66	255
Farside													
S-21.5	121/74	0.02	126.7°E	24.0°S	1461	1530	49*	6.4*	70.0	−1.4	70.5	13	182

*Framelet width applies only at center of photo.

Table 4.4: SECONDARY—SITE SUPPORTING DATA (Cont'd)

PHOTO SITE	SPACECRAFT EXPOSURE NO./ORBIT	SHUTTER SPEED (sec)	LOCATION OF PHOTO CENTER		SPACECRAFT		APPROXIMATE FRAMELET WIDTH		PHASE ANGLE (deg)	ALPHA (deg)	ANGLE OF INCIDENCE (deg)	CAMERA AXIS TILT	
			Long. (deg)	Lat. (deg)	Altitude (km)	Slant Distance (km)	Wide Angle (km)	Telephoto (km)				Angle (deg)	Azimuth (deg)
Scientific Interest													
S-6	73/56	0.04	6.5°E	8.2°N	62	104	3.4*	0.43*	101.0	−21.6	83.4	52	21
S-8	78/58	0.01	26.5°E	9.9°S	55	170	5.4*	0.70*	78.5	−58.5	59.8	69	180
S-9	79/59	0.01	17.6°E	1.8°S	47	47	1.5	0.56	69.5	−2.9	66.7	7	22
S-13	85/63	0.04	0.4°W	5.0°N	49	93	3.0*	0.38*	99.4	−30.1	78.0	57	21
S-15	103-106/67	0.04	5.6°W	0.6°N	45	49	1.6*	0.20	69.5	5.2	76.6–75.1	19	203
S-16	107/69	0.02	5.7°W	0.3°S	44	44	1.4	0.18	70.5	1.8	72.4	5	204
S-18	112-115/71	0.02	8.1°W	2.2°S	44	54	1.7*	0.22*	63.0	3.5	71.5	35	200
S-20	123/76	0.04	27.7°W	7.4°N	53	148	4.7*	0.62*	85.2	−18.0	82.4	67	0
S-23	132-135/78	0.02	17.5°W	3.8°S	47	56	1.8*	0.23*	60.4	2.6	68.8–67.1	33	200
S-26	162/84	0.04	38.3°W	6.5°N	53	166	5.3*	0.69*	104.2	−44.2	79.0	69	21
S-29	213/94	0.04	59.7°W	3.1°S	57	156	5.0*	0.65*	68.8	−2.5	82.5	66	201
S-30	214/96	0.04	64.4°W	7.0°N	61	166	5.3*	0.69*	86.0	−14.1	84.0	66	0
S-31	215/97	0.06	66.7°W	2.1°N	63	63	2.0	0.26*	83.2	1.2	84.3	1	291

*Framelet width applies only at center of photo.

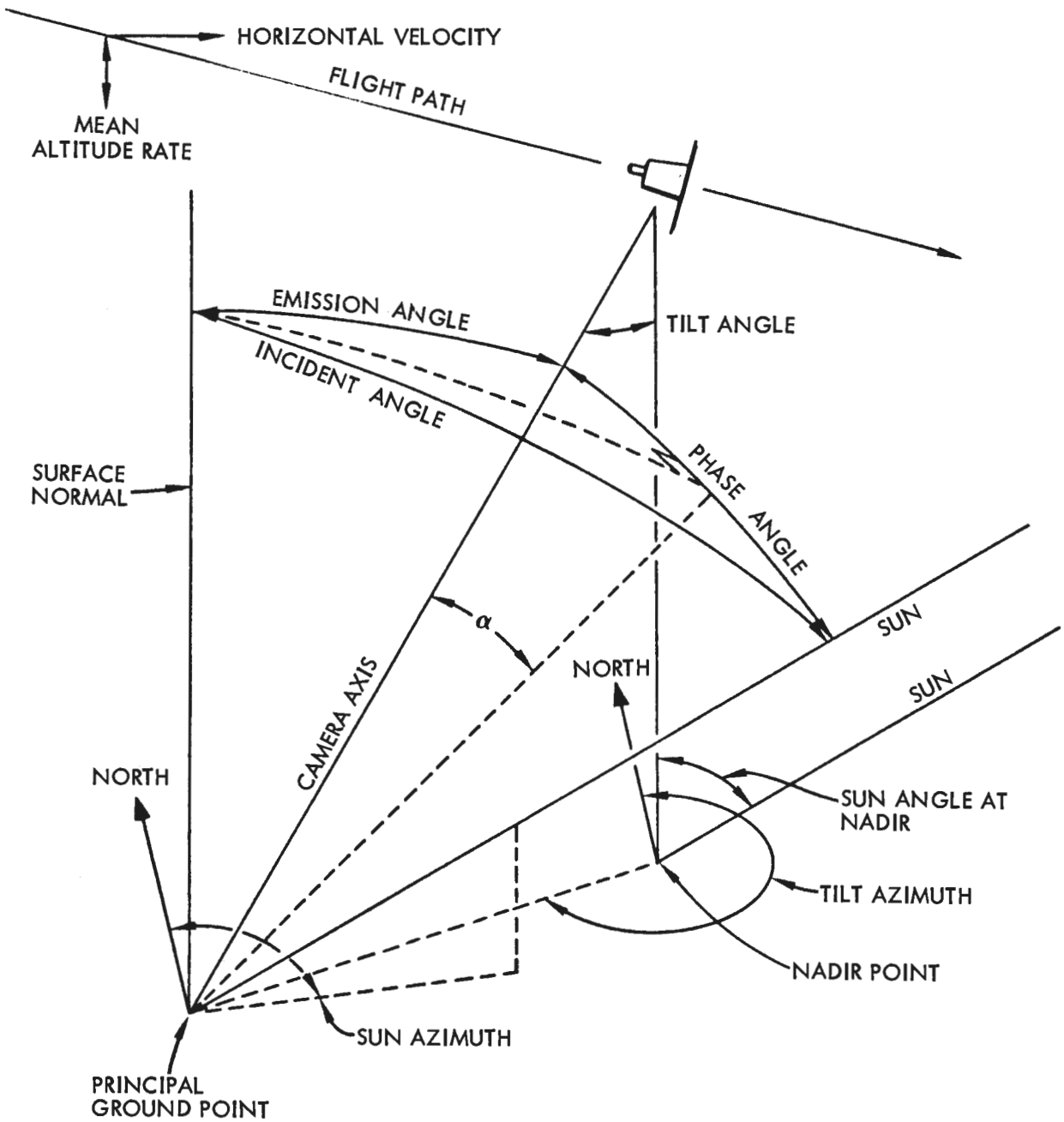

Figure 4-4: Geometrical Parameters of Photography

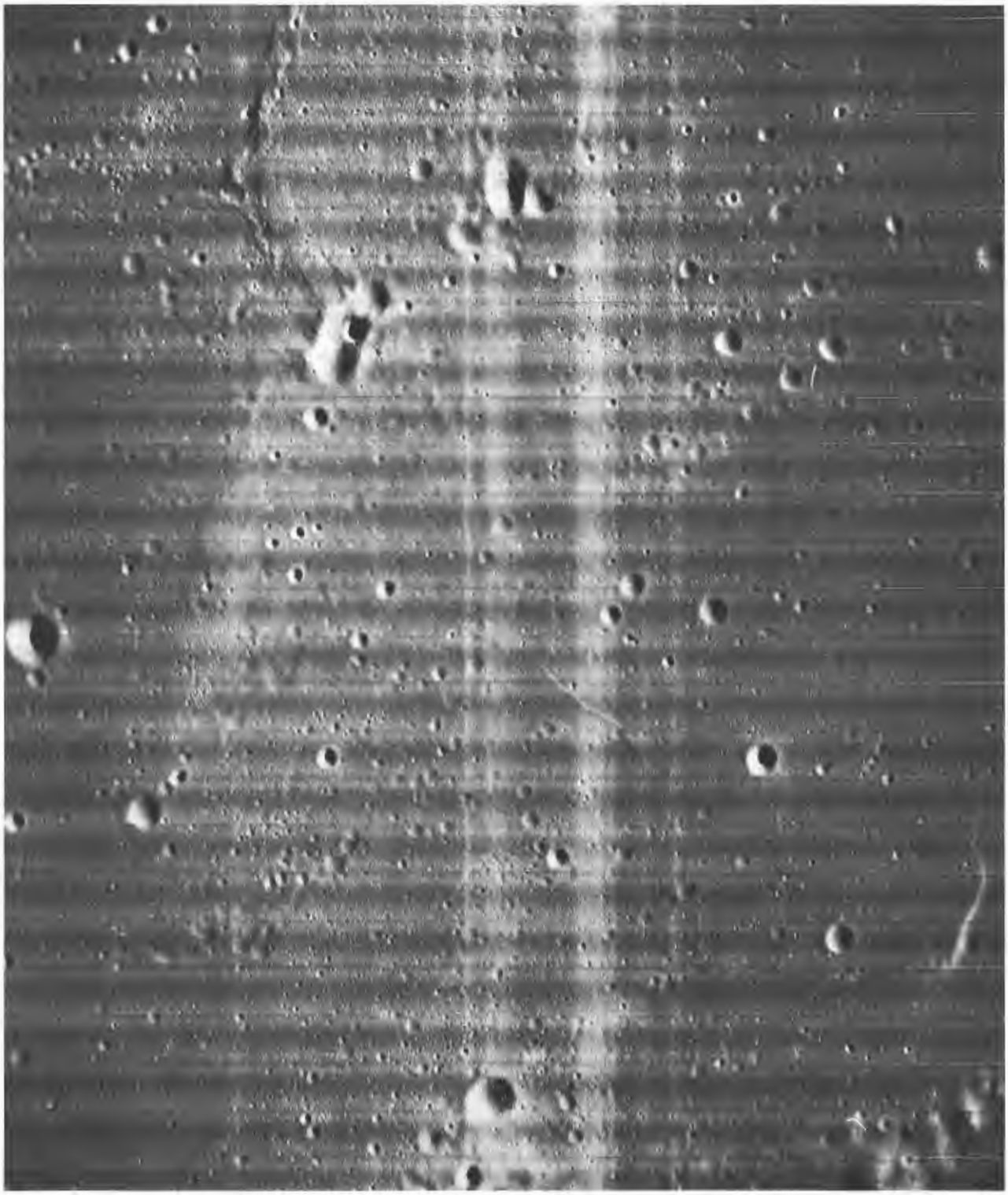

Figure 4-5: Wide Angle Frame 15—Site III P-1
Framelet Width: 1.7 km
(Vertical white bands in center of photo attributed to periodic static discharges from a teflon film separator)

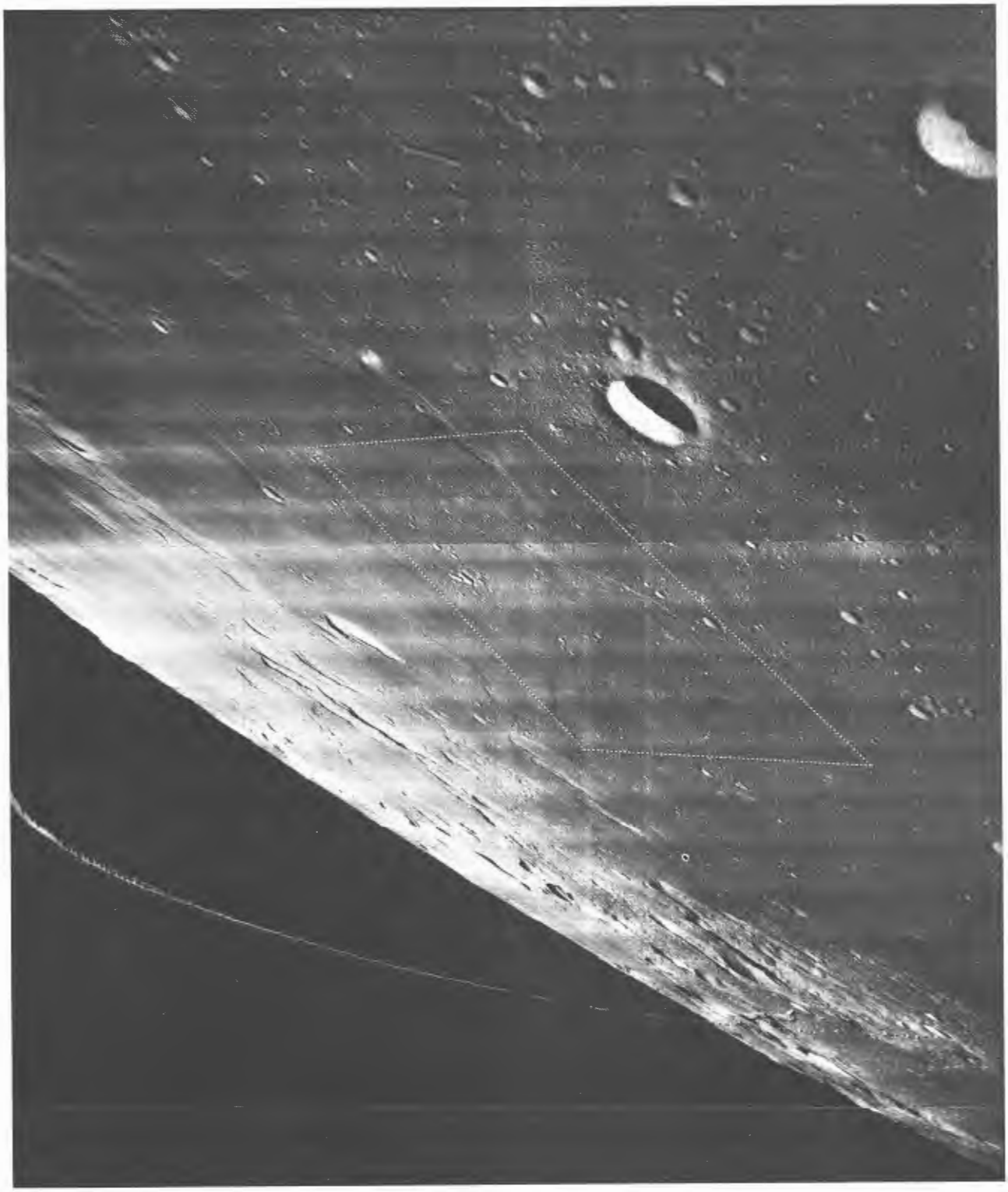

Figure 4-6: Wide Angle Frame 84—Site III S-11
Oblique photo centered on Site III P-7 coordinates
(Outlined area covered by Figure 4-7)

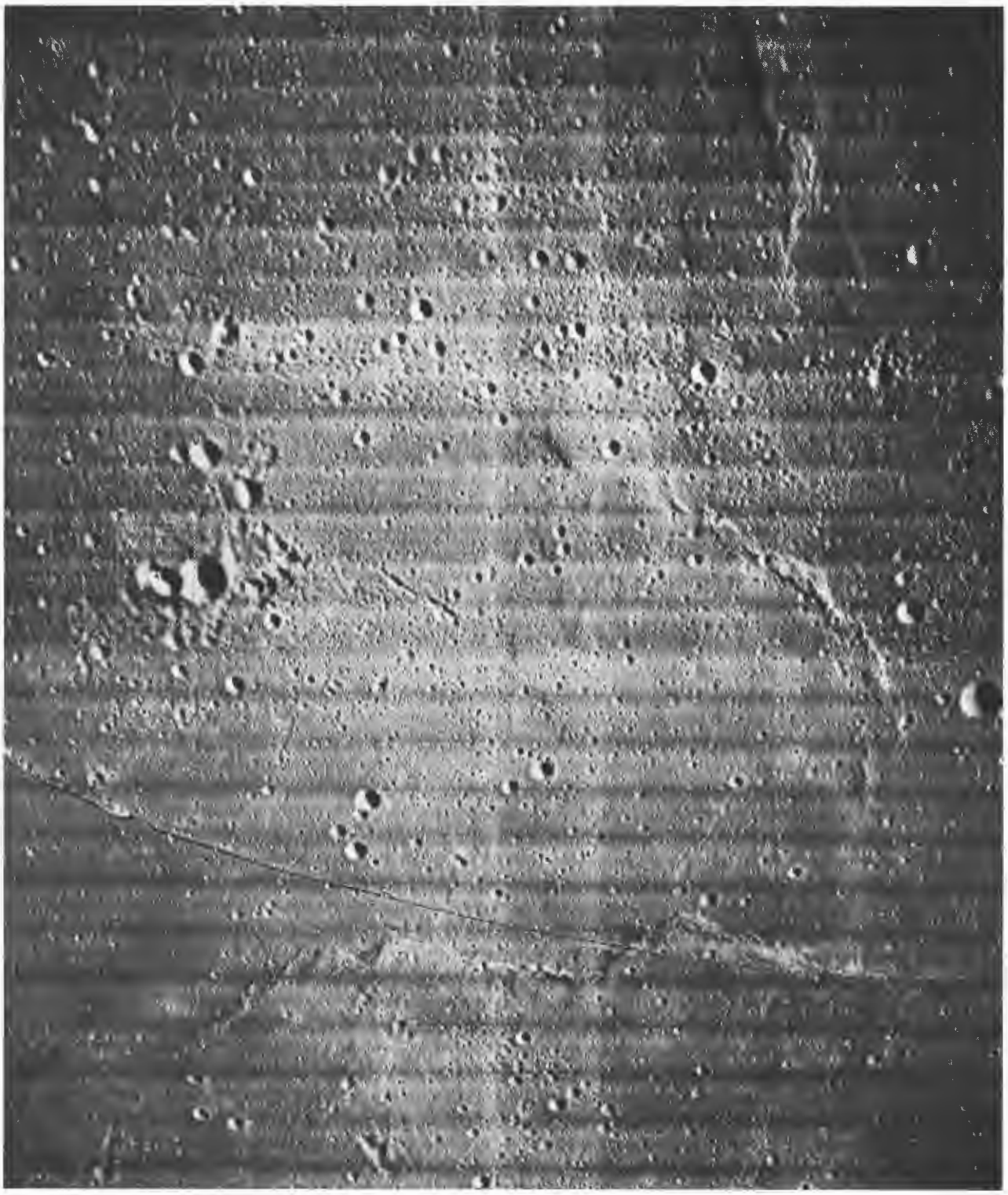

Figure 4-7: Wide Angle Frame 92—Site III P-7
Framelet Width: 1.6 km
(Outlined area covered by Figure 4-8)

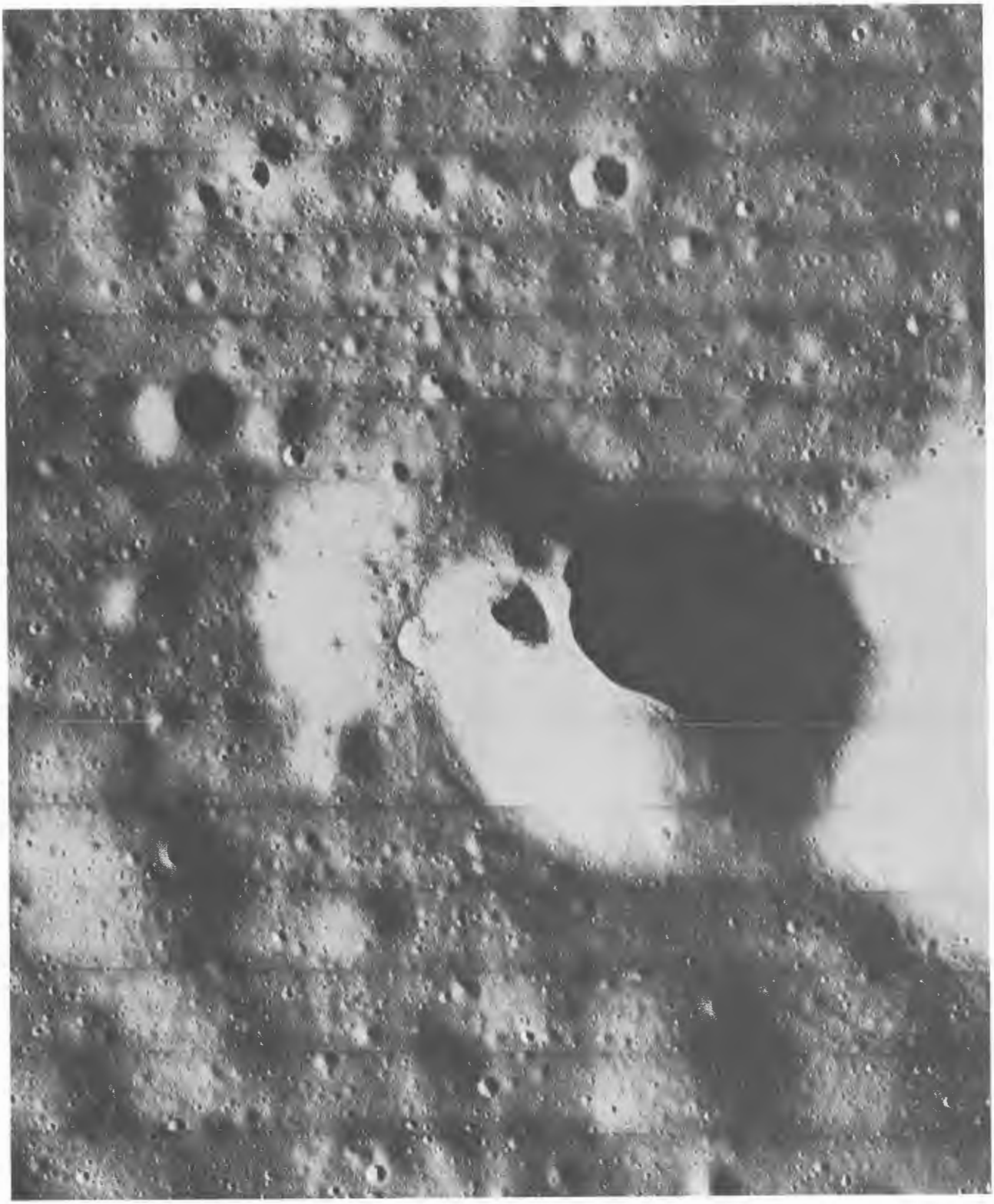

Figure 4-8: Telephoto Frame 89—Site III P-7
Framelet Width: 210 meters

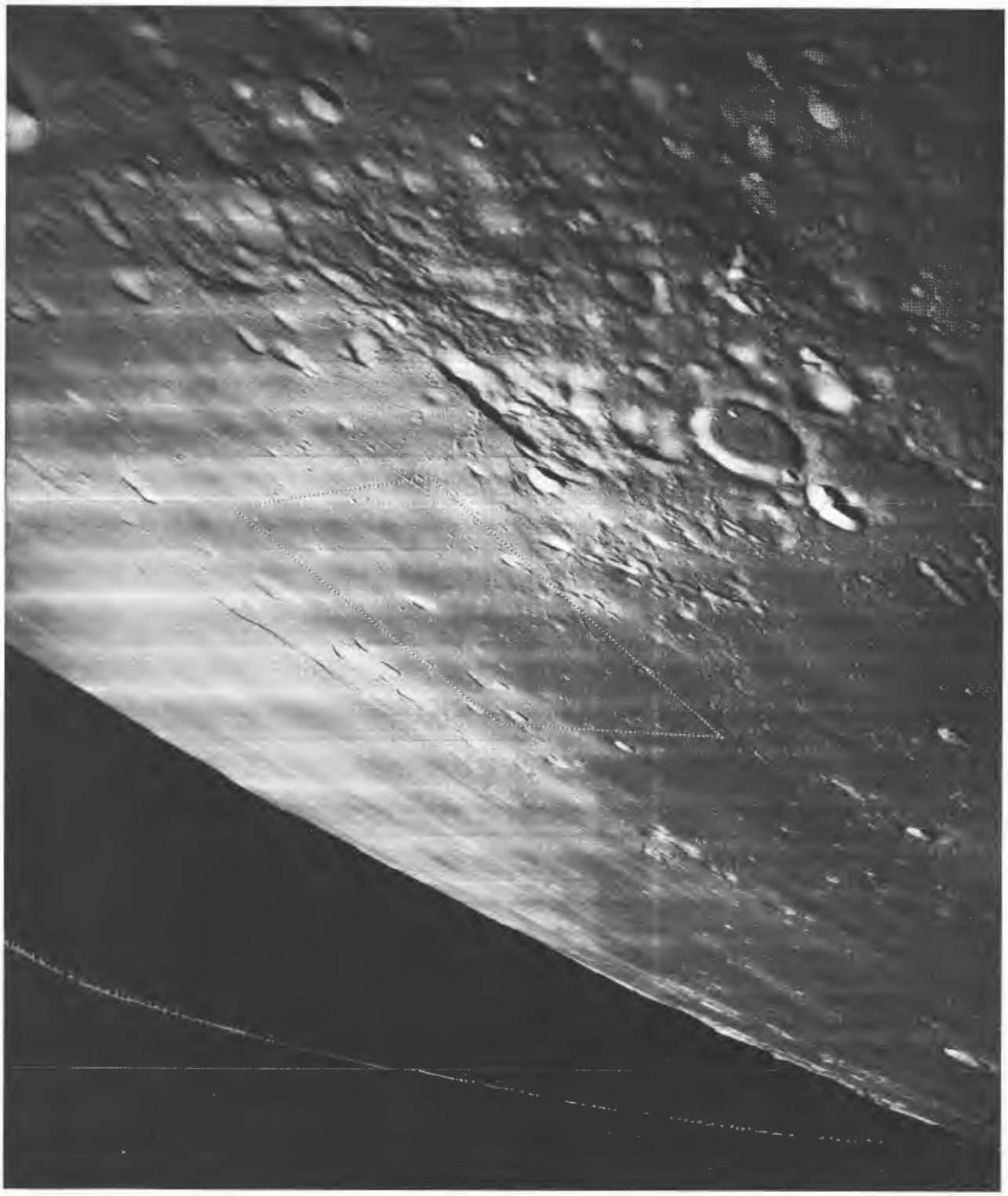

Figure 4-9: Wide Angle Frame 120—Site III S-21
Oblique photo centered on Site III P-8 coordinates
(Outlined area covered by Figure 4-10)

Figure 4-10: Wide Angle Frame 126—Site III P-8
Framelet Width: 1.5 km

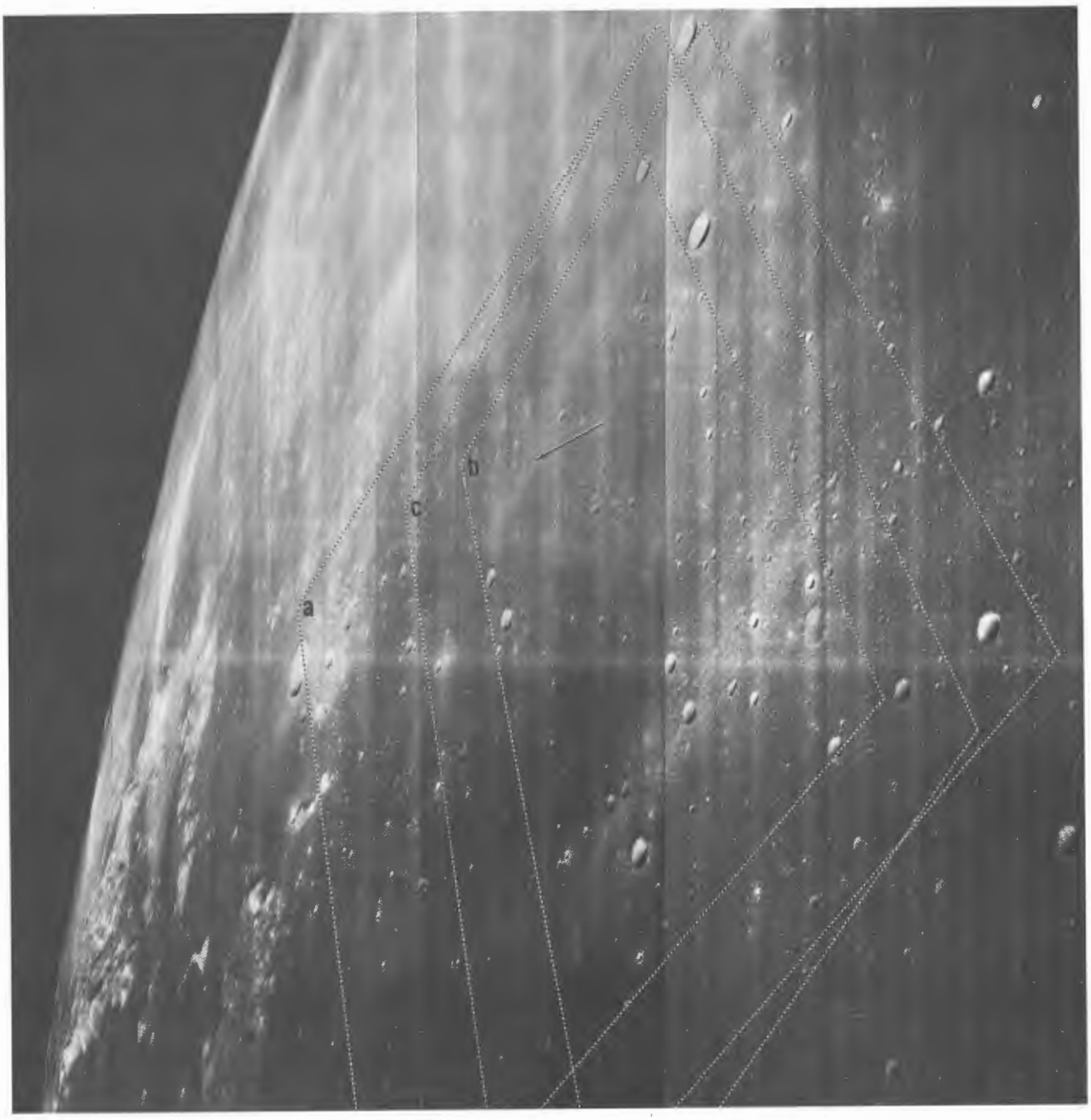

Figure 4-11: Wide Angle Frame 136—Site III S-24
Oblique photo centered on Site III P-9 coordinates for Surveyor III landing site and showing vertical photographic coverage.
(Letters identify photo passes)

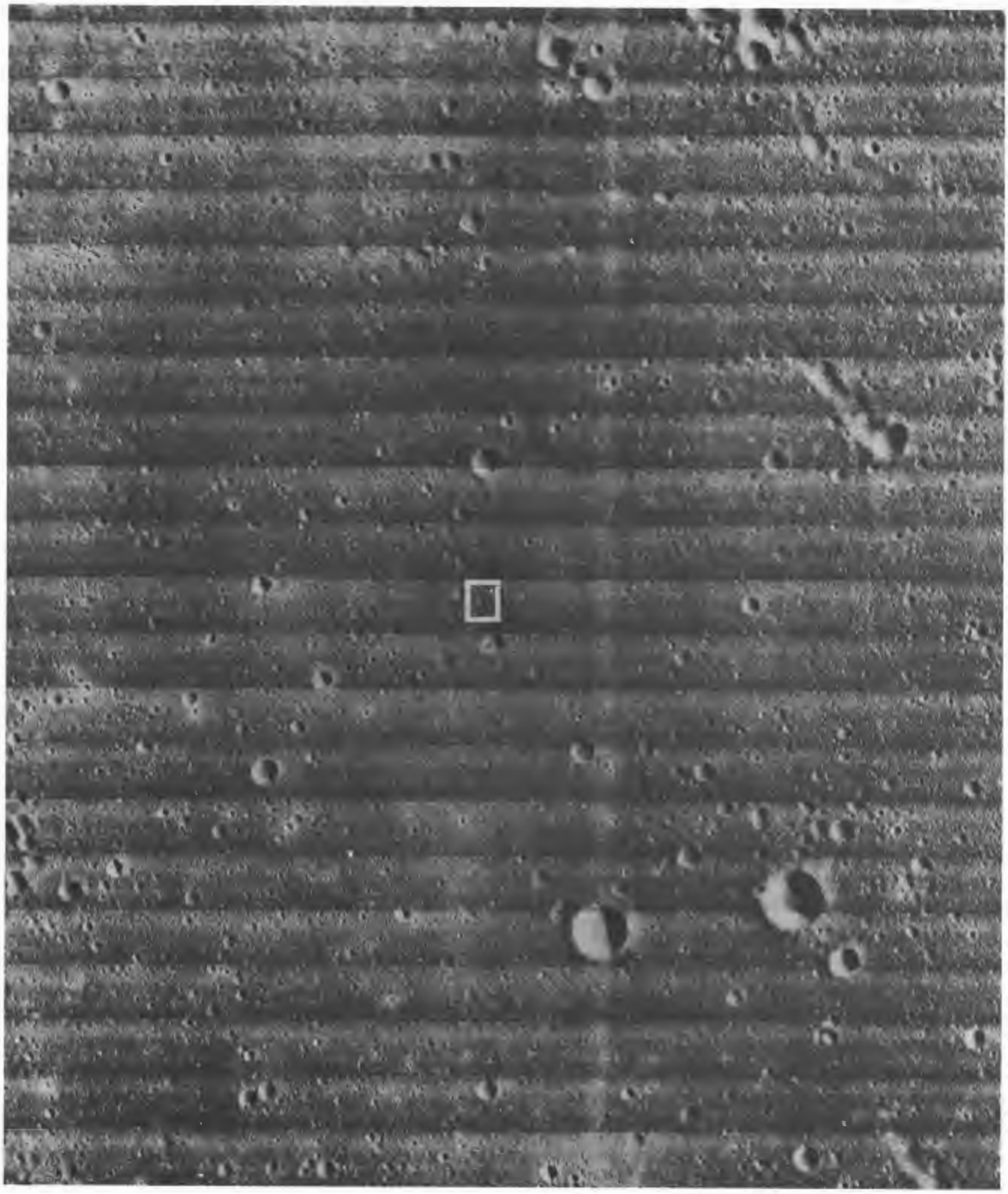

Figure 4-11a: Wide Angle Frame 154—Site III P-9
Framelet Width: 1.6 km
(Outlined area covered by Figure 4-11b)

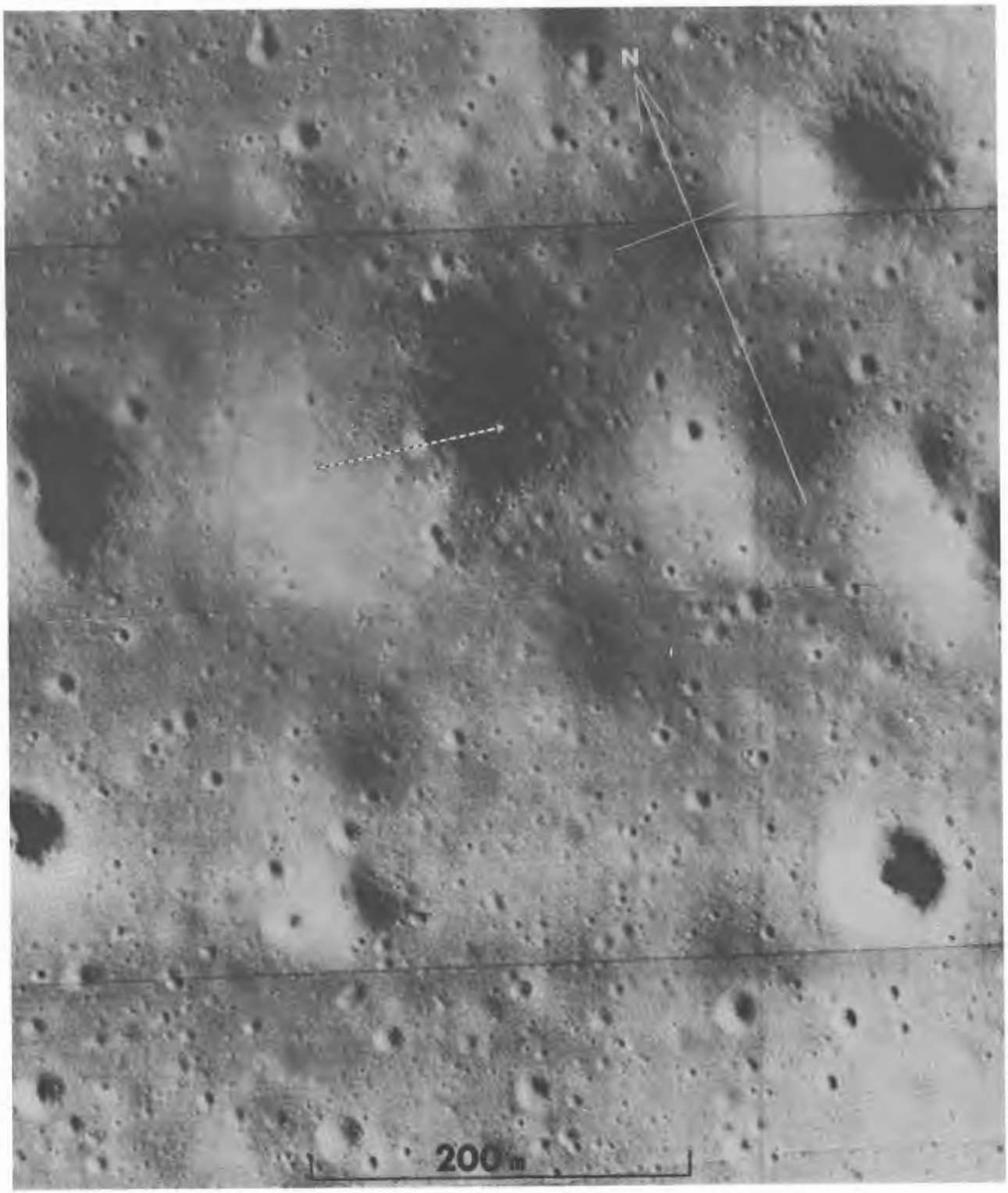

Figure 4-11b: Telephoto Frame—Site III P-9
Framelet Width: 200 meters
(Crater where Surveyor III landed)

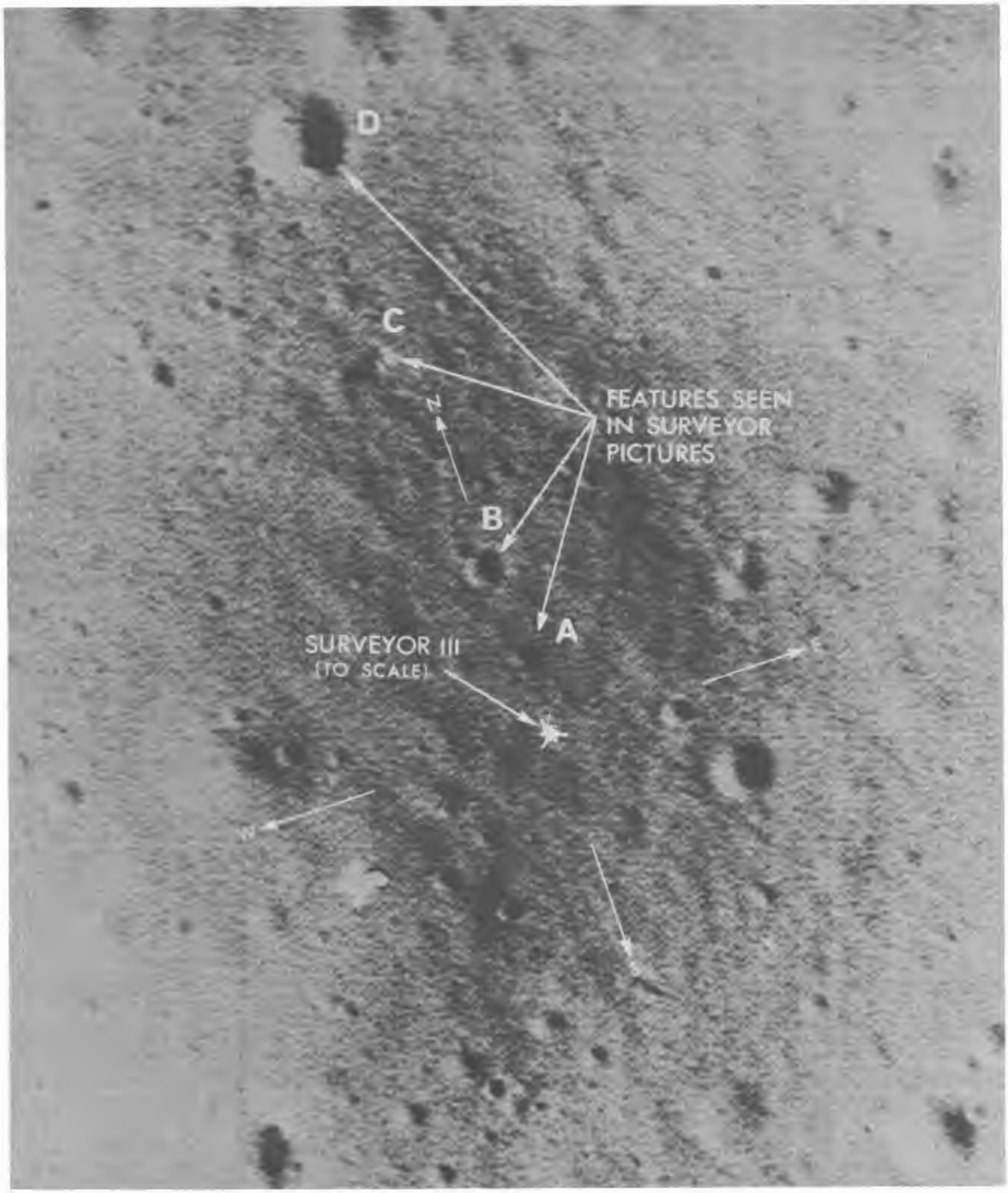

Figure 4-11c: Telephoto Frame—Framelet—Site III P-9
Enlargement of Surveyor III landing point

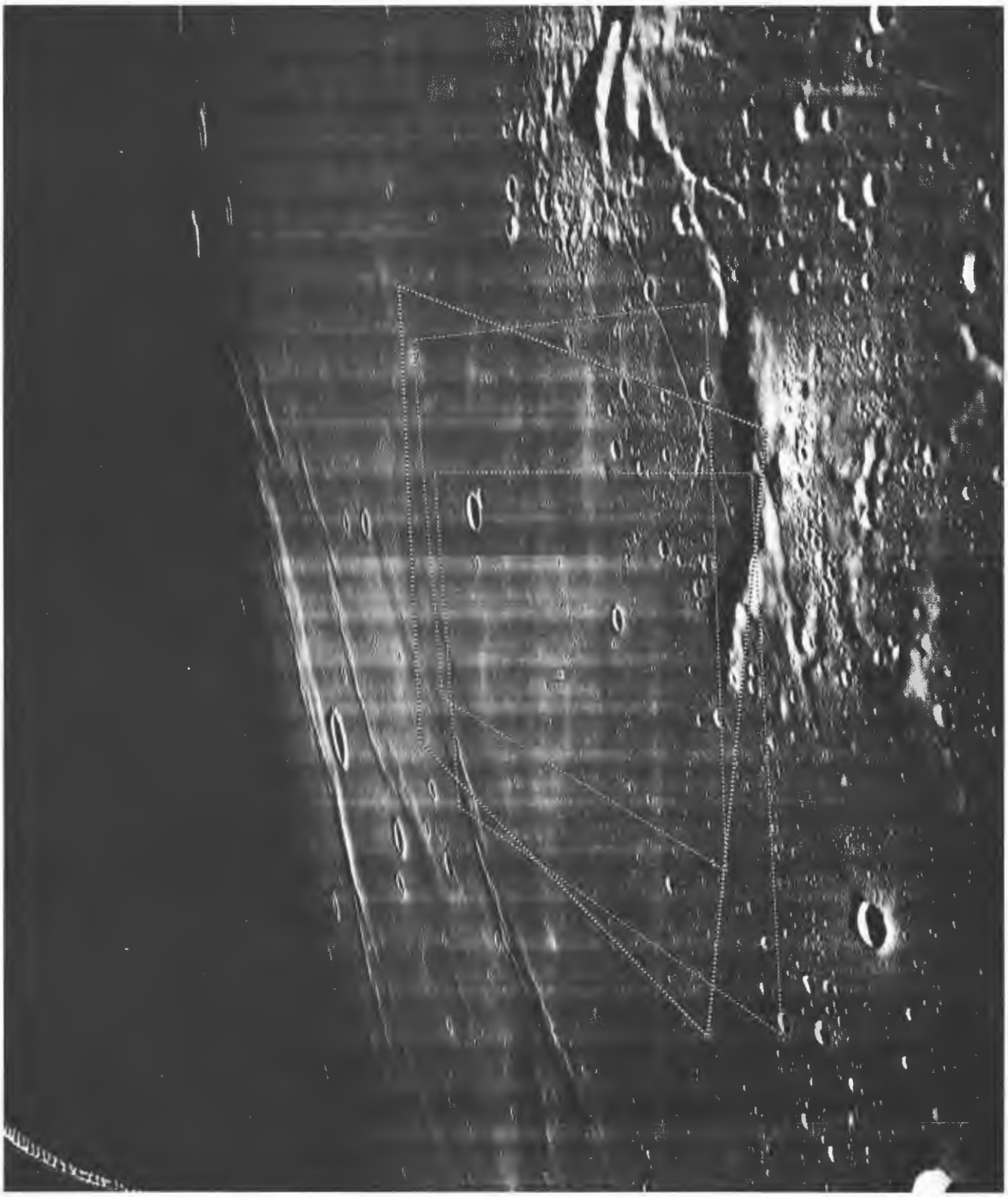

Figure 4-12: Wide Angle Frame 161—Site III S-25
Oblique photo centered on Site III P-10 and II P-13 coordinates
(Mission III coverage superimposed on Mission II site.
Identified crater shown in Figure 4-13)

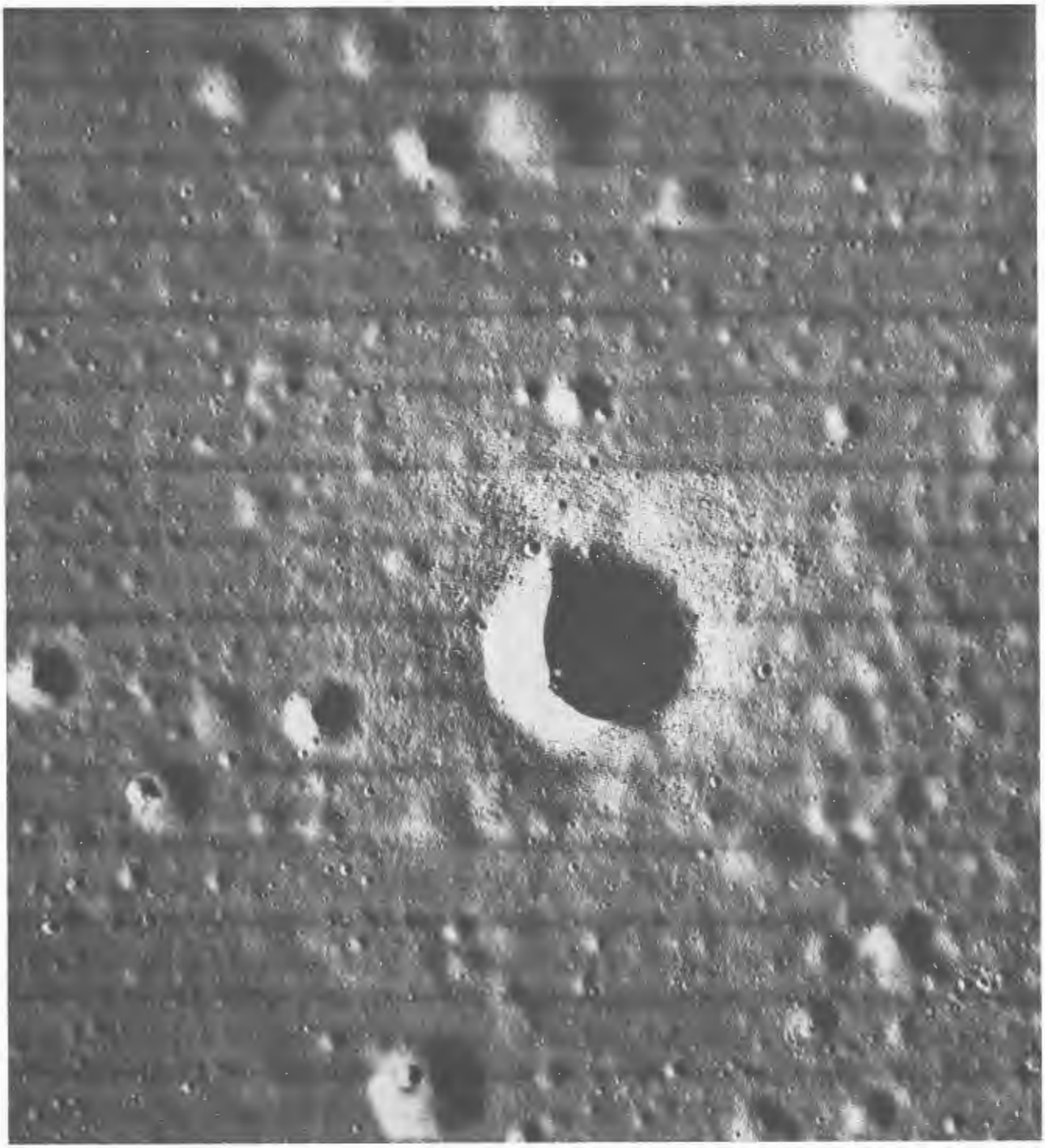

Figure 4-13: Telephoto Frame 168—Site III P-10
Framelet Width: 220 meters
(Surface detail and ejecta about crater)

Figure 4-14: Wide Angle Frame 172—Site III S-28
Oblique photo centered on Site III P-12 coordinates
(Wide angle vertical coverage and Frame 197 outlined)

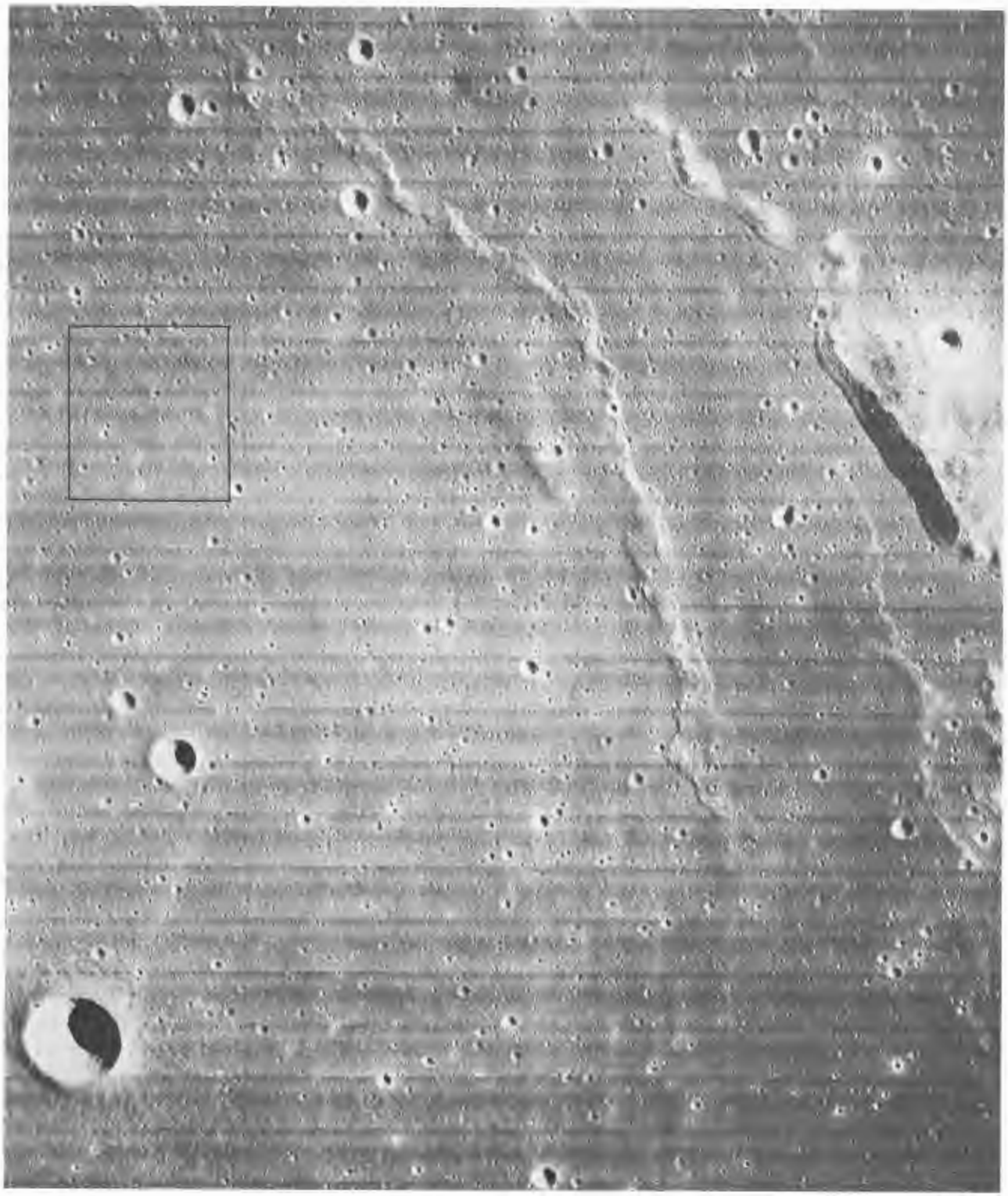

Figure 4-15: Wide Angle Frame 197—Site III P-12
Framelet Width: 1.7 km
(Outlined area covered by Figure 4-17)

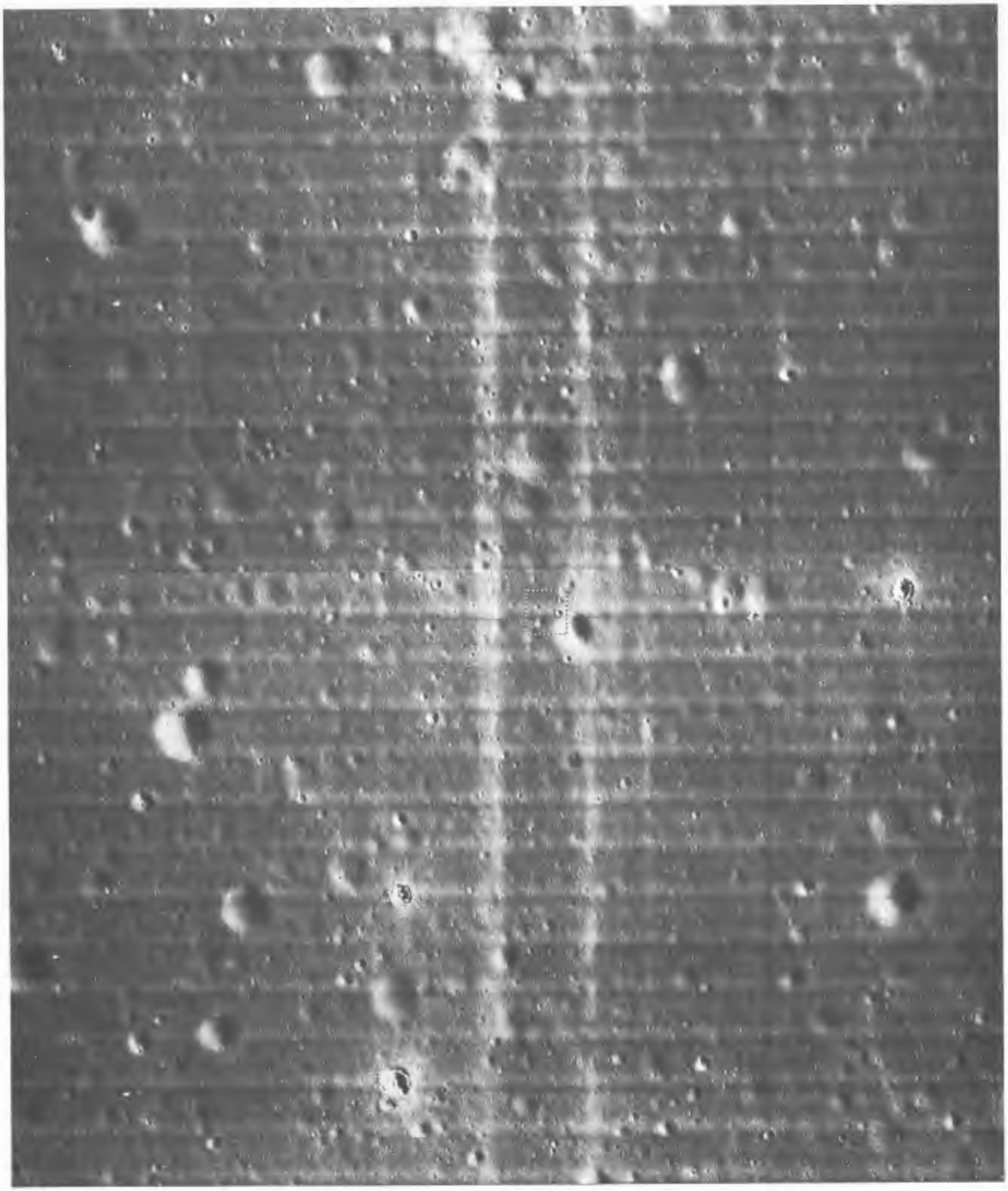

Figure 4-16: Wide Angle Frame 194—Site III P-12a
Framelet Width: 1.7 km
(Outlined area shows Surveyor I landing area)

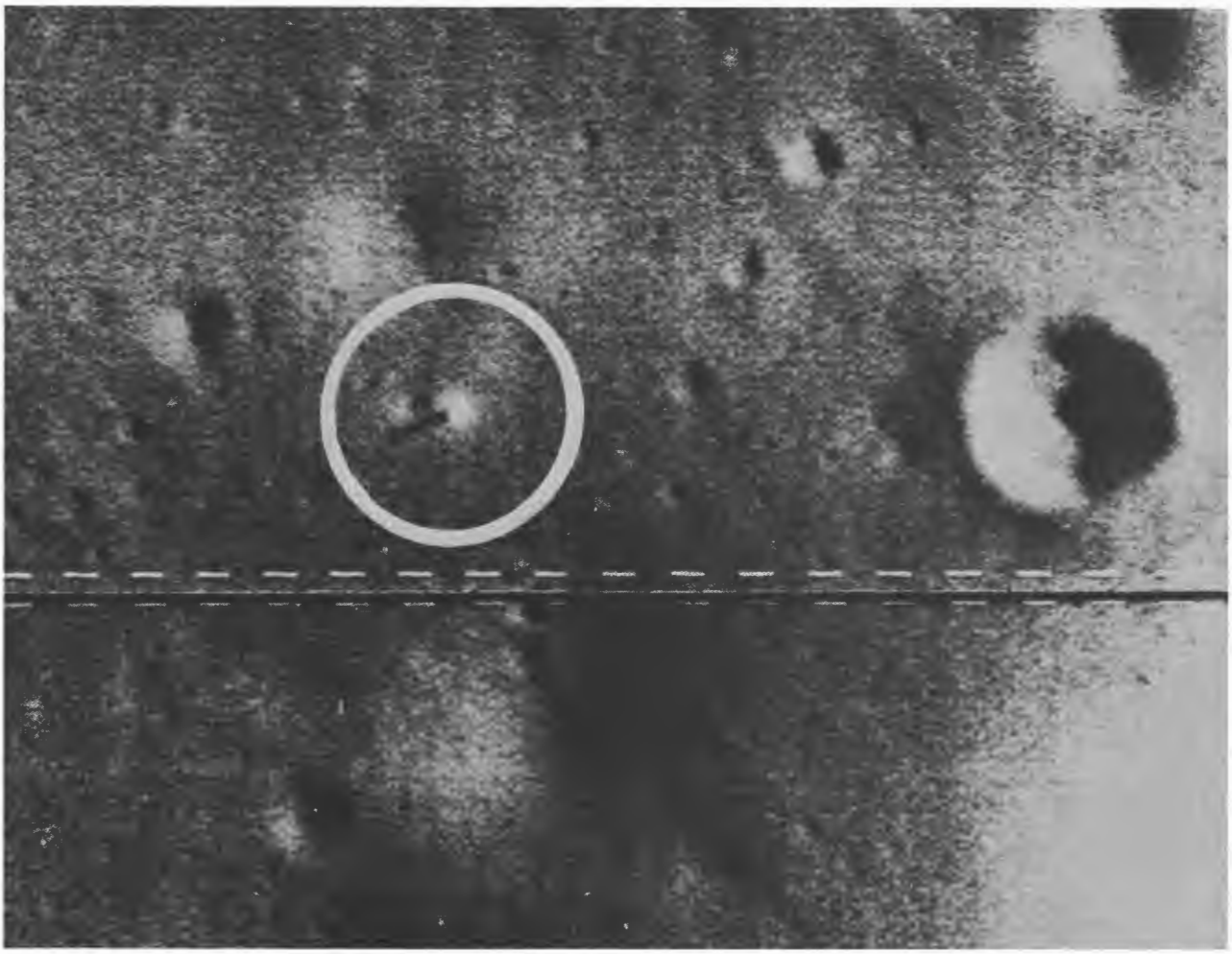

Figure 4-17: Telephoto Frame 194—Site III P-12a
(Enlargement of Surveyor I spacecraft)

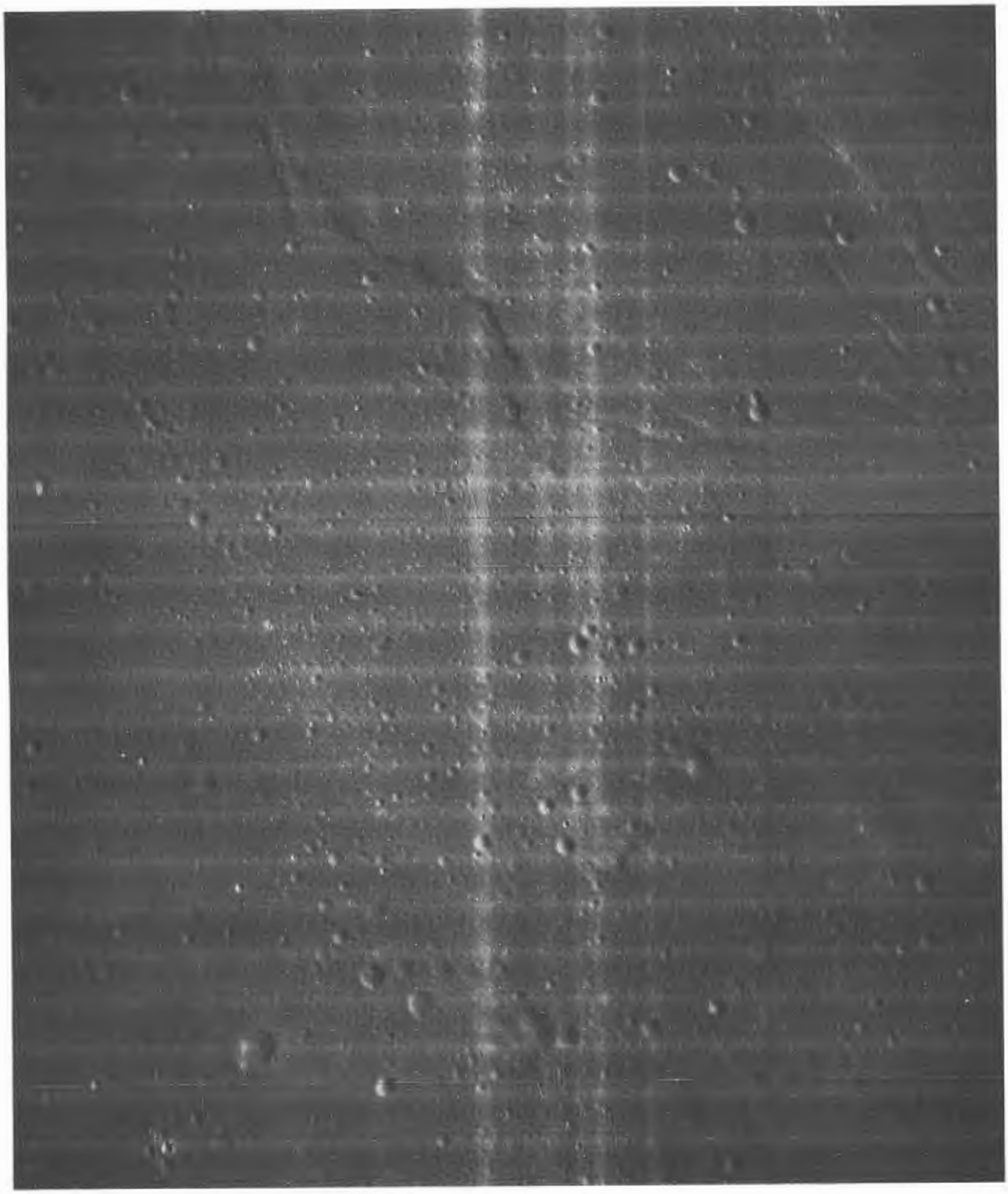

Figure 4-18: Wide Angle Frame 60—Site III P-5
Framelet Width: 1.6 km
(Vertical white bands in center of photo attributed to periodic static discharges from a teflon film separator)

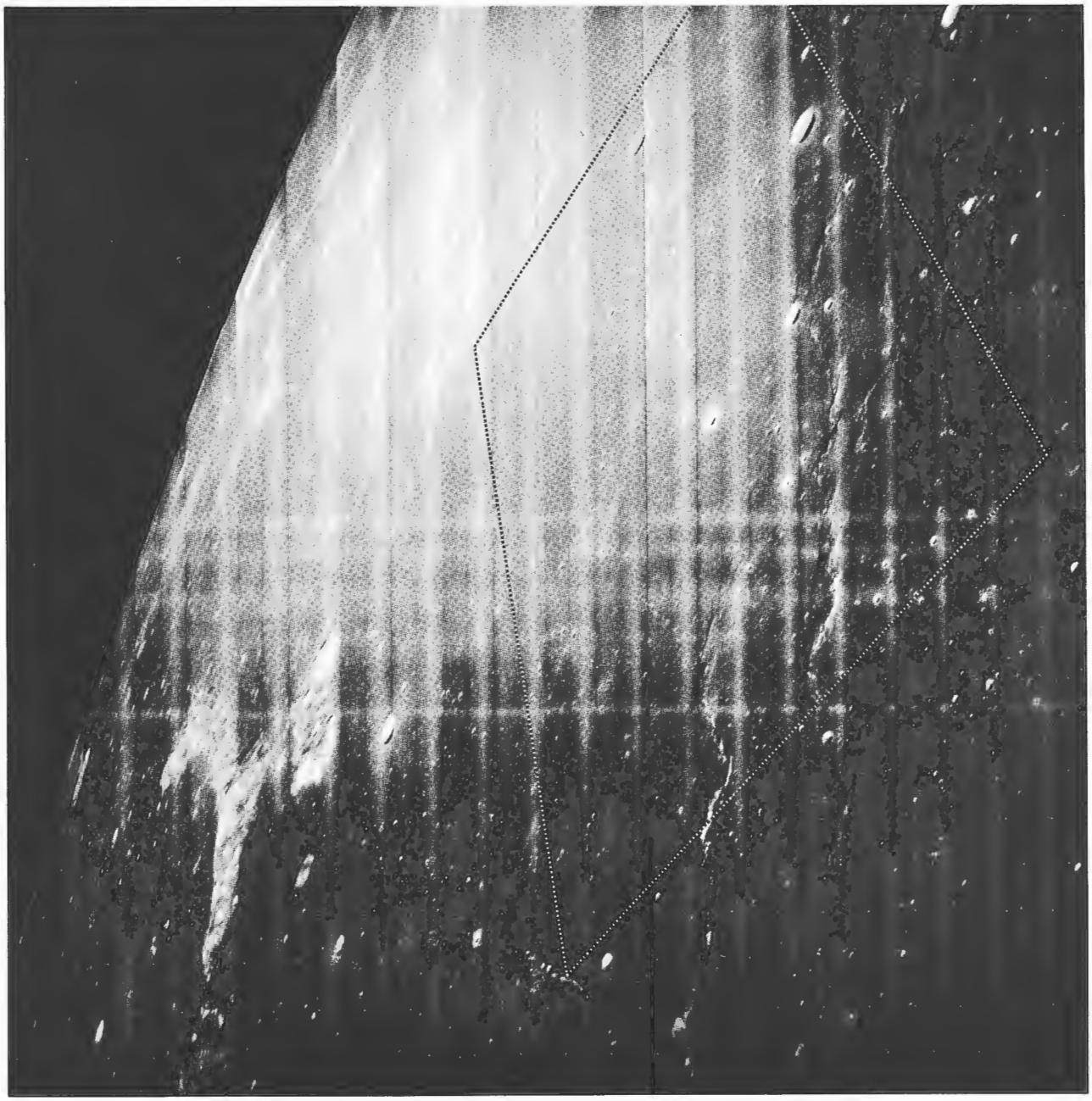

Figure 4-19: Wide Angle Frame 171—Site III S-27
Oblique photo centered on Site III P-11 coordinates
(Wide angle vertical coverage outlined)

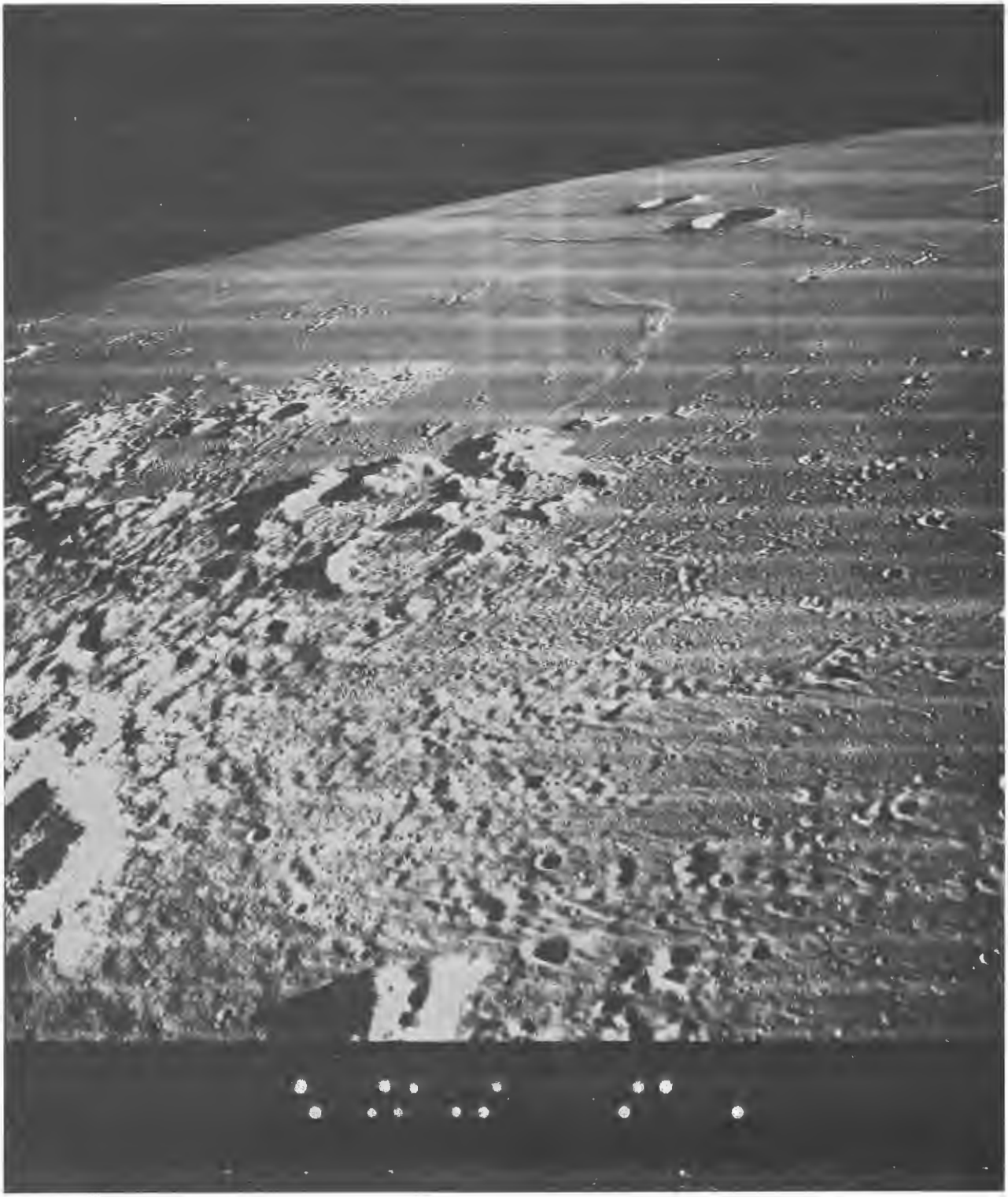

Figure 4-20: Wide Angle Frame 214—Site III S-30
Oblique photo of Luna 9 landing area

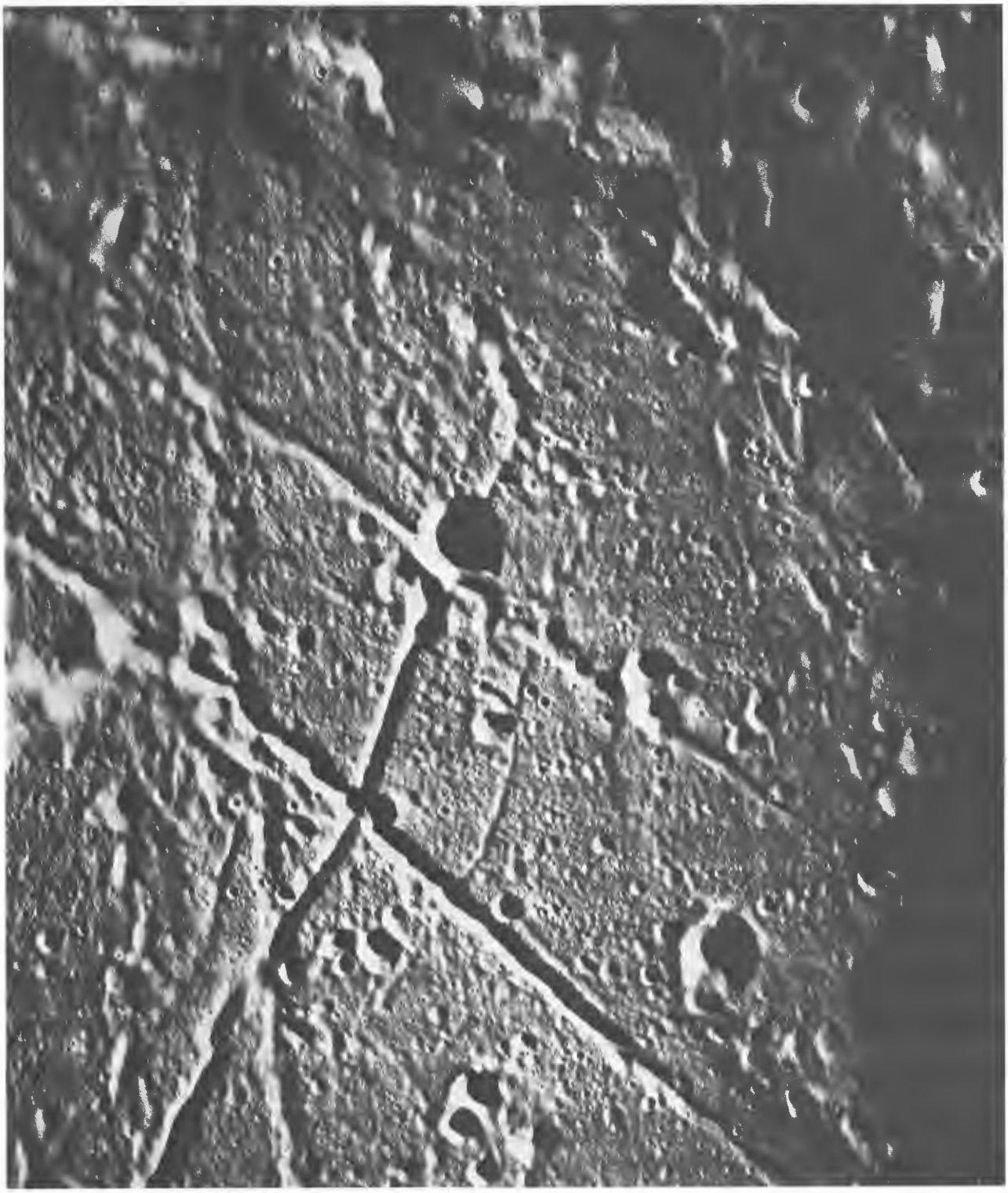

Figure 4-21 : Wide Angle Frame 215—Site III S-31
Framelet Width : 2.0 km
Floor structure of crater Hevelius

4.2 ENVIRONMENTAL DATA

Two types of telemetry instrumentation were installed on Lunar Orbiter III to monitor lunar environmental conditions. Two radiation dosimeters were mounted adjacent to the photo subsystem. Twenty individual micrometeoroid detectors were circumferentially mounted on the tank deck.

4.2.1 Radiation Data

Dosimeter 1, located near the film cassette, had a sensitivity of 0.25 rad per count, with a capacity of 0 to 255 counts. Dosimeter 2, located near the camera looper, had a sensitivity of 0.50 rad per count and a similar capacity of 0 to 255 counts. Due to the inherent shielding of the spacecraft, the photo subsystem structure, and the 2-grams-per-square-centimeter aluminum shielding provided by the film supply cassette, it was estimated that solar flares of magnitude 2 or less would have negligible effect on the undeveloped film. Flares of magnitude 3 or greater would produce considerable fog on the film.

The radiation dosimeter measurement system functioned normally throughout the mission and provided data on the Earth's trapped radiation belts as well as the radiation environment encountered in transit to the Moon and in orbits about the Moon. Radiation data obtained during the photographic mission are tabulated by state changes in Table 4-5.

Table 4-5:
RADIATION DATA SUMMARY

GMT OF CHANGE				RADIATION COUNTER READING (rad)	
Day	Hour	Min.	Sec.	Dosimeter 1	Dosimeter 2
36	02	00	—	0.75	—
36	07	35	41	—	Turn-on
37	01	03	37	—	0.5
37	10	29	39	1.0	—
37	17	33	35	—	1.0
38	13	30	08	—	1.5
39	17	50	29	—	2.0
42	04	49	49	1.25	—
45	11	23	48	1.50	—
48	12	55	12	—	2.5
49	10	30	12	1.75	—
53	12	21	47	2.00	—
57	08	10	0	2.25	—
59	12	22	10	—	3.0
60	07	49	09	2.50	—

Data from Dosimeter 1 indicated that the spacecraft was exposed to a total dosage of 0.75 rad while penetrating the inner Van Allen belt. There was no indication of any increase in level in transit through the outer belt. Dosimeter 2 was turned on after the spacecraft had passed through the Earth's trapped radiation belts.

Dosimeter 2 data indicated the presence of residual flux from the low-energy protons from the solar particle event of January 28. This was confirmed by the count increases during the 3-day period from turn-on through Day 38. Thereafter the increase was as expected for the normal cosmic-ray density and dosimeter noise observed on the two previous missions.

At 17:43 GMT on Day 44 (February 13), one of the largest optical flares, measured as Class 4, was observed by the solar observatory at Sacramento Peak, California. Pioneer VII recorded increases in low-energy proton flux. This occurrence was unexpected as it did not develop from a sizable sunspot group. Considerable concern was evidenced that this event would seriously damage the spacecraft film before lunar photography was planned to start. Fortunately, the particle energies were not present in the lunar areas traversed

by Lunar Orbiter III since they were not detected by either dosimeter and the film was not fogged.

4.2.2 Micrometeoroid Data

As of the end of the photographic mission there were no hits recorded by Lunar Orbiter III data. Detector 17 was found to be punctured prior to launch and a decision was made not to replace the detector.

4.3 TRACKING DATA

Lunar Orbiter III continued to provide lunar orbit tracking data to augment the data obtained on the first two missions. The orbit inclination of 20 degrees provided new data for determining the lunar model coefficients for this orbit. As of March 11 a total of 941.7 station hours of doppler tracking data had been recorded. Approximately 168 hours of spacecraft ranging data were recorded. A total of 35 station-time correlation checks were completed. All of this data has been furnished to NASA and will be further evaluated to refine the mathematical model of the Moon. The following discussions are pertinent to the quality of the tracking data obtained and the performance accuracy of the tracking system.

4.3.1 Deep Space Instrumentation Facility

Overall performance of the DSIF tracking data system was excellent in support of Mission III. There were no major data outages and better than 90% of the data received was classified as good. The DSIF continued to receive and record good doppler data during the photo readout phases by using Receiver 2 in the AGC mode as developed during Mission II. Ranging data was also obtained to aid in orbit determination.

DSS-62 was commissioned and replaced DSS-61 as a prime tracking station at Madrid, Spain. The station performed in a satisfactory manner with very little time between commissioning of the station and launch of the spacecraft.

The prediction program performed without any troubles and maintained a high degree of accuracy due to improved lunar harmonic coefficients and to accurate state vectors. The first occultation at DSS-12 was predicted within 1 second of the actual occurrence. There were no prediction outages and all stations were supplied with the current predictions.

Tracking Data Validation—The tracking data validation function was accomplished by back-feeding the tracking data to the Goldstone computer facility for processing by the Tracking Data Monitoring program (TDM), which compared the received data against a set of predictions and computed the residuals. This program also calculated the standard deviation of the last five data points and provided an estimate of data noise. Program outputs were transmitted to the SFOF by teletype and printed in tabular form. The program outputs were also plotted on the Milgo 30 X 30 plotter through the IBM 7044 plot routine.

During the cislunar phase the TDM generated its own predicted quantities by using an internal trajectory subprogram. The residuals were less than 1 Hz and the noise was computed to be less than 0.1 Hz, indicating a high quality of data.

The internal trajectory subprogram of the TDM does not compute predictions for the lunar orbit phase. In this phase the JPL predictions are used and the residuals increased, which reflects inaccuracies of the lunar model in the prediction program. No deviations in the rf carrier were observed during Mission III. Noise estimates of the TDM remained fairly accurate, indicating the overall good quality of the data. Spacecraft velocity changes were also monitored through the tracking data and showed good agreement with the other data.

Overall performance of the data validation system was very smooth and trouble-free.

Tracking data quality reports were made consistently throughout the active mission. The data quality was excellent, surpassing DSN's performance on Lunar Orbiter II. There were fewer anomalies and TTY data received at JPL was cleaner and much more usable,

not only due to DSN obtaining two- and three-way doppler and ranging throughout, but also due to good spacecraft performance.

4.3.2 Deep Space Network

Tracking data were recorded at the Deep Space Stations and the Space Flight Operation Facility to satisfy requirements for the selenographic data. The Deep Space Station recording was a five-level teletype paper tape. During the mission, the tracking data were transmitted to the SFOF via normal teletype messages. At the Space Flight Operations Facility teletype data were received by communications terminal equipment and passed to the raw-data table on the 1301 disk by the IBM 7044 I/O processor. These data were processed by the TTYX program to separate the telemetry data and tracking data in the messages received, and stored on the tracking raw-data file on disk. The tracking data processor (TDP) program generated the master tracking data table on the 1301 disk by smoothing and sorting the data from the tracking raw-data file by Deep Space Station identification. The output of this program was also recorded on magnetic tape and identified as the tracking data deliverable to NASA. An orbit data generator routine extracted selected master data file tracking data, smoothed it, sorted it according to time, and inserted it in the orbit determination program input file. Upon command from the FPAC area, orbit parameters were computed as predicted—based upon selected data from the orbit determination program input file and the orbit determination program—and inserted into the data display for subsequent display by the user.

The raw-tracking-data paper tapes recorded at each Deep Space Station and the output of the tracking data processor at the Space Flight Operations Facility, recorded on magnetic tape, were collected and delivered to NASA for follow-on selenodetic analysis.

4.4 PERFORMANCE TELEMETRY DATA

Spacecraft performance telemetry data was obtained by three different methods. Prior to spacecraft separation the data was transmitted via assigned subcarriers of the VHF Agena telemetry link. This data was recorded at AFETR and, after real-time demodulation, transferred to DSS-71 (Cape Kennedy) for retransmission to the SFOF computers. In addition, the AFETR stations recorded the S-band signal directly from the spacecraft. After separation, the performance data was received directly from the spacecraft by the Deep Space Stations and reformatted for transmission to the SFOF. In all cases, the data was available for the subsystem analyst to continuously monitor the operational status of all spacecraft subsystems and environmental conditions.

Mission support by the DSN began 6 hours prior to liftoff on February 5, 1967, on a 24-hour-coverage basis, and terminated with the conclusion of photo readout on March 2, 1967. Table 4-6 summarizes the data recorded by the DSN during the period from liftoff through the completion of priority readout on February 23. Early termination of DSN telemetry data, monitoring was required to facilitate scheduled work within the SFOF. The data continued to be processed and used by the operations personnel after the termination of data monitoring.

Table 4-6: DSN TELEMETRY SUMMARY

DEEP SPACE STATION	TOTAL PASSES	TELEMETERED FRAMES		PERCENT RECOVERED
		Transmitted	Recorded	
Goldstone	18	19,455	19,323	99.3
Woomera	19	17,373	16,640	95.8
Madrid	18	17,366	16,482	94.9
Total		55,363	53,577	96.4

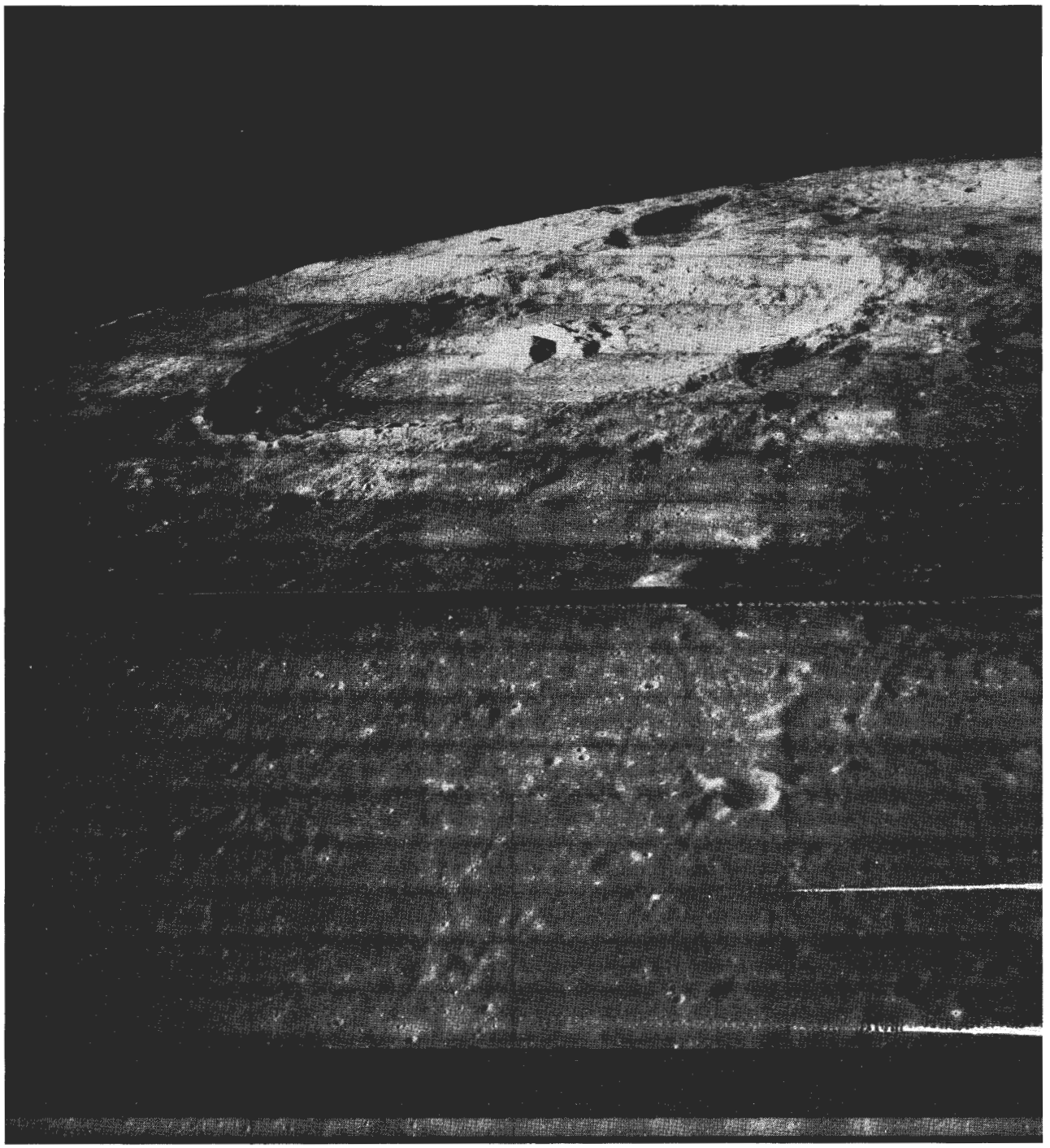

Wide-Angle Frame 78—Site III S-8
(Oblique to south toward crater Theophilus)

5.0 MISSION EVALUATION

Lunar Orbiter III added significant data to the major accomplishments of Lunar Orbiters I and II as related to the techniques and data required to land a man on the Moon and provide for his safe return to Earth. These accomplishments included but were not limited to:

- Provided sufficient photographic data from which eight candidate sites for the first Apollo landing were selected.
- Completed the first extensive site-examination photographic mission of the Moon.
- Employed greater diversity of photographic techniques to enhance the data recoverable from the lunar photos. This included the integrated use of vertical, forward overlap, side overlap, converging telephoto stereo, and low- and high-angle obliques.
- Positively identified the location of the Surveyor I spacecraft and landing site.
- Provided high-resolution photos of Surveyor III's landing site sufficient to establish its landing point within 1 meter.
- Provided data from which to determine the lunar mathematical model coefficients for a 21-degree orbit inclination.
- Successfully completed a 13-degree plane change at lunar orbit injection.
- Provided many photographs of areas of scientific interest with excellent resolution capabilities.
- Provided photos with nearly equal exposure characteristics of the two lenses.
- Demonstrated the spacecraft maneuver versatility and control in the many photographic maneuvers.
- Developed a tape playback capability that compensates for known spacecraft readout system density characteristics.

Mission III was considerably more complicated than either of the previous missions, as evidenced by the number of primary and secondary sites and the integrated use of many photography modes. Performance data during the active photographic period indicated that the complex mission was completely accomplished, except for the cancellation of the 32nd secondary site. A voltage transient or interruption within the photo system caused an improper logic status in the internal programmer, resulting in failure of the film-advance motor and premature termination of final readout. This failure occurred after 275 telephoto and wide-angle photos of the 422 taken had been read out. Fifty-one of the remaining photos were read out in whole or in part during the priority-readout phase. This failure was the only event that resulted in loss of any of the four types of mission data obtained.

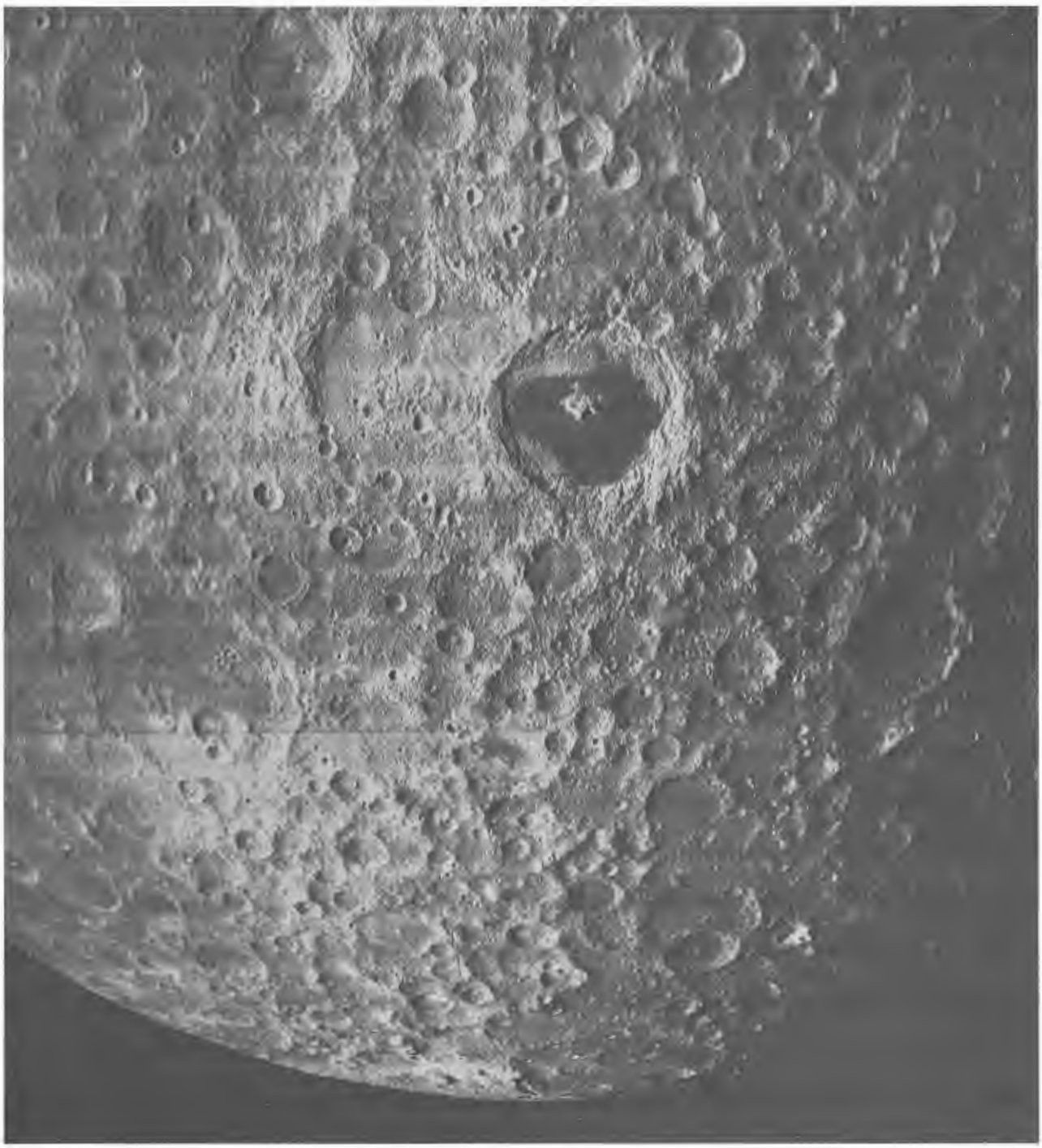

Wide-Angle Frame 121—Site III S-21.5
(Farside photo centered at 126.7° E and 24.0° S)

6.0 PROGRAM SUMMARY

The primary task of the Lunar Orbiter program was essentially completed during the first three missions. Potential landing areas within the established Apollo zone of interest (±5° latitude and ±5° longitude) had been selected based on Earth observations as augmented by Ranger and Surveyor program data. Lunar Orbiters I and II accomplished photographic site-search missions of preselected areas grouped in southern and northern latitude bands, respectively. Lunar Orbiter III accomplished a comprehensive site-confirmation mission of the 12 most promising sites selected from the Mission I and II photographs. Eight candidate sites for early Apollo missions were selected by the NASA Flight Evaluation Group after analysis of photographs from the three missions. Three primary sites will be chosen by Apollo from this set of eight candidates, for the first manned landing on the Moon.

In addition to the primary objectives, the first three Lunar Orbiter missions provided extensive detailed photographic coverage of the farside of the Moon and many areas of scientific interest on the nearside. Many of these photos can be described as spectacular. Other major accomplishments included: determination of the mathematical model of the Moon for 12-and 21-degree orbit inclinations, and precision achievement of the desired orbit characteristics.

Accomplishment of these objectives began with the Lunar Orbiter I flight 28 months, 15 days after the start of the program and the subsequent flights at the prescribed intervals. The on-board digital programmer, with its 128-word magnetic core memory, controls 120 separate spacecraft function and provides the inherent high degree of operational flexibility. It has the capability of providing up to 16 hours of stored information and instructions that can be interrupted at virtually any time during radio communication to update the stored sequences or introduce new real-time commands. The designed flexibility of the operational command and control concept and the adaptability of the supporting computer programs and software were exercised to greater limits on each successive mission. As operating experience was gained, the ability to perform extremely complicated photographic missions, including real-time changes in photo site locations and the reaction to nonstandard events, was routinely implemented.

This capability was employed to initiate special test sequences to support real-time analysis of operational problems and implement corrective action or alternate procedures that allowed the mission to continue to completion with a minimum loss of data.

During the Mission I design period, there was no indication or requirement for the photo subsystem operational constraint (film-set) exposures to be used to photograph any specific lunar sites and the primary-site photography was limited to vertical photography. As the program developed, it became more desirable and important to use the film-set photos to obtain additional information on potential sites for subsequent missions as well as other lunar terrain features from Apollo considerations and scientific interests. Sufficient planning permitted changes in site location during the conduct of the mission and procedures were developed for accurately orienting the camera axis and timing the exposure to obtain any desired photo coverage. (The most spectacular photo of this type was the Earth and the Moon's limb.)

The outstanding quality and detail of the Moon's topography, evident in the Earth-Moon photo, led to the development and employment of more off-vertical photography for succeeding missions. A Mission II experiment in converging telephoto stereo photography was a complete success and produced a considerable improvement in surface contouring. Based on the results obtained, the promising Apollo landing sites have been photographed by comprehensive series of vertical, oblique, forward and side vertical (wide-angle) stereo, and con-

vergent telephoto stereo photography. The combination of these photos during any analysis effort provides an enormous source of detailed topographic and geological data of the lunar surface.

As each operational mission became more complex, it was necessary to improve the corresponding operation of the space flight operations system. The flight operations team (composed of NASA, Boeing, JPL, and other supporting government agencies) personnel developed improved and simplified operating procedures, data displays, communications, and computer routines based upon the experience gained on successive missions and intermission training exercises. Changes were also made in the organization of the flight operations team to change or eliminate the manning of operational positions for succeeding missions. An off-line planning group was added to work in parallel with the on-line team to handle the planning and command preparation necessitated by nonstandard events and other deviations to the basic mission plan. A detailed flight operations plan was developed prior to each mission based upon the specific objective and photo sites defined. The flexibility of the flight operations team, supported by the inherent capability of the spacecraft command and control system and the operational software, made it possible to react quickly and effectively to changes in mission requirements, abnormal spacecraft performance, and problem diagnosis. These efforts resulted in real-time changes or adjustments to the basic mission plan or operating procedures to ensure the maximum possibility of satisfactorily completing the assigned mission.

The following tables (Tables 6-1 through -5) compare specific parameters of the first three missions and compare the predicted and actual performance when significant. Although Lunar Orbiters II and III are currently in the extended-mission phase, the data presented herein is limited to the period from launch to the end of the photographic mission. The data has been arranged in separate tables where related data are presented and include launch and boost, velocity control, trajectory, operational, environmental, and photographic parameters.

Table 6-1 : LAUNCH AND BOOST PARAMETERS

FUNCTION	LO I		LO II		LO III	
	Predict	Actual	Predict	Actual	Predict	Actual
Launch Date (GMT)		8-10-66 19:26:01		11-6-66 23:21:00		2-5-67 01:17:01
Launch Azimuth (deg)		99.9		93.8		81.6
Spacecraft Launch Weight (lb)		852.84		855.22		856.71
Earth Orbit Coast Period (sec)		1671.4		677.1		578.1
Velocity Imparted by Atlas (ft/sec)		18,520		18,509		18,534
Cislunar Injection Time (sec)		2282.2		1287.0		1194.4
Cislunar Injection Parameters						
$\bar{B}\cdot\bar{T}$ (km) } Prior to	6,630	15,643	6120	10,426	5,590	5,077
$\bar{B}\cdot\bar{R}$ (km) } Midcourse	−1,135	-1,686	−410	−1,475	−2,460	-1,801
$\bar{B}$ (km) } Maneuver	6,431	15,734	6134	10,529	6,107	5,387
Time of Closest Approach (GMT)	8-14-66 14:05:54	8-14-66 15:55:58	11-10-66 20:39:00	11-10-66 21:21:07	2-8-67 22:06	2-8-67 21:47

Table 6-2: OPERATIONAL PARAMETERS

FUNCTION	LO I	LO II	LO III
SPACECRAFT CONTROL			
Velocity Change Maneuvers	16	12	12
Photography Maneuvers	92	216	280
Attitude Update Maneuvers	144	30	11
Thermal Pitch-off Maneuvers	77	9	67
Star Map, Canopus and Other Maneuvers	45	17	13
Total	374	284	383
Real-time Commands Transmitted (words)	1,988	1,289	1,266
Stored-Program Commands Transmitted (words)	2,522	2,282	2,349
TWTA Operation Hours	211.1	198	155
TWTA On-off Cycles	148	129	114
FILM CASSETTE RADIATION DOSAGE			
Van Allen Belt	1.0	0.75	0.75
Cislunar Period	0.0	0.0	0.25
Solar Flares	10.0	0.0	0.0
Total	10.5	1.75	2.50
CAMERA LOOPER RADIATION DOSAGE			
Van Allen Belt	turned off	turned off	turned off
Cislunar Period	0.5	0.0	2.0
Solar Flares	135.0	0.0	0.0
Total	138.0	1.0	3.0
MICROMETEOROID IMPACTS	0	3 known 1 possible	0

Table 6-3: VELOCITY CONTROL PARAMETERS

FUNCTION	LO I		LO II		LO III	
	PREDICTED	ACTUAL	PREDICTED	ACTUAL	PREDICTED	ACTUAL
MIDCOURSE MANEUVER						
Time From Launch	–	28h34m	—	44:33	—	37:43
ΔV Imparted (meters/sec)	37.8	37.8	21.1	21.1	5.1	5.1
Burn Duration (sec)	32.7	32.1	18.4±0.6	18.1	4.5+0.5	4.3
Specific Impulse lb-sec / lb	275.2	276.0	276.0	276.5	273.2	276
Thrust Developed (lb)	99.8	101.6	100.0	100.5	99.6	102.5
DEBOOST MANEUVER						
Time From Launch	–	92h8m	—	93h6m	—	92h37m
ΔV Imparted	790.0	789.7	829.7	829.7	704.3	704.3
Burn Duration	588±10	578.7	618±10	611.6	541±10	542.5
Specific Impulse	274.7	276.0	276.0	276.0	276	277
Thrust Developed	99.8	101.3	100.0	101.0	100	99.9
ORBIT TRANSFER						
Date (GMT)	–	8-21-66 09:50	—	11-15-66 22:58	—	
ΔV Imparted	40.2	40.2	28.1	28.1	50.7	50.7
Burn Duration	22.7±1.6	22.4	17.5±0.9	17.4	33.4±1.6	33.7
Specific Impulse	274.5	276	276	276	277	277
Thrust Developed	112.6	113.6	101.5	102.3	101.3	100.3
ORBIT ADJUSTMENT						
Date	–	8-25-66				
ΔV Imparted	5.4	5.4				
Burn Duration	3.0±1	3.0				
Thrust Developed	114	113.6				

Table 6-4: TRAJECTORY PARAMETERS

FUNCTION	LO I		LO II		LO III	
	PREDICTED	ACTUAL	PREDICTED	ACTUAL	PREDICTED	ACTUAL
LUNAR ENCOUNTER PARAMETERS						
$\bar{B}\cdot\bar{T}$(km)	6,402	6,458	6,010	6,044	5605	5607
$\bar{B}\cdot\bar{R}$(km)	−1,171	−1,120	−391	−373	−2465	−2479
$\bar{B}$(km)	6,509	6,555	6.023	6,055	6123	6131
Time of Closest Approach	8-14-66	8-14-66	11-10-66	11-10-66	2-8-67	2-8-67
(GMT)	15:50:01	15:50:34	20:39:00	20:39:00	22:06:00	22:06:05
INITIAL ORBIT KEPLER ELEMENTS						
Perilune Altitude (km)	199	189	202	196	213	210
Apolune Altitude (km)	1,850	1,866	1,850	1,871	1850	1802
Orbit Inclination (day)	12.04	12.16	11.99	11.97	21.05	20.94
Ascending-Node Longitude (deg)	325.3	325.9	341.8	341.7	311.7	310.3
Argument of Perilune (deg)	180.8	180.3	162.1	161.6	176.2	177.3
Eccentricity		0.303		0.302		0.289
Orbit Period (hours:min)	3:37	3:37		3:37		
Number of Orbits		43		33		26
ORBIT TRANSFER KEPLER ELEMENTS						
Perilune Altitude	57.9	56.0	50.2	49.7	54.8	54.8
Apolune Altitude	1855	1853	1858	1853	1846	1847
Orbit Inclination	12.04	12.05	11.91	11.89	20.87	20.91
Ascending-Node Longitude	234.1	234.0	272.8	273.3	258.6	257.9
Argument of Perilune	181.5	181.2	163.3	162.8	178.3	178.9
Eccentricity		0.333		0.335		0.334
Orbit Period		3:29		3:28		3:28
Number of Orbits		30		146		123
ORBIT ADJUSTMENT KEPLER ELEMENTS						
Perilune Altitude	40.0	40.5		N.A.		N.A.
Apolune Altitude	1824	1817				
Orbit Inclination	12.03	12.0				
Ascending-Node Longitude	176.7	177.0				
Argument of Perilune	186.0	185.3				
Eccentricity		0.333				
Orbit Period		3:26				
Number of Orbits		135				
TRACKING DATA RECORDED						
Doppler (hours)				819		942*
Ranging (hours)				200		168*
Station Time Correlations				36		35*

*DSN Data through 3-11-67

Table 6-5: PHOTOGRAPHIC PARAMETERS						
FUNCTION	LO I		LO II		LO III	
	PLANNED	ACTUAL	PLANNED	ACTUAL	PLANNED	ACTUAL
DUAL FRAMES EXPOSED	212	211	211	211	212	211
FIRST PHOTO DATE		8-18-66		11-18-66		2-15-67
LAST PHOTO DATE		8-29-66		11-25-66		2-23-67
TELEPHOTO FRAMES READ OUT	212	211	211	209□		170□
WIDE-ANGLE FRAMES READ OUT	212	211	211	208□		157□
FINAL READOUT STARTED		8-29-66		11-26-66		2-23-67
LAST READOUT COMPLETED		9-14-66		12-7-66		3-2-67
PRIMARY SITES PHOTOGRAPHED	10	10	13	13	12	12
Frames Exposed	180	156	184	184	156	156
Photo Sequences	11	11	22	22	19	20
Altitude Range (km)		45-54		44-57		45-62
SECONDARY SITES PHOTOGRAPHED (NEARSIDE)		41	13	13	31	30
Frames Exposed	42	44	23	23	55	54
Photo Sequences	42	41	14	14	31	30
Altitude Range (km)		46-239		41-51		44-63
FARSIDE SITES PHOTOGRAPHED		7	4	4	1	1
Frames Exposed	0	11	4	4	1	1
Photo Sequences	0	7	4	4	1	1
Altitude Range (km)	0	1295-1454		1450-1517		1460
AREA PHOTOGRAPHED (km^2) +		*		1×10^4		5×10^3
Primary-Site Telephoto		5×10^4		3.6×10^4		3.5×10^4
Primary-Site Wide Angle						

Table 6-5: PHOTOGRAPHIC PARAMETERS (Cont'd)

FUNCTION	LO I		LO II		LO III	
	PLANNED	ACTUAL	PLANNED	ACTUAL	PLANNED	ACTUAL
Secondary-Site Telephoto		*		2×10^3		2.5×10^4
Secondary-Site Wide Angle		2.1×10^5		1.2×10^4		5×10^5
Farside Telephoto		4×10^5		3.3×10^5		1.2×10^4
Farside Wide Angle		3×10^6		3×10^6		2.2×10^5
READOUT SEQUENCES						
Priority Readout		45		53		53
Final Readout		93		73		56
Total		138		126		109
%PRIMARY SITES COVERAGE READ OUT						
Telephoto		100		96		63
Wide Angle		100		100		75
%SECONDARY SITES COVERAGE READOUT						
Telephoto		100		100		78
Wide Angle		100		100		80
TYPES OF SITE PHOTOGRAPHY (FRAMES)						
Vertical	212	209	196	196		79
Near Vertical		0	11	11		80
High Obliques		2	4	4		52
High Obliques		0	8	8		36
Convergent Telephoto Stereo						

*Telephoto photos smeared by camera abnormality.
+Redundant coverage eliminated.
□Contains some partial frames.

NATIONAL AERONAUTICS AND SPACE ADMINISTRATION
WASHINGTON, D.C. 20546

OFFICIAL BUSINESS

FIRST CLASS MAIL

POSTAGE AND FEES PAID
NATIONAL AERONAUTICS AND
SPACE ADMINISTRATION

POSTMASTER: If Undeliverable (Section 158 Postal Manual) Do Not Return

"The aeronautical and space activities of the United States shall be conducted so as to contribute . . . to the expansion of human knowledge of phenomena in the atmosphere and space. The Administration shall provide for the widest practicable and appropriate dissemination of information concerning its activities and the results thereof."

—NATIONAL AERONAUTICS AND SPACE ACT OF 1958

NASA SCIENTIFIC AND TECHNICAL PUBLICATIONS

TECHNICAL REPORTS: Scientific and technical information considered important, complete, and a lasting contribution to existing knowledge.

TECHNICAL NOTES: Information less broad in scope but nevertheless of importance as a contribution to existing knowledge.

TECHNICAL MEMORANDUMS: Information receiving limited distribution because of preliminary data, security classification, or other reasons.

CONTRACTOR REPORTS: Scientific and technical information generated under a NASA contract or grant and considered an important contribution to existing knowledge.

TECHNICAL TRANSLATIONS: Information published in a foreign language considered to merit NASA distribution in English.

SPECIAL PUBLICATIONS: Information derived from or of value to NASA activities. Publications include conference proceedings, monographs, data compilations, handbooks, sourcebooks, and special bibliographies.

TECHNOLOGY UTILIZATION PUBLICATIONS: Information on technology used by NASA that may be of particular interest in commercial and other non-aerospace applications. Publications include Tech Briefs, Technology Utilization Reports and Notes, and Technology Surveys.

Details on the availability of these publications may be obtained from:

SCIENTIFIC AND TECHNICAL INFORMATION DIVISION

NATIONAL AERONAUTICS AND SPACE ADMINISTRATION

Washington, D.C. 20546